Utilization of Ferrochrome Slag in Bitumen Base Stabilisation

A Dissertation Submitted in Fulfillment of the Requirement for the Award of the Degree of

MASTER OF ENGINEERING

In

Infrastructure Engineering

Submitted By

Utkarsh Singh

Roll No.: 802023023

Under Supervision of

Dr. Tanuj Chopra
(Assistant Professor)

Dr. Siksha Swaroopa Kar
(Principal Scientist)

DEPARTMENT OF CIVIL ENGINEERING

THAPAR INSTITUTE OF ENGINEERING AND TECHNOLOGY
(A DEEMED TO BE UNIVERSITY), PATIALA, PUNJAB
June, 2022

DECLARATION

I, Utkarsh Singh hereby declare that the work presented in this dissertation entitled "Utilization of Ferrochrome Slag in Bitumen Base Stabilisation" in fulfilment of the requirement for the award of degree of Master of Engineering submitted at Civil Engineering Department, Thapar Institute of Engineering & Technology (Deemed to be University), Patiala is an authentic record of work carried out under the of Dr. Tanuj Chopra (Assistant Professor, Civil Engineering Department, Thapar Institute of Engineering &Technology, Patiala) and Dr. Siksha Swaroopa Kar (Principal Scientist, Flexible Pavement Division, CSIR-CRRI, New Delhi) from 28th July 2021 to 30th June 2022. The matter presented in this has not been submitted either in part or full to any other university or institute for the award of any other degree.

Date: 01/07/22

Utkarsh Singh
(Roll No.: 802023023)

(Dr. Tanuj Chopra)
Assistant Professor,
Civil Engineering Department
Thapar Institute of Engineering &Technology
Patiala

(Dr. Siksha Swaroopa Kar)
Principal Scientist,
Flexible Pavement Division
CSIR-CRRI
New Delhi

ACKNOWLEDGEMENTS

First of all, I would like to thank God Almighty, the Giver of life and all knowledge, for giving me everything to accomplish this dissertation, patience, health, wisdom, blessing, and for granting me the capability to proceed successfully.

I wish to tender my unreserved appreciation to my Supervisor **Dr. Siksha Swaroopa Kar,** Principal Scientist, CSIR-Central Road Research Institute (CSIR-CRRI), New Delhi for her overwhelming support and advice, both technically and morally throughout the period of my M.E. dissertation work. Dr Siksha have given me a leap in my career, I will ever be grateful to for her kind heart and support that made my stay in CSIR-CRRI, New Delhi enjoyable. Also giving precious time, and great ideas that enable me to complete this dissertation. Their dynamism, vision, sincerity, and motivation have deeply inspired me.

I will also like to appreciate my Guide**, Dr. Tanuj Chopra,** Assistant Professor, Civil Engineering Department, Thapar Institute of Engineering &Technology (A Deemed to be University), Patiala for his contribution and input, without your help, this goal would not have been achieved. His Technical Guidance, valuable suggestions, and encouragement have been a tremendous help throughout this research study.

I would like to thank my parents for allowing me to realize my own potential and taught me the value of hard work, time, and education.

It is my great pleasure to acknowledge **Dr. Ranjana Aggarwal,** Director, CSIR-Central Road Research Institute (CSIR-CRRI), Delhi for his generous support and useful advice to accomplish my project work.

Special thanks to Ms. Anupriya, Mr Saurav Kumar Verma, and Mr Saurabh Chandra of CSIR-CRRI for their help during laboratory testing investigations. I am also thankful to the entire staff of the Flexible Pavement Department, CSIR-CRRI for their support and for creating an amiable environment in the division to carry out my dissertation work.

I also wish to appreciate the efforts and support of my friends Vedant Purohit, Imran Wasil, Amiya Thakur, Piyush Prasad, Joshua Divakar, Chandu Yadav, Mohini Patel, and Muskan Verma for helping out in times of difficulties and need.

My deepest gratitude to all who are closest to me, for their endless love, prayers, Assistance, advice, and encouragement without which this study would not have been possible.

ABSTRACT

The industrial waste such as steel slag, copper slag etc. in road construction industries is gaining significant importance in India considering the disposal, environment problems and gradual depletion of natural resources like aggregates and soil. These industrial waste products can be employed in the building of various layers of road pavement either as full replacements for standard materials or in combination with cement/lime with or without chemical stabilisers. Through experimental examination, the current study investigates the engineering features of ferrochrome slag, an industrial waste, with the goal of improving its applicability as a subgrade, subbase, and base material for road building.

Bitumen binder (VG-10) with three different RAP material percentages (45%, 65%, 85%) and two different slag content (with slag and without slag), along with two different binders (Foam bitumen and emulsion bitumen) were considered in this research study. Detailed laboratory performances of FBM and EBM as well as foaming characteristics were investigated. The foam was characterized for expansion ratio and half-life. The ideal foam binder and emulsion binder contents of the mix were determined statistically using the response surface technique (RSM). The effects of different percentages of RAP material and slag content on the resilient modulus, split tensile strength, tensile strength ratio, conditions of FBM and EBM were evaluated. Image analysis and X-ray diffraction pattern (XRD) were used to visualize the effect of different percentages of RAP material and slag content of FBM and EBM. The main harmful element found in the ferrochrome slag that is most likely to contribute to environmental pollution issues during use and disposal is chromium. Although there is a significant quantity of residual chromium in the slag samples, almost all of it is well immobilised in the spinel phase, allowing for very little chromium leakage from the slag samples. Results after exhaustive laboratory studies indicate that the warm aggregates having Slag content with 65% of RAP content gives the best performance of FBM and EBM.

TABLE OF CONTENTS

LIST OF Figures

LIST OF TABLES

LIST OF PHOTOS

CHAPTER 1
INTRODUCTION

1.1 Background

India is having world's second-largest road network in terms of length with a total length of 3.3 million km (approx.). Large-scale road-building projects, including Pradhan Mantri Gram Sadak Yojna (PMGSY) and National Highway Development Programme (NHDP), as well as numerous other state road development projects, have created a huge demand for high-quality natural stone aggregates. In addition to road development, the upkeep of this road network consumes a significant quantity of quarried materials each year. Rapid depletion of excellent quality aggregate resources, along with ever-increasing demand from infrastructure projects, has resulted in unsustainable mining of natural aggregates in many regions of our nation. Recent government actions, such as a prohibition on natural aggregate mining in many locations and incentives for the use of industrial waste in building operations, have sparked various projects to investigate alternate materials for construction of road. The main aim of current study is to examine the viability of employing such wastes in various forms in different pavement layers.

Large-scale industrialization has resulted in the build-up of a massive number of industrial by-products, harming natural environment through contamination of air, water and land. Appropriate management and usage of these by-products are now critical to the sustainability of the industries. Several initiatives being made to gainful utilisation of these wastes in place of natural resources in significant quantities. Use of fly ash, red mud, blast furnace slag (bfs), steel slag, copper slag and other materials has been attempted in numerous civil engineering infrastructure projects. In present study, efforts were made to gainful utilization of ferrochrome slag in pavement construction. The process of cooling the melted mass of slag determines the formation of ferrochrome slag. The metal slag produced during the production of ferrochrome slag is known as water granulated slag. Overflow slag from the ladle goes through slag launder towards granulation pond, in which high-pressurised water was put to break the slag into minute portions and cooled down by water quenching. Air-cooled ferrochrome slag is generated by the air-cooling technique. Ferrochromium slag forms at a rate that is 1.1 to 1.5 times that of ferrochromium metals. The annual production of ferrochromium slag is estimated in order of 12 to 16 million tonnes. The majority of this waste is dumped as a landfill, resulting in a massive deposit overtime. A few studies showed slowly release of chromium (Cr^{+6}) into

the environment over time causing contamination of ground water. As a result, cost-effective waste use in an ecologically responsible manner remains a concern for ferrochrome companies. Concerted efforts are therefore needed to explore the possibility of using ferrochrome slag in other sectors to solve the disposal problem. Road construction is one such sector where huge quantities of these waste materials could be gainfully used. Detailed investigations, therefore, needed for sustainable utilization of ferrochrome slag in roads.

In India, Ferro Alloy Plant of Tata Steel Limited situated at Raw Mat, Cuttack produced ferrochrome slag as shown in Fig 1.1. This report brings out the details of laboratory investigations carried out at CSIR-CRRI to discover the suitability of ferrochrome slag as alternate road construction material. Solid waste products created by industry not only take up precious landmass, but it also contaminates the environment and offer significant problems to safe disposal. Working toward the 5R's of trash reduction, recycling, recovery, research, and reuse, is the best solid waste management plan. (Su et al. 2001).

It is well-accepted fact that the roads are used for the transportation of various personnel and goods from one place to another. Also, the road network is the most important infrastructure required for the prompt growth of the country. It contributes significantly to a nation's economic and social development. Given India's federal system of government, numerous government entities are in charge of managing the country's road system. As of March 31, 2020, India had the second-largest road network with around 6,215,787 kilometres (3,862,337 miles) (MoRTH, 2020). India National Highways (NH) constitutes only about 2.7% of total national road network with 151,000 kilometres approximately (Department of Road Transport and Highways, 2021). It carries approximately 40% of road traffic. State Highways (SH) and District Roads which are managed by the state/union territory of Public works department constitute about 3% and 10.17% of the road network respectively. Rural Roads (RR), which is overseen by the Panchayats and the Pradhan Mantri Gram Sadak Yojana (PMGSY), serves as a catalyst for fostering and sustaining agricultural growth, enhancing basic health, granting access to educational possibilities, and improving economic chances. Rural Road carries the major length share of about 72.97% (MoRTH, 2020).

Major objectives of the road construction are to ensure a suitable material that focuses on the overall stability of pavements and the economy. It designates that extensive knowledge of the aggregate and the soil properties is requisite as it affects the pavement's, performance and strength, also it majorly affects the binding material which improves these pavement characteristics. (Amu et al. 2011).

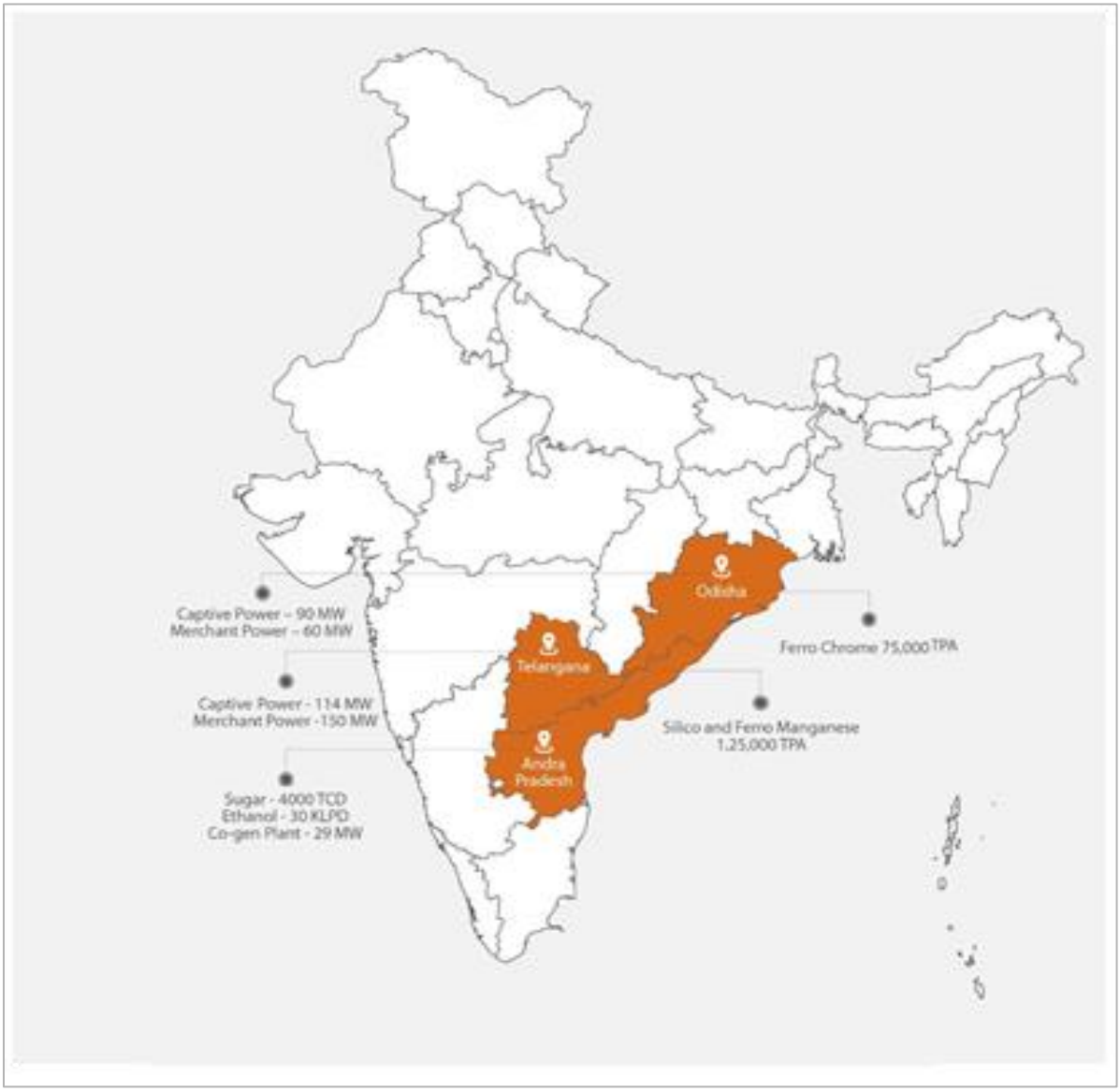

Fig 1.1: Domestic operations – Facilities chart on Indian map

1.2 Recycling Options

Pavement recycling, in which recycled asphalt pavement (RAP) components are utilized to produce new pavement. It has several advantages since its introduction into the realm of pavement repair and maintenance.

RAP is a pre-existing asphalt pavement material that was removed during pavement resurfacing, rehabilitation, or rebuilding. RAP includes asphalt binder and aggregate, and they are valuable long after their service life has expired. As urban life expands, so does the building, repair, and maintenance of pavements to boost the growth, which has resulted into the disposal of a vast amount of RAP materials. The majority of which have been utilised to manufacture

hot mix asphalt (HMA). According to various sources, up to 80% of recycled materials have been utilized in the building of pavements, and 100% can be used by completing the material cycle and allowing RAP to be used in the same high-value application as conventional asphalt (Zaumanis et al. 2014).

In the cold recycling process, RAP material is used as an aggregate. It is typical practise to mill or remove old, existing pavement before breaking it up into pieces of various sizes of aggregate and mixing it along with emulsified and foamed bitumen. In flexible pavement repair, this mix is often used as a stabilised base course. While cold recycling entails adding the foamed bitumen or emulsion to the aggregates at room temperature before mixing. In contrast, in the current study, the temperatures of the aggregates were raised by heating them in an oven and then adding foam bitumen prior to mixing. By briefly heating the aggregates and lowering the bitumen temperature to form the foam (this process decreases the viscosity of a bitumen), it "spot welds" the aggregates, boosting the workability of the mix. This method improves the mix's shear strength, indirect tensile strength, and moisture susceptibility.

1.3 Scope and Objectives

In this study, Water Granulated (WG) ferrochrome slag is collected from Raw Mat Plant, Cuttack, Odisha. The objective of this assignment is to explore feasibility of using water granulated ferrochrome slag in place of natural aggregate used for road construction through laboratory experiments. Prime goal of current research work is to establish feasibility of using water granular slag in bitumen base stabilized layers of road construction.
The objectives and scope of the study are as follows:

- Study of ferrochrome slag in granular layer and bituminous in companion on to natural aggregate.
- Characterization of granular and bituminous mixes as per MoRTH 2013 specification.
- Toxicity characteristic leaching procedure (TCLP) study of the ferrochrome slag.
- Studies on foam bitumen in relation to binder temperature and content of water using the Expansion Ratio (EL) and Half-Life (HL)
- Determination of mixing moisture content and optimum foam binder content for mix design with the increase in temperature of aggregates and RAP material at different RAP material percentages.
- Determination of bitumen emulsion characteristics.
- Calculating the optimum fluid and emulsion concentrations.

- XRD test to find out the different phases in materials

1.4 Summary

The chapter discusses the gap area with the reason of motivation as well as the scope of the entire research work. It also describes the need and importance of the present research work on the use of FBM and EBM and also the methodology adopted to conclude the research work.

CHAPTER 2

LITERATURE REVIEW

The most popular type of pavement for building roads and highways around the world is flexible pavement. For a substance used in paving, there are various standards and laws in every nation. All recycled and salvaged materials being used construction must go through a similar property test to that of regular materials. The end product made from waste material should also meet the minimal standards for strength, durability, stability, longevity, and other pertinent qualities (used whether as a some or all substitution of virgin material). Resources are the most exploited resource in road building comparable to other civil engineering fields. Massive amounts of natural resources, gravel, rocks, and sand are constructed into kilometres of newly-made roads or in the rehabilitation of old highways.

A country's socio-demographic growth of extensive road net is critical. Number of materials necessary for the building is usually rather significant. Soil is the most affordable and accessible resource that man uses for a variety of construction-related objectives. Due to a lack of acceptable graded soil on the building site, scientists and engineers have been forced to use waste items, which either harm the environment or cause disposal issues. Thus, it is imperative to pay close attention towards utilization of industrial solid wastes including fly ash, steel wastes/slag, granular blast furnace slag (gbfs), cement kiln dust, etc. in geotechnical construction (Singh et al. 2008).

One of the key elements of flexible pavement structure that influences stresses and strains throughout the structure is the granular material layer. Two key failure modes in the flexible pavement consume a significant influence on rutting and asphalt concrete fatigue (Andrew et al. 2004).

For many years, industrial wastes and by-products have been investigated by way of green building materials. Some industrial wastes and products, such as fly ash, crushed ggbfs and silica fume, have already been standardised as green construction materials in numerous codes of practice. However, ferrochrome slag (FCS) is one of the by-products that has yet to be standardised, notably in the concrete manufacturing process. (Fares et al. 2021). In general, this chapter discusses many studies on the efficient use of ferrochrome slag in various applications. Since 2001, numerous initiatives have been launched to characterise and use ferrochrome slag for various engineering purposes.

2.1 Characteristics of Ferrochrome Slag

Chromite and iron oxides are used as raw materials in the manufacturing of ferrochrome. The chromite is utilised as a charge in the furnace in the form of irregular ores or granular concentrated that need to be core component. Prior to being sintered in the furnace at 1400°C, the granular concentrate is treated and shaped into pellets in the sintering plant. The Ferrochrome slag is an excellent material for construction applications because it possesses excellent physical characteristics that are comparable to those of natural aggregates. FCS is created during process of extracting ferrochrome (FC) from natural materials. FCS has lately developed the interest of researchers as a potential green and sustainable construction material, notably as an aggregate, because to its chemical composition, physical nature, and mechanical capabilities (Fares et al. 2021).

A by-product of producing high carbon ferrochromium amalgam is ferrochrome slag. Ferrochrome is composed mostly of $Si0_2$, $Al0_3$, and MgO in various proportions, but also contains CaO, chromium, and iron oxides, with considerable amounts of chromium in the form of PAC an entrained alloy (Hayes 2004).

To achieve the correct slag composition, fluxing elements such as quartz, lime, olivine, bauxite, dolomite, corundum, and limestone are used. Slag and ferrochrome alloy are melted down products of melting furnaces. Depending on the input materials, the output ranges from 1.1 to 1.6 t/t ferrochrome. The chemical composition of ferrochrome slag has been given in Table 2.1 as suggested by Kauppi and Keppa (2007).

Table 2.1: Chemical composition of ferrochrome slag

Elements	**Al_2O_3**	**SiO_2**	**MgO**	**CaO**	**Cr_2O_3**	**FeO**
Kauppi and Keppa (2007) (% by Weight)	16-43	13-39	10-29	1-6	6-18	3-11

Ferrochrome slag is made up of silica, aluminium, iron, calcium, chromium, and magnesium oxides. The values may be seen to be comparable to those published in the works (Kauppi and Keppa, 2007). It should be highlighted that elevated levels of magnesium oxide (MgO) are

cause for worry as they can lead to enlargement/expansion. The physical properties of ferrochrome slag has been given in Table 2.2.

Table 2.2: Physical properties of ferrochrome slag (Das et al. 2017).

Property	Ferrochrome Slag
Specific Gravity (g/cm^3)	2.84
Water Absorption (%)	0.63
Flakiness Index (%)	9.83
Elongation Index (%)	10.50
Impact Value (%)	11.00
Crushing Value (%)	17.89
Abrasion Resistance (%)	18.19

Both fine grain and coarse grain ferrochrome slag have pH values of 9.79 and 9.88, respectively. These samples therefore interact with alkali's present in atmosphere, and higher pH value is caused by the large MgO value (Yudhbir and Honjo. 1991).

According to reports, the slag's structure is primarily polycrystalline and partially glassy. Significant phases include forsterite, Mg-Al-silicate, Fe-Mg-Cr-Al-spinels, metal alloys and amorphous glass. Chemically, ferrochrome slag products are quite stable. Thus, the PXRD test conducted in raw ferrochrome slag may be validated, as indicated in the figure below (Kauppi et al., 2007).

Singh et al. (2014), investigated the phases present, by analysing the sample using XRD. The Bruker D8 Advance having Cu K (= 1.54056 A°) with 2θ values of 5° and 80° at a scan rate of 3°/min was used. Powder X-ray diffraction patterns of raw ferrochrome slag were observed. Crystallite phase analysis of raw ferrochrome slag was shown in Fig. 2.1.

The phases found in raw FCS slag were Spinel (MgAl2O4) (JCPDS No.-01-085-1798), Entatite (MgSiO3) (JCPDS No.-00-007-0216), and Forterite (Mg2(SiO4)) (JCPDS No.-00-

001-1290), whereas Spinel was as the major phase. The individual XRD patterns was compared with the JCPDS-recommended library/database, phase identification analysis was performed (PDF-2 database 2003).

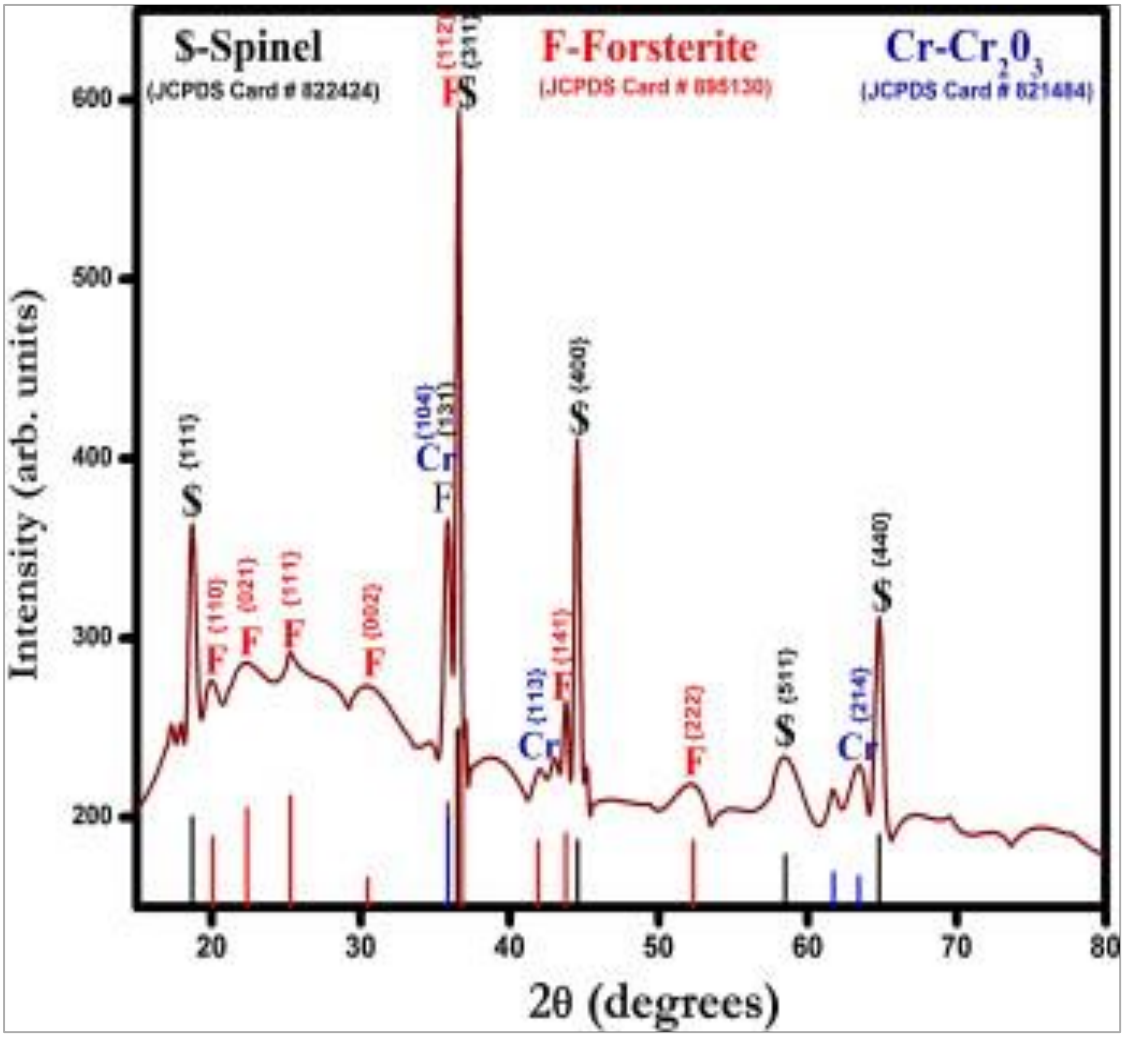

Fig 2.1: X-ray diffraction pattern of ferrochrome slag (Singh et al. 2014)

FCS has been investigated for use in at least 3 major fields: ceramic and refractory industries, hazardous hexavalent chromium treatments, and civil engineering applications. Utilization of FCS in civil engineering has been investigated for a range of applications, including building and road construction as shown in Fig. 2.2 (Karhu et al. 2020).

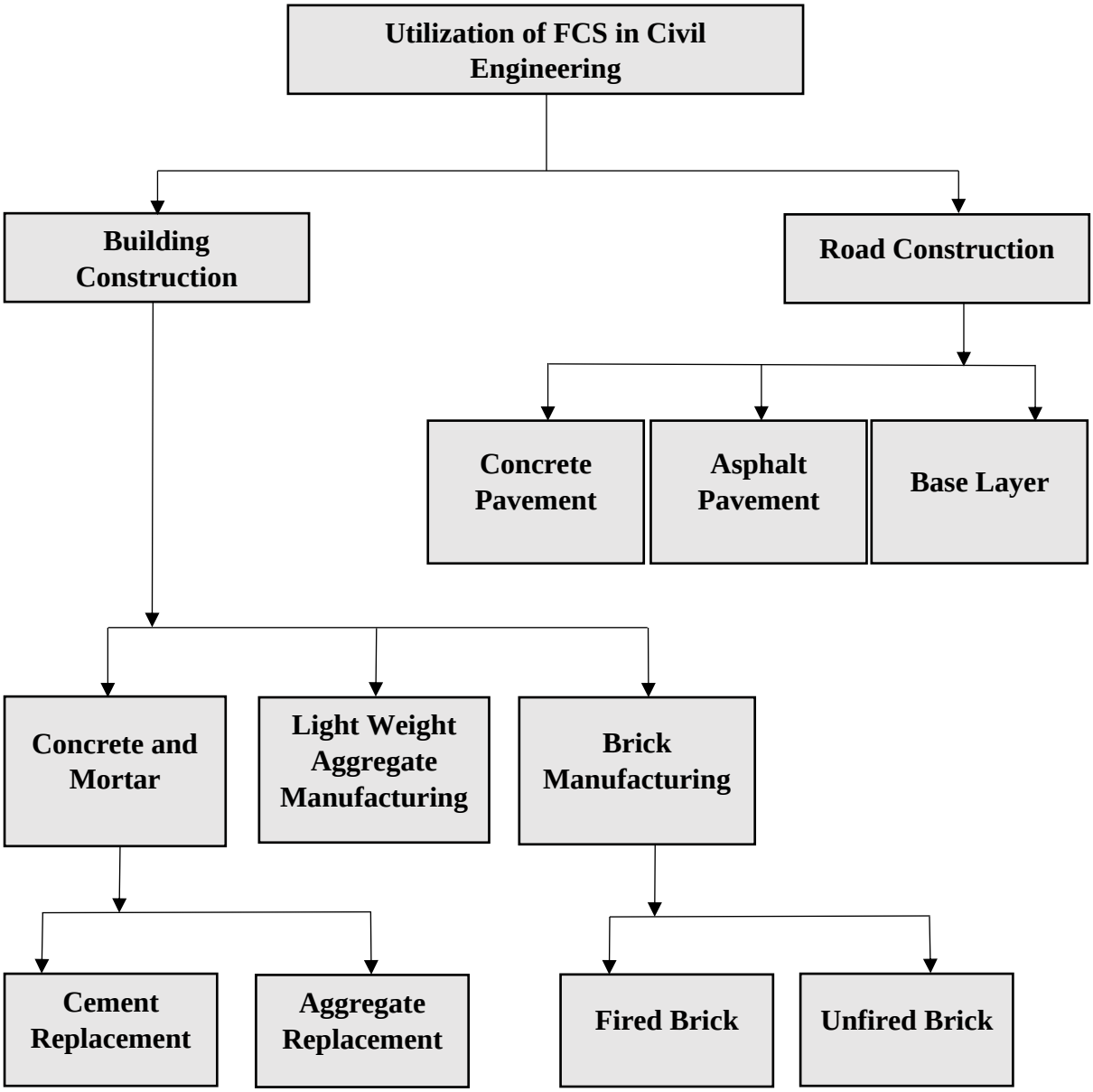

Fig 2.2: Utilization of FCS in civil engineering applications (Karhu et al. 2020)

Determination of the engineering properties of ferrochrome slag is necessary for the feasibility study in pavement application. The main goal of the experimental programme was to carefully examine the engineering characteristics in order to study potential applications in various pavement layers.

When ferrochrome slag is crushed and screened, its engineering properties are to be investigated to find out whether it can be used in place of natural aggregates. In order to use ferrochrome slag in place of stone aggregates, it is required to be hard, durable and tough. Hardness is a parameter to measure resistance of road aggregate to crushing and abrasion. Rigidity of aggregate ensures safety against crushing due to load coming on pavement and against the abrasive action of the wheels on the surface. Toughness of road stones is the

property which enables them to resist any fracture when subjected to impact due to moving vehicles. Apart from this the aggregate must provide a good resistance to skidding and resist weathering action and be not prone to polishing.

2.2 Usability of Ferrochrome Slag in Road Construction

In comparison to other fields of civil engineering, road construction makes the best use of natural resources. Large amounts of natural resources, such as gravel, rocks, and sand, are used to create kilometres of new roads or to rehabilitate deteriorating highways. At the same time, the notion of sustainable development necessitates more effective waste management and environmental protection (Ivana et al. 2008).

It is crucial to assess the quality of the aggregates being used in road building in terms of physical as well as mechanical characteristics. It's critical that the aggregates operate well in a road setting. In the Ferro Chrome, Slag aggregates are evaluated to fulfil the basic requirements of natural aggregates for pavement application as stipulated in the Ministry of Road Transport & Highway Specifications for Road and Bridge Work (5th Revision).

Led to a significant progress rate of population, progress of science & infrastructure, and the expansion of acquisitiveness, yields of industrial by-products and by-products have increased rapidly in recent decades. Due to growing environmental challenges, waste and pollution reduction. Many areas allowed waste resources such as ferrochrome slag as substitute materials in bridges, road constructions, and road pavement. Slag is utilized businesswise in road construction industries in countries like India, South Africa, Norway, China, Sweden, the United States & East Europe. This material is utilized in road construction as aggregates in pavement construction, as well as engineered fill (Al-Jabri, K. S.,2018).

Slag is extensively utilised in the road construction industry as aggregate in rigid and flexible pavements, as a source material in base and sub-base films and hot asphalt mixtures. Slags are an excellent material for creating roads because of their amazing characteristics, including volumetric stability, information driven mass, good abrasion resistance, and crushability (Zeli et al. 2005).

Flexible pavements cover over 95 percent of the world's roads. As indicated in Fig. 2.3 below, it is made up of tetrad layers: subgrade, subbase, base, and surface course (Mulungye et al. 2007).

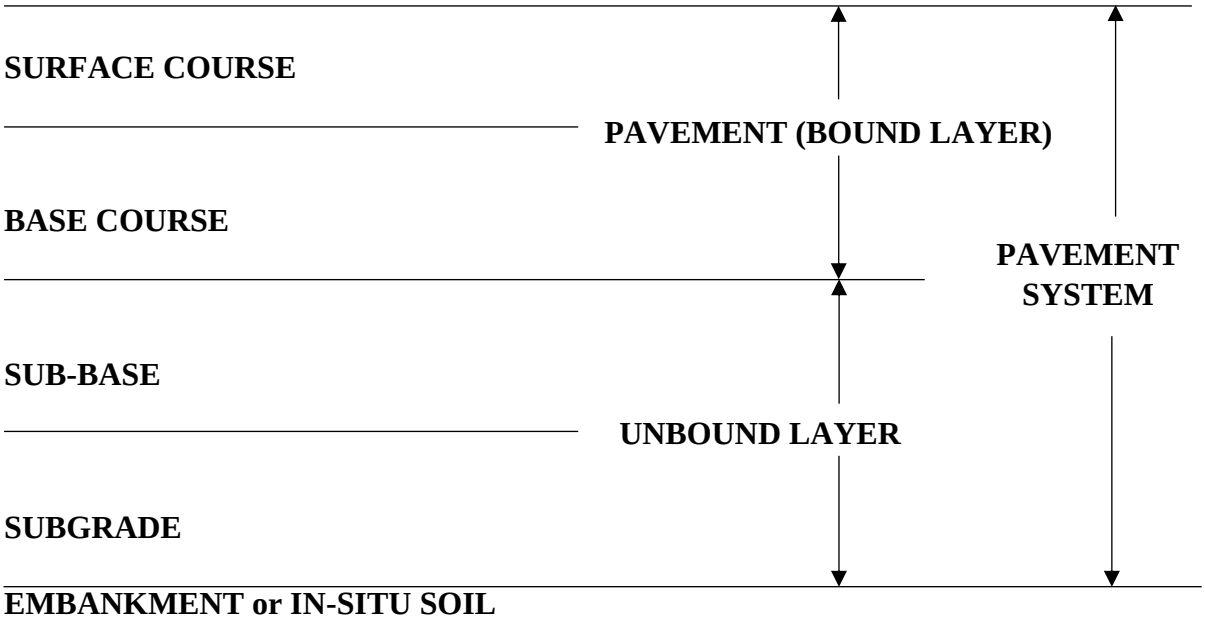

Fig 2.3: Pavement system

The natural soil on which the other levels are constructed is the sub-grade. It is frequently found that the current subgrade is fragile or expansive, meaning that a little change in the moisture state results in a large volume change in a short amount of time. Circumstances where, the sub-grade is altered with the addition of particular chemicals. Subbase is the name given to this modified sub-grade. The base course, a load-bearing layer made up of premium aggregates in a range of sizes, sits above the sub-base. The top layer of the surface course is made up of aggregates, grits, filler, and binder. Because layer is close touch with traffic, better quality materials are required (Dakshanamurthy et al. 2001).

The outcomes of research on using ferrochromium slag as aggregate in granular layering of flexible pavements are discussed. According to the findings, air-cooled ferrochromium slag has physical and mechanical properties that are on par with or better than among aggregates. Because of this, SiFeCr and ferrochrome slag have the ability to be used in applications that typically call for destroyed aggregate materials as pavement foundation layer materials (Yilmaz et al. 2009).

2.2.1 FCS used with cement

As a base layer material for roads, blends of ordinary Portland cement (OPC) and ferrochrome slag, can be utilised in certain proportions. At 3 percent and greater PC levels, ferrochrome slag and cement combinations fulfil the requisite compressive strength qualities of standards. In vibratory compacted specimens, this effect results in greater air spaces and reduced density.

Grinding and sieving operations of ferrochrome slag must also be prioritized in the material's utilization as an aggregate (Yilmaz et al. 2013).

When it comes to the generation of ferrochrome slag, its utility is restricted. To some extent, they are employed in civil engineering and highway building. The usage of ferrochrome slag can minimize the need for natural aggregates while also having a lower environmental effect. Although waste slag has remarkable qualities, its use has been restricted due to the risk of releasing harmful chromium compounds into the environment. In this study, the ability of ferrochrome slag to partially or entirely substitute conventional coarse aggregate in M50 Grade concrete is assessed (Niemela et al. 2007).

Petrographic analysis was used to investigate the physicochemical characteristics of low-carbon ferrochrome slags. Ferrosilicon-aluminium was used as a solvent to produce ferrochrome. The occurrence of helenite in various forms is confirmed by a petrographic analysis of slags. Melilite, larnite, and vitreous phase discrete impregnations are distinct from one another, indicating that further processing may be used to isolate them from the helenite phase (Konarbaeva et al. 2010)

The concretes with the highest splitting strengths were those incorporating activation blast furnace slag and ferrochrome aggregate as shown in fig. 2.4. Except 0.45 w/b (water/binder) ratio, the unbearable strengths of "all-waste concrete" remained higher than those of concretes incorporating Portland cement and FCS aggregate. Concretes made from Portland cement and waste ferrochromium slag aggregate have inferior chloride permeability than those made from limestone. However, at high water/binder ratios, the chloride porousness of combinations including alkali-activated blast furnace slag was significantly greater (Salihpasaoglu et al. 2020).

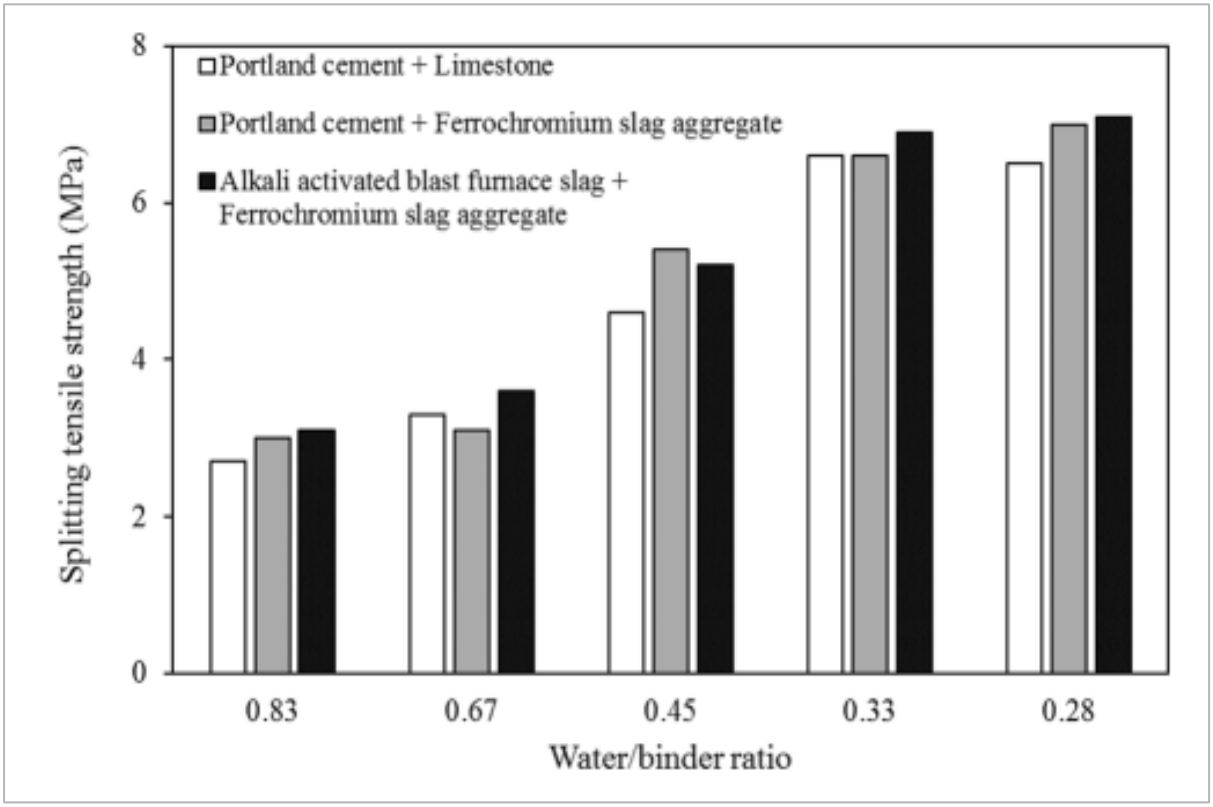

Fig 2.4: Splitting tensile strength

2.2.2 Used as geopolymer

When compared to Portland cement binder, geopolymer manufacturing is less damaging to the environment and produces products that are more robust. Powder of alumino-silicate could be utilized for production of geopolymer. As a result, several organically produced and synthetic solids are being evaluated for use in the synthesis of geopolymers. Additionally, it has the capacity to immobilise large and dangerous components inside the building and valorize industrial waste materials (Part et al. 2015; Jaarsveld et al. 1999).

Geopolymer binder is a block of cement made by combining aluminosilicate material with alkaline or phosphoric acid solutions. When compared to GPC with natural coarse aggregate, this aggregate produced acceptable strengths. Lightweight GPC with a recycled lightweight block was demonstrated as an effective building material for wall and partition walls (Davidovits et al. 1991).

In GPC, ferrochrome slag (FeCr) is used as coarse aggregate. The waste product generated by the stainless-steel production sector is ferrochrome slag (FS). This slag is created at a temperature of much more over 1600 degrees celsius as the liquid. In India, roughly 3.36 MT of FS is produced from 118 units out of a total of 229 furnaces (C.N. Harman, 2007).

Other mechanical parameters of the FSGPC, such as split tensile strength and flexural strength, improve with proportion of FS up to 30% when compared to the comparable value of controlled GPC. However, the strengths diminish by 35% and 40% at FS content (Jena et al. 2019).

The structural rearrangement of the mixture during polymerization is confirmed by XRD analysis, which shows a decrease in the FCS peak's crystalline peak intensity and a modification in the amorphous hump's composition (Nath 2018).

FCS can be utilised as the starter for geopolymer production. Geopolymer's quality is determined by the stimulating solutions, KOH content, and L/S ratio. When compared to silicate activation, aluminate activation of the ferrochrome slag provides a more competent geopolymer.

Geopolymerisation reduces metal leachability through the probable inclusion of metals in geopolymer's CSH/CASH phases, which are also responsible for the increased UCS in synthesised geopolymers. The best curing period for GPA, GPS, and pure ferrochrome is 28 days at ambient temperature.

The GPA may be utilised for light traffic pavement construction, resulting in high slag usage. When compared to GPS and pure ferrochrome slag geopolymers, the GPA's potential for environmental degradation with prolonged usage is negligible.

Mechanical strength of firm geopolymer paste specimen was investigated. Compressive strength reduces as FCS is replaced. Microstructural and calorimetric investigations support this observation even more.

After 28 days, a sample of 100% FCS that has been cured yields the maximum strength as shown in Fig. 2.5. This is caused by FCS's higher reactive element, which hydrates more quickly and produces additional Ca-carrying gel in addition to the geopolymer's sodium incorporating alumino-silicate hydrated (N-A-S-H) gel. (Gao et al. 2015; Djobo et al. 2016)

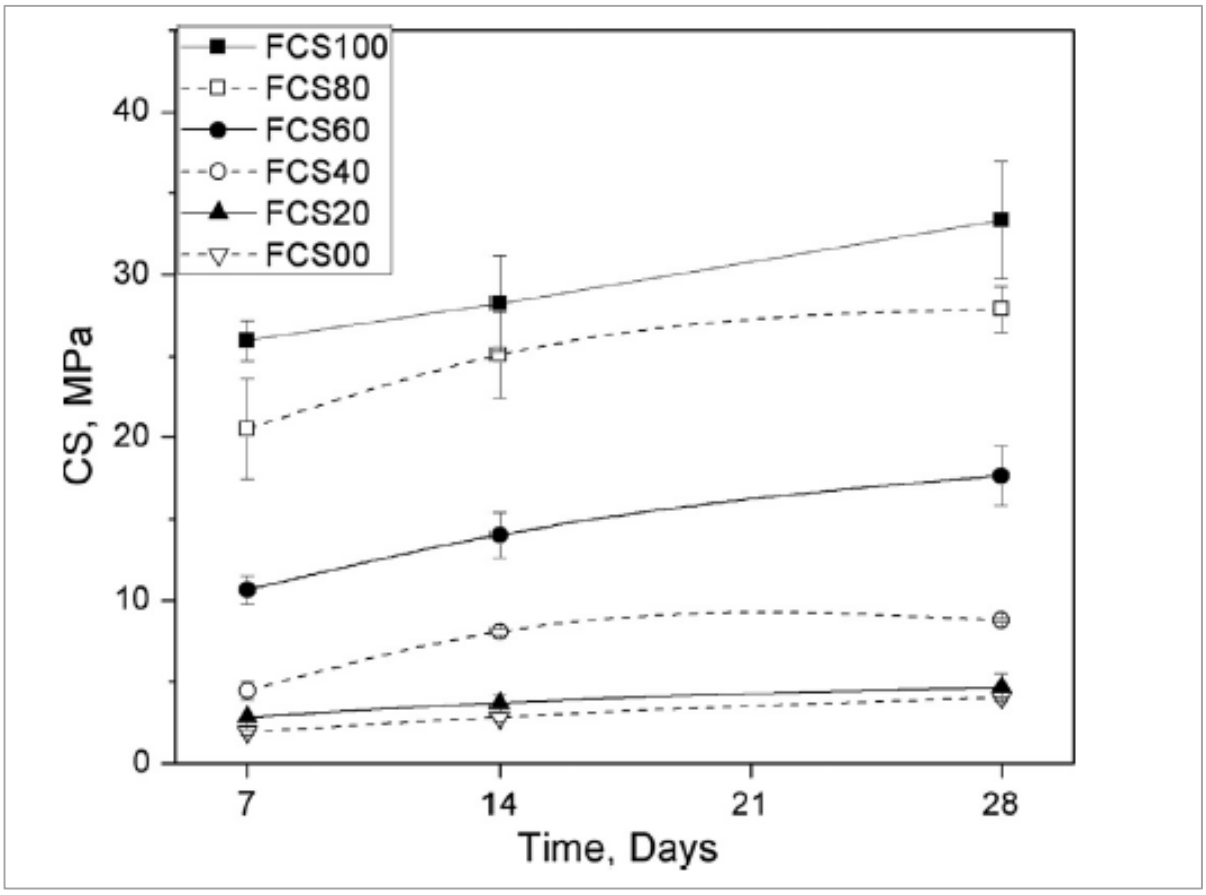

Fig 2.5: Compressive strength of geopolymer-cement paste specimens.

2.3 Use of Ferrochrome slag in Bitumen Mix

Literature survey reveals good performance of ferrochrome slag in bituminous mixtures in other countries. Both laboratory and field studies available in published literature, showed that ferrochrome slag incorporated bituminous mixes has equivalent mechanical properties than bituminous mixes produced from natural aggregates.

Hot bituminous mix (HBM) being used in flexible pavements contains aggregate in excess of 90% by weight of the mixture. These pavements demand a substantial quantity of aggregate resources for development and upkeep. The aggregate resource management doesn't really appear to be in accordance with country's sustainable building plan, which calls for environmental protection and a reduction in natural resource use.

Because of the high demand for aggregates, numerous mountains are being mined, resulting in pollution and environmental degradation. The utilisation of waste materials will be definitely lower the demand of natural resources. Prior to utilise waste materials on a wide scale,

engineering, environmental, and economic considerations must be addressed (Karasahin et al. 2007).

Ferrochrome slag is employed by way of aggregate in the hot bituminous mix, and tests showed that it enhances the mechanical qualities of hot bituminous mix. There are various probable uses for ferrochrome slag:

1) Included in hot mix asphalt and as aggregate in concrete.

2) Sub-base or base material.

3) Landfill & embankment material.

Bitumen's rheological behaviour is a very complicated phenomenon that varies from fully viscous to elastic according on loading duration and temperature. Bitumen, being a visco-elastic substance, has a significant impact on many elements of road performance. To prevent cracking of pavement at low temperatures and permanent deformation at high temperatures, bituminous binders must be stiff. Numerous studies conducted on incorporation of polymer modified bitumen to generate flexible pavement at low temperatures and stiff pavement at high temperatures (Yilmaz et al. 2008).

The aggregates form a skeleton or matrix in a bituminous mixture which provides the stiffness to the mix in the presence of a suitable binder, thus aggregates have to be tested properly before the preparation of bituminous mixes. Before use, the aggregates were tested as per relevant Indian Standards to check whether they meet the requirements specified as MoRTH, The natural aggregates are replaced by the water granulated and air-cooled ferrochrome slag in bituminous mix, so it is important to confirm the various requirements of the slag as aggregate for bituminous mixes. Slag can be used as aggregates replacing natural stone aggregates in bituminous mixes. To evaluate feasibility of usage in bituminous mixes, ‘Bituminous Concrete (BC)’ and ‘Cold Mix Bituminous Maccadam (CMBM)’ were selected. BC is used as wearing surface for high traffic volume roads like National Highways and it is constructed as per MoRTH Specification Clause 507. Cold bituminous macadam and cold mix seal surfacing samples using slag are also prepared and evaluated as per IRC Code (IRC SP: 100-2014).

Hot bituminous mixtures are utilised to create flexible pavements, along with ferrochromium slag and strong, uncomplicated styrene-modified binders. According to test results, ferrochromium slag did not perform well in terms of stability and stiffness when used as a full

aggregate. However, the ferrochromium slag-only combination showed excellent moisture resistance. (Kok et al. 2009).

2.4 Economic Analysis

Sweden is listed among the top manufacturers of ferrochrome slag in Europe (Lind et al. 2000). Physical testing showed that ferrochrome slag is particularly well suited for application as a material for road construction, consequently many roads made of FCS were finished in year 1994. Even while leaching under normal circumstances is extremely low. Laboratory leaching experiments on FCS demonstrated that significant chromium content is found, ranging from 1 to 3 percent chromium, nickel, zinc, and other elements all showed very little leaching potential, with exception of potassium (K), which showed a theoretical leaching value of roughly 16 percent. There was some uncertainty, nevertheless, as to how well these laboratory tests represented what actually happened in the field when acid rain and biological activity were present.

In the ferrochrome smelting process, a large amount of slag (slag: alloy = 1.1to 1.5:1) is created, and the entire volume cannot be used locally. Furthermore, metallurgical waste such as ferrochromium slag is typically generated in distant places where the availability of new materials is low. Transporting this raw material to other areas is therefore unprofitable in light of the available natural resources, and only a tiny amount of rubbish is utilised. The resulting product or process may occasionally become unprofitable after additional ferrochromium slag treatment and modification for other usage. For use in ceramics and refractories, ferrochromium slag must undergo a number of processing steps, including grinding, milling, shaping, and high-temperature firing. Because of this, the techno-economics of such a process or product relative to current competitor's affects how widely it is used (Sahu et al. 2016)

Developed nations have enforced the mandatory laws to utilise effective waste management techniques. Future ferrochrome industry viability will be reliant on the cost-effective use of metallurgical waste by-products from a societal and environmental perspective. There is still room for cost-effective and environmentally beneficial ferrochromium slag solutions, according to the examination of its application.

2.5 Environment Impact

Mankind is growing increasingly worried about the environmental consequences of his actions. ferrochrome manufacturers are no exception, especially given the impact of hexavalent chromium leakage into the environment, water, and soil. In addition to endangering the environment. Cr (VI) endangers human and animal life. However, if correctly handled, ferrochrome manufacturing has no negative consequences on either man or the environment. Nonetheless, it is vital to be mindful of the dangers and hazards inherent in every industrial process, and ferrochrome manufacturing is no different (Gericke 1995). The ferrochrome slag's chemical composition contains three key constituents: aluminium (Al), silicon (Si) and manganese (Mg). These components in oxide form alone account for 83 percent of ferrochrome slag (Larsson 1995).

Chromium (Cr) level among the heavy metals is notably higher (3%), which is 1000 times the concentration in area's natural soils. Nearly a hundred times more Ni, Co, Sn, and W are present than in the soil's normal state. Because of its great technical material qualities, slag is appealing as a construction material. However, environmental issues have been expressed concerning heavy metal levels and leachability, particularly chromium (Eguchi et al. 2007).

The slag is generally disposed of in landfills, which causes environmental issues due to the use of potentially agricultural land and metal seeping into the environment. ferrochrome slag is a very well polluter with high quantities of hazardous metals. (Falayi 2019)

Most elements have limited leachability from the FCS slag when tested with saline saltwater and PH adjusted water. Additionally, it was asserted that the migration of nanoparticles from the ferrochrome slag to the subsurface during road building was restricted and that, with the exception of potassium, the leaching of the elements tested from FCS slag into groundwater was minimal (Lind 2001).

The ferrochrome slag structures in the environment could be regarded as a geochemical anomaly. Geochemical Cr-anomalies can also be found in the environment, such as in ultramafic rocks with Cr concentrations between 1000 and 3000 mg/kg.

On samples gathered from diverse places, three tests (ground water sampling, plant analysis, and soil sampling) was carried out. The soil samples were treated through a multi-acid digestion, pulverised in an agate mill, and then analysed with inductively coupled plasma spectrometer. After being examined, the nearby plants' roots were cleaned with purified water

and allowed to dry for two months. Dried roots that had been manually ground up were heated to 100 °C and digested in HNO_3 acid. The identical samples were decanted, diluted, and their composition was evaluated after 5 hours of sedimentation. Groundwater samples were taken three times throughout a year. We measured the temperature, pH, and redox potential. After that, the samples were filtered and checked for metal contamination.

The conclusions were that:

• Low levels of tiny particles from the slag migrate to the soil.

• Even though large uptake of chromium, there is only a little amount of leaching into the groundwater (Nicholls. 2004).

2.6 Research Gap

Based on extensive literature review, followings are identified research gaps:
a) The limited studies were reported to use FCS slag in the construction of road.
b) Limited studies were also reported FCS slag in base stabilised layer.
c) A few literatures reported utilizing two binder system for road construction.

CHAPTER 3

MATERIALS & METHODOLOGY

The material used for the inquiry, as well as its processing and characterization, are covered in this chapter. Generally, the Pavement recycling purpose is to retrieve the overall properties of reclaimed asphalt pavement (RAP) mix without coming to terms with the performance. Foam Bitumen mix (FBM) contains RAP material, aggregate, bitumen binder (VG-10) and fills. Thus this chapter presents the testing process of recycling that necessitates mixing of the RAP material and additive material in suitable proportion, which is used in research and results eventually obtained. Physical testing of materials used was required to ensure their suitability for use in bituminous layers. This chapter describes the various tests performed on aggregates, emulsions, foam bitumen etc.

3.1 Material Characteristics

3.1.1 Aggregates selection

The meta-quartzite aggregate was utilized in this work, which was sourced of a quarry near New Delhi (NCR), India. Aggregates of 10mm and 20 mm size along with stone dust (Photo 3.1) were tested for volumetric properties, shape and strength. The tests were carried out as per relevant Indian standards and ASTM specifications.

3.1.1.1 Testing of Aggregates

In the presence of a suitable binder, the aggregates form a skeleton or matrix that provides stiffness to the mix. As a result, aggregates must be tested to ensure their suitability for use in bituminous mixes. Table 3.1 shows results of aggregate testing, as well as the specifications of aggregate properties provided by MoRTH (2013). The results show that the aggregates met all of the requisite criteria as per specifications. The aggregates were sieved to determine particle size distribution as given in Table 3.2. The aggregate impact test was conducted to determine appropriateness of aggregate against load impact breaking. The flakiness and elongation test, which is used to measure aggregate shape, was performed in accordance with Indian standards IS:2386 (Part 1). Water absorption and specific gravity tests, which aid in determining aggregate strength, were performed in accordance with Indian standards IS: 2386 (Part III) and IS: 2386 (Part IV), respectively.

(A)

Photo 3.1: View of (A) 10mm and 20mm Size Aggregate (B) Stone Dust

Table 3.1: Test results of physical characteristics of aggregates

Properties Tested	Test Methods	Test Results			MoRTH Specification,2013
		Aggregates		Stone Dust	
		10mm	20mm		
Impact Value	IS 2385 (Part IV)	21%	18%	-	30% Maximum
Combined (EI + FI) Index	IS 2386 (Part I)	29%	28%	-	35% Maximum
Water Absorption	IS 2386 (Part III)	1.0%	0.5%	1.5%	2% Maximum
Specific Gravity	IS 2386 (Part III)	2.76	2.78	2.64	-

Table 3.2: Gradation of aggregates and stone dust

Sieve size (mm)	Percentage Passing			
	10mm	20mm	Stone Dust	MoRTH Limits
45	100.00	100.00	100.00	100
37.5	100.00	100.00	100.00	87-100
26.6	100.00	100.00	100.00	77-100
19	100.00	96.84	100.00	66-99
13.2	99.85	16.44	100.00	67-87
4.75	0.57	0.13	100.00	33-50
2.36	0.22	0.13	93.41	25-47
0.6	0.22	0.13	57.45	12-27
0.3	0.22	0.13	38.52	8-21
0.075	0.22	0.13	10.26	2-9

3.1.2 Virgin Bitumen

The research study used one binder (VG 10) that was acquired directly from the Indian Oil Corporation Ltd. (IOCL) refinery near Delhi and evaluated according to Indian standards (IS:73, 2013). This section goes over the various test methodologies for evaluating binder characteristics.

3.1.2.1 Testing

The characteristics of the bitumen binder were assessed to confirm that they met Indian standards IS: 73, 2013. The viscosity was measured by means of a Brookfield Viscometer at temperatures ranging from 100°C to 180°C, as specified in the ASTM D 4402 specification (Photo 3.2). A U-tube viscometer was used to determine absolute viscosity at 60°C and kinematic viscosity at 135°C according to ASTM D 2171 and ASTM D 2170, respectively (Photo 3.3). The penetration test was achieved at 25°C using a standard penetrometer in accordance with the IS:1203 requirements. The softening point test was carried out in accordance with IS:1205 guidelines.

3.1.2.2 Results

Table 3.3 lists the physical characteristics of the VG 10 binder. Results of the physical property tests reveal that bitumen binders comply with the IS:73, 2013 specification.

Viscosity is a key attribute of bitumen that characterizes the resistance of the binder to flow, and it is important to guarantee that the bitumen binder has the required viscosity for ease of pumping and improved bitumen foaming. As a result, bitumen viscosity is an essential component in the performance of foam bitumen, and optimum foaming temperature is determined by the viscosity value. Figure 3.1 depicts the viscosity variation results as a function of temperature for VG 10. At temperatures of 100°C, 120°C, 135°C, 150°C, 160°C, 180°C, and 200°C, the viscosity of the binders was determined using a rotational viscometer while maintaining a constant speed of 20 RPM. Results showed that there were no observable difference. According to data, there was no discernible difference in the viscosity of binders at higher temperatures, or over 140°C.

Photo 3.2: Brookfield viscometer

Photo 3.3: U-tube viscometer

Table 3.3: Properties of VG 10

Properties	Test Results	Specification Limit (IS:73, 2013)	Test Method
Penetration Test at 25°C,	120	80 (minimum)	IS 1203
Softening point (°C)	45.6	40	IS 1205
Absolute viscosity at 60°C, Poises	872	800-1200	IS 1206 (Part 2)
Kinematic viscosity at 135°C, cSt	275	250 (minimum)	IS 1206 (Part 3)

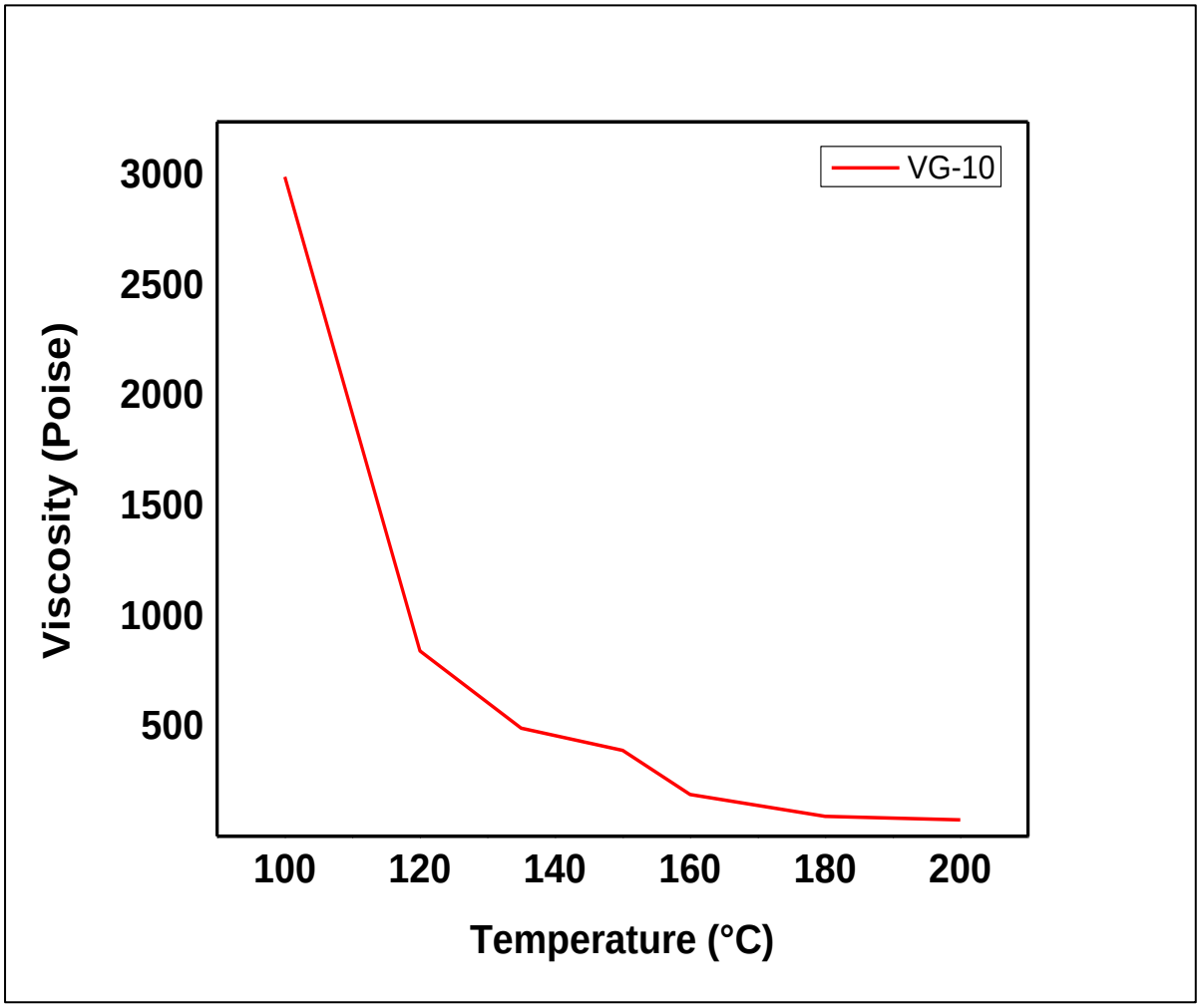

Figure 3.1.: Effect of temperature on viscosity of binder

3.1.3 RAP Material

The RAP material with the nominal size was milled and taken from an existing pavement in New Delhi, India. (Photo 3.4). The material was later manually cleaned by visualization for any potentially harmful material before being tested.

The results indicate that the RAP material gradation was well within the desired limit specified in the Requirements of MoRTH and thus blending with fresh aggregate was performed to allow for use of high RAP content in the mix design.

Photo 3.4: RAP Aggregate

3.1.3.1 Gradation of Washed Aggregates from RAP/ Gradation of RAP

The sieve analysis of the aggregates was performed. The gradation obtained is given in Table 3.4, which showed the deficiency in fine aggregate as shown in Fig. 3.2.

Table 3.4: Gradation of the RAP material

Sieve Size (mm)	Gradation of RAP Material
45	100.00
37.5	100.00
26.6	98.19
19	86.36
13.2	70.96
4.75	35.17
2.36	24.29
0.60	9.62
0.30	4.29
0.075	0.26

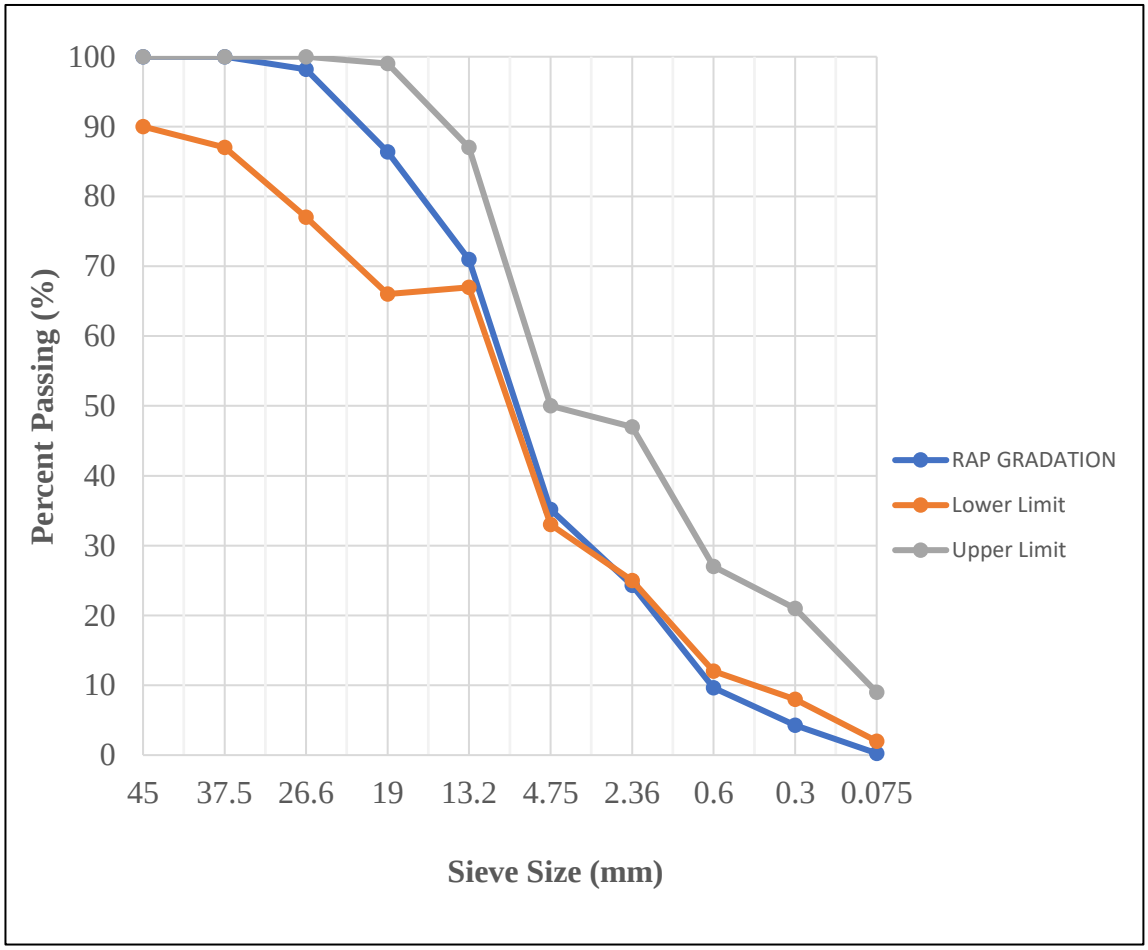

Fig. 3.2: Gradation of the RAP (IRC:37, 2012)

3.1.4 Ferrochrome Slag (FCS)

The water granulated (WG) ferrochrome slag was used in this study. FCS slags were obtained from the dumping site and supplied to CSIR-CRRI by the Raw Mat plant, Cuttak. The chemical composition of ferrochrome slag reported by TATA Steel to CSIR-CRRI is presented in Table 3.5. A view of supplied 10 mm water granulated ferrochrome slag is given in Photo 3.5. In India, MoRTH i.e., Ministry of Road Transport and highways guidelines had defined properties of aggregate to be used in road construction. For application in different layer-specific chemical and physical properties are defined for aggregates. Only those aggregates which confirm these properties are used in road construction.

Table 3.5: Chemical composition of ferrochrome slag

Oxide	Content, %
FeO	2-3 %
MgO	25-28 %
Al2O3	22-25 %
SiO2	28-30 %
Cr2O3	8-15 %
CaO	2-3 %

Photo 3.5: Water granulated ferrochrome slag

3.1.4.1 Gradation of ferrochrome slag

The sieve analysis of the slag was performed. The gradation obtained is given in Table 3.6, which showed the deficiency in fine aggregate as shown in Fig. 3.3.

Table 3.6: Gradation of the ferrochrome slag material

Sieve Size (mm)	Gradation of RAP Material
45	100.00
37.5	100.00
26.6	100.00
19	100.00
13.2	100.00
4.75	79.21
2.36	73.96
0.60	31.98
0.30	11.63
0.075	2.92

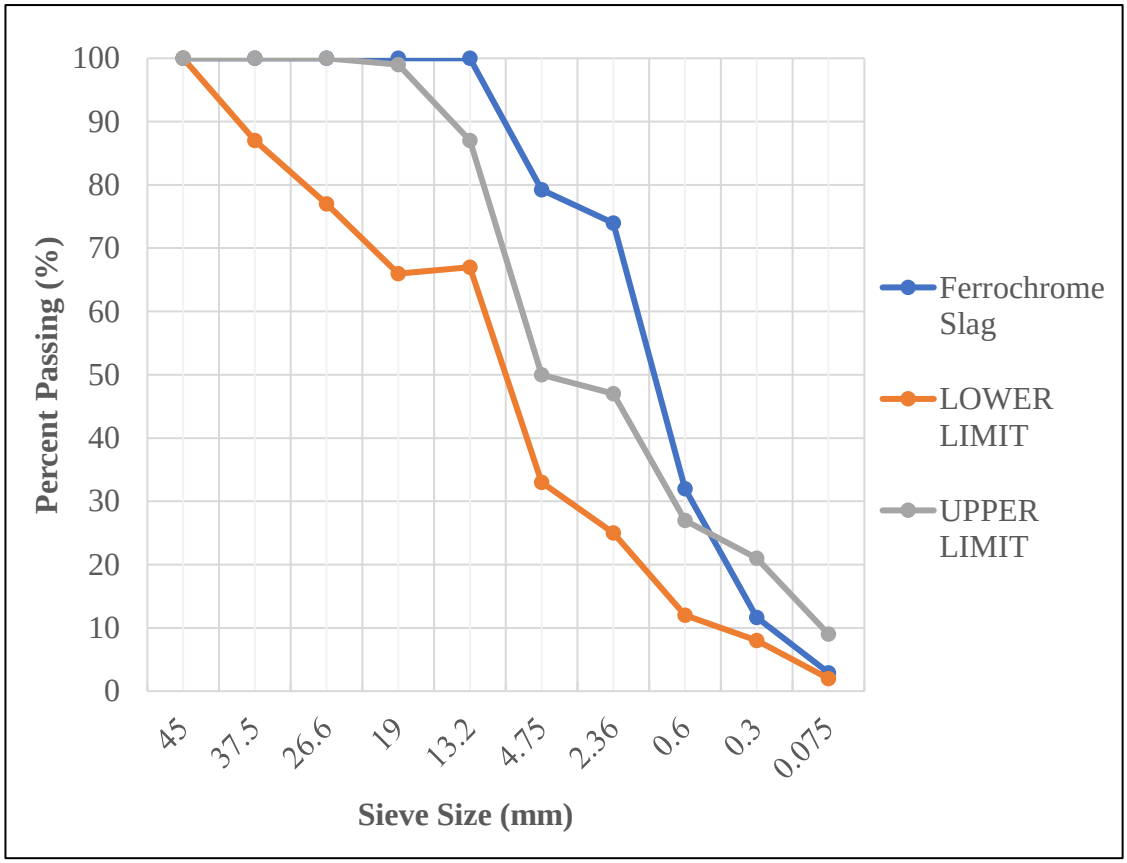

Fig. 3.3: Gradation of the FCS (IRC:37, 2012)

3.1.4.2 Physical properties

Table 3.7 lists mechanical and physical characteristics of ferrochrome slag as measured by CRRI. When compared to natural aggregates, ferrochrome slag has a slightly higher water absorption value. Because slag is properly dried during the creation of hot asphalt mixes, this degree of water absorption is typically not a big concern when utilising ferrochrome slag in asphalt mixtures. However, higher absorption levels could result in a greater demand for bitumen. Ferrochrome slag showed a good affinity with bitumen and retained bitumen coating as per specification limits. The specific gravity of slag is a little higher compared to natural aggregates. Calculating the void content in compressed hot mix asphalt and performing weight-to-volume conversions both benefit from an understanding of aggregate specific gravity.

Table 3.7: Properties of ferrochrome slag

Property Tested	Test Results	MoRTH Specification Limits for aggregates	IS Code
Water Absorption Test	0.92	2% Max (Soundness test required if it is more than 2%)	IS 2386 (Part III)
Specific Gravity	2.89	-	IS 2386 (Part III)
Soundness	3.0	12% Maximum	IS 2386 (Part V)

3.1.4.3 Chemical and leaching properties

Detailed report of Water leaching test, Toxicity characteristic leaching procedure (TCLP) test and total extraction of water granulated, sample is shown in this study. The total compositions of three samples are presented in Table 3.8.

Table 3.8: Total Concentration

Parameters	Test Results	Unit
Iron [as Fe],	2260	mg/kg
Potassium [as K],	122	mg/kg
Sodium [as Na],	45	mg/kg
Manganese [as Mn]	118	mg/kg
Total Chromium [as Cr],	688	mg/kg
Magnesium (as Mg),	6444	mg/kg

In the ferrochrome slag, chromium has already been recognized as the primary harmful element that is likely to contribute to environmental contamination issues during use and disposal. Although there is a sizable quantity of residual chromium in the slag samples, almost all of it is well immobilised in the spinel phase, allowing for very little chromium leakage from the slag samples.

This water leaching test findings show that there is no appreciable chromium leaching. The findings of the toxicity characteristic leach procedure (TCLP) testing are shown in Table 3.9. According to the findings, the chromium concentration in TCLP extracts made from samples of ferrochromium slag is 0.3 mg/l, which complies with US EPA regulations of 5 mg/l. Less than 0.1 mg/l of Cr is present in TCLP extraction from the bitumen-coated, air-cooled sample. It may be determined from results of the TCLP tests that perhaps FCS would not be a potential pollutant. Results indicate that there is no appreciable chromium leaching from normal water.

Table 3.9: TCLP Test results

Parameters	Test Results	Unit
Antimony and anitomony compounds	<0.03	mg/l
Arsenic and arsenic compounds	<0.03	mg/l
Cadmium and cadmium compounds	<0.1	mg/l
Mercury and mercury compounds	<0.01	mg/l
Selenium and selenium compounds	<0.03	mg/l
Total chromium compounds	0.3	mg/l
Cobalt compounds	<0.1	mg/l
Lead and lead compounds	<0.1	mg/l
Molybdenum compounds	<0.1	mg/l
Nickel compounds	<0.1	mg/l

3.1.5 Emulsion

The emulsion grade used in this study is SS-2 which is used to determine the aggregate type and gradation, as well as emulsion's capacity to coat aggregate. In the case of SS-2, the specified tests should be conducted in accordance with IS 8887:2004. As a result, mixes should be made with SS-2 grade Emulsion, which will be used to compare outcomes with mixes containing varied RAP amounts.

Moisture evaporates as the combination dries, and the leftover bitumen from the emulsion begins to perform its twin function of keeping the intermediate together while it's promoting a denser medium. Optimum moisture content would not be enough for entire content of fluid since technique of compaction is subtly different while both moisture and binder are added to mixture *(*Ibrahim. 1998 and Thanaya 2003) while it specifies the region in which entire fluid content lies. Due to these properties, it was necessary to calculate the amount of pre-wetting water suitable for research composition before adding the emulsion. Specimens will be prepared at varying pre-wetting water concentrations while maintaining the emulsion content constant. In most cases, four one-percent increments of water content are sufficient to define the stability curve. Finally, for appropriate coating, employ suggestive tests such as ITS to evaluate pre-wetting water content and overall fluid content.

Binder content in total fluid content must be optimised now that the Total Fluid Content (TFC) has been determined. The emulsion content is changed by keeping the FC constant. Therefore, specimens will be created with emulsion content differences of 1%. Thus best emulsion content is then determined using the ITS test. The Total Fluid Concentration is used to calculate Optimum Emulsion Content (OEC) by estimating trial emulsion and water content (FC).

A RAP bitumen content mix can only be compacted to its highest density when it has the ideal fluid content. To determine the appropriate fluid content, compaction experiments should be performed at various fluid contents. Procedures for mix design have been recommended in Manual 14 The Design and Use of Granular Emulsion Mixes published by the South African Bitumen and Tar Association (SABITA) (7) and TG-2 of South Africa (64) Other methods of mix design are described in the Asphalt Institute's 'Cold Mix Recycling' and 'Asphalt Cold Mix Manual (MS-14).

3.2 Foam Bitumen Characterization

An enclosed space, hot bitumen and cold water combine to create foam bitumen, which swells up to 15-20 times larger than its initial liquid volume under normal air pressure. The foaming process is accompanied by a series of events. In the current study, VG-10 grade bitumen was used, and its physical properties were in accordance with Indian standards. The goal of the bitumen foaming procedure test is to identify the ideal water content needed to produce greatest foam qualities for a particular asphalt binder. Ideal water content is established using the optimum expansion ratio and half-life of both the foamed bitumen. At temperatures exceeding 150°C, good foaming can be accomplished using low viscosity bitumen binders. Water and higher foaming temperatures both boost the expansion ratio thus shortening the half-life. The Wirtgen WLB 10 foaming apparatus was used to conduct the asphalt foaming test. Thus, the following test conditions were used to optimize the foaming water content and bitumen temperature:

- Bitumen: VG-10
- Air pressure: 500 kPa;
- Water pressure: 550 kPa;
- Temperature of asphalt binder: 150°C
- Water content: 2.0-8.0 % at 2.0 % increments.

The flow chart of the optimising process for foaming characteristics used in the current studies is shown in Fig. 3.4.

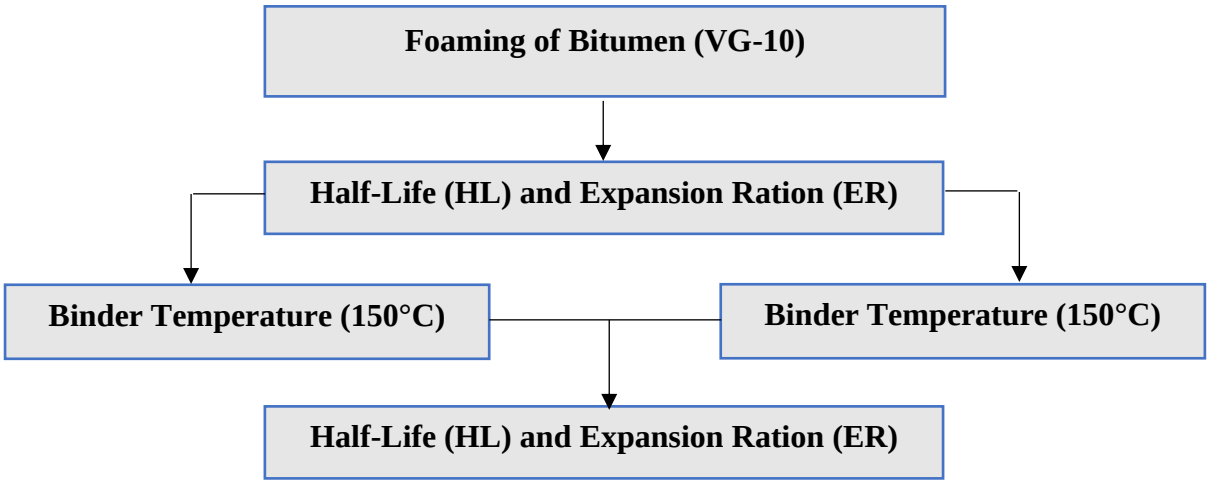

Figure 3.4: Flow chart for optimizing foaming characteristics

3.2.1 Adopted foaming approach and characteristics

The following method was employed to ascertain both bitumen temperature and amount of water addition. The foaming plant is a WLB 10 S plant developed by the Wirtgen group (Photo 3.6). This foaming plant generates foamed bitumen that is very similar to that produced by plants mounted on large recycling machines like the WR 2500. Start by heating bitumen in the kettle of Wirtgen WLB 10S laboratory unit and maintaining proper temperature by pumping the bitumen through the system. Set the timer on the unit to discharge 500g of bitumen after calibrating the discharge rate to 50g/s. Additionally, set water flow metre to necessary water injection rate Pour the foam bitumen together into steel drum that has been heated up and set to spray 500g of bitumen. As immediately as foam discharge stops, start the stopwatch. Using dipstick, determine the highest level of foamed bitumen that is reached in the drum shows in Photo 3.7, supplied with the Wirtgen WLB 10S.

Photo 3.6. Foaming plant (WLB 10S) used for the present study

Photo 3.7: Dipstick supplied with Wirtgen WLB 10 S

This recorded as the maximum volume in order to calculate the expansion ratio. Use the stopwatch to time how long it takes the foam to dissolve to half of its extreme value in seconds, which is known as the half-life of foamed bitumen. Using same set of axes, plot expansion ratio vs half-life at various water injection rates. Ideal water addition is calculated by averaging the two water contents required to satisfy the minimal requirements of ER 8 and HL 6 seconds. (TG-2, 2009 and Wirtgen, 2012).

At 150°C, the relationship between the expansion ratio and half-life was restrained at various water contents ranging as of 2.0 to 8.0 percent, with 2.0 percent increment intervals. The results of the foaming experiment at asphalt temperatures are summarised in Table 3.10. At 150°C and foaming water content of 6.5 percent, as shown in Fig. 3.5, a high expansion ratio is achieved though maintaining a suitable level of half-life. As results, in foaming temperature of 150°C was chosen for the VG-10 asphalt binder, with an optimum foaming water content of 6.5 percent. Later, the design of foamed mixtures takes these temperature and water content conditions into account. According to literature, higher temperature leads to more aging of the bitumen, as well as, consuming more energy. To minimize and prevent this, the lowest temperature at which ER and HL are 6 and 8 respectively was used as the optimum temperature for foaming conditions. It shows that optimum water content needed to produce foam bitumen for the mix is 6.5%. The high-water content is due to existence of higher asphaltene content in

bitumen which means that to achieve a maximum expansion ratio, higher water content is required (Eleyedath et al. 2019).

Table 3.10. Foaming characteristics of VG-10 binder at 150°C

Water Content (%)	Expansion Ratio (ER)	Half-Life (HL)
2%	6	10.19
4%	8	9.5
6%	12	13.09
8%	12	8.59

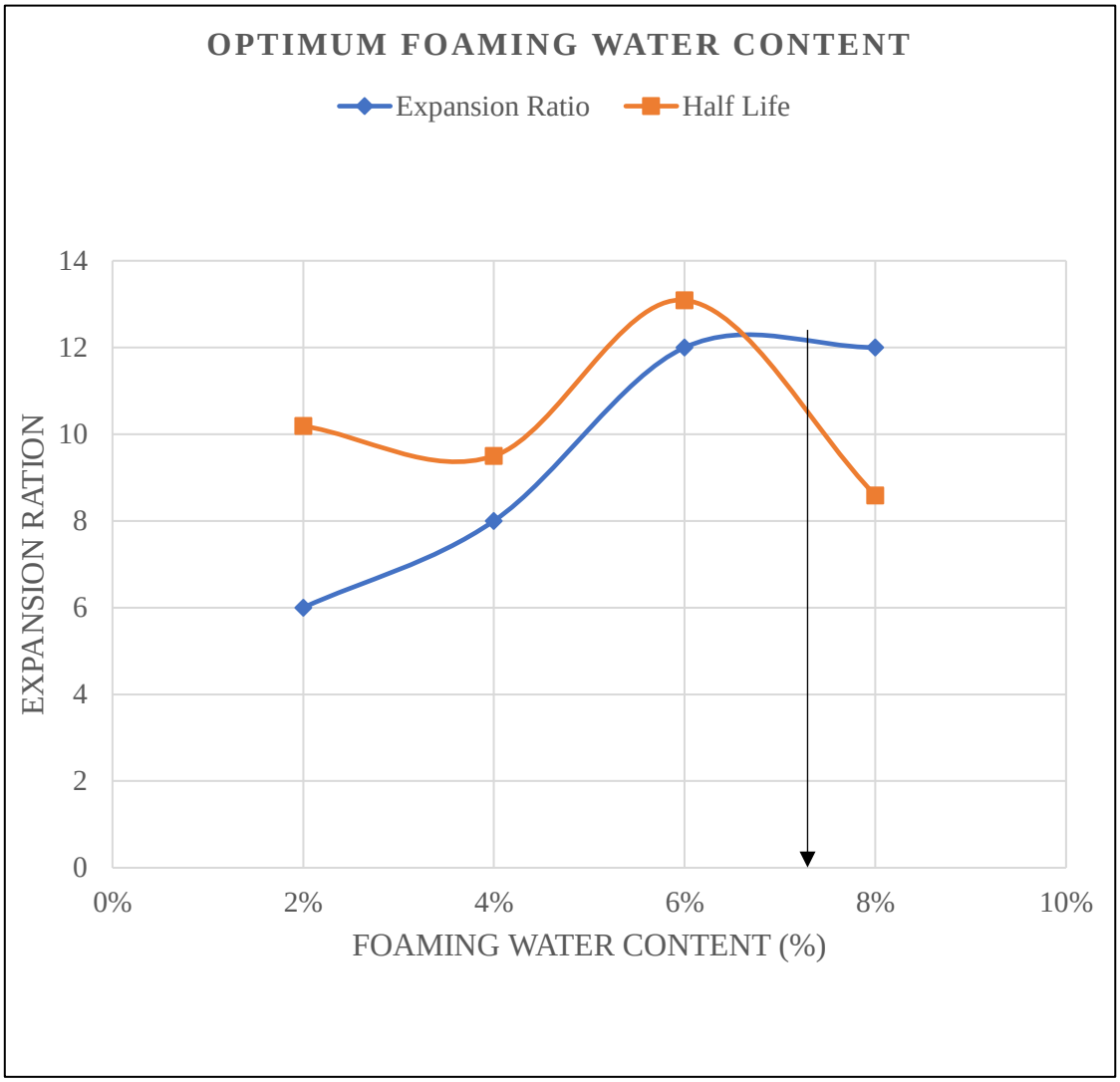

Figure 3.5. Expansion Ratio and Half-Life measured at 150°C

3.3 Testing Methodology

3.3.1 Modified proctor test

The water content, also known as the optimum moisture content, required during material mixing is a critical factor that must be carefully determined in accordance with IS 1702-8 specifications (1983). The blended/graded aggregate was thoroughly mixed with a known amount of water, and resulting mixture was compacted in multiple layers in a 2250 cm3 capacity mould, with every layer getting 55 blows from 4.9 kg rammer fell from a 457 mm (18 inches) height (Photo 5.1). Compacted sample was then detached from mould and kept on a mixing pan. Water content of representative sample was determined in accordance with IS: 2720. (Part: 8). This process was then repeated for different moisture contents, RAP percentages, slag percentages. The dry densities of each compacted mixture were calculated. A dry density graph is plotted against moisture content to produce a compaction curve, the peak point of which is considered maximum dry density (MDD), and the moisture content is considered Optimum Moisture Content (OMC).

Photo 3.8: Apparatus for modified proctor test

3.3.2 Dry and wet indirect tensile strength (ITS)

Indirect tensile strength (ITS) is measured on both dry and wet situations, according to IRC 120. (2015). ITS_{dry} test specimens were preconditioned for 1 hour at 25°C, whereas ITS_{wet} test specimens were preconditioned for 24 hours in a 25°C water bath. Specimens were then placed in the loading apparatus with their centres on the border of the bottom loading strip. The assembly was placed in the centre of the upper loading strip under the compression testing device's loading ram (Photo 3.9). After that, the specimen was exposed to a vertical compressive load until it achieved its maximum load. This method was then performed for wet ITS specimens, with the highest load P (in N) being recorded. After then, ITS values were determined in Equation 5.1; ITS = $\frac{2000 \times P}{\pi \times D \times T}$

Where, ITS = Indirect Tensile Strength (kPa)

P= max. applied load (N)

T = avg. height of specimen (mm)

D = diameter of specimen (mm)

Photo 3.9: Indirect Tensile set-up

3.3.3 Resilient modulus testing

A material's resilient modulus is an estimation of its elastic modulus. Resilient modulus is described as stress divided by strain for quickly applied loads, such as those that pavements encounter. The robust modulus method is used to calculate input for pavement design, evaluation, and analysis as well as to judge the relative quality of the material. Modulus of resilient of bituminous mixes including variable amounts of the mix was examined at various temperatures. The ASTM D7369, "Standard Test Method for Determining the Resilient Modulus of Bituminous Mixtures by Indirect Tension Test," was used to conduct the test on a Universal Testing Machine (UTM-16). The compressive load was applied with a haversine waveform at 25°C, 35°C, and 45°C during test. After preparing specimens, they were placed in a temperature-controlled chamber for at least 6 hours to reach the specified test temperature. The specimen was loaded into the loading apparatus, with the loading strips parallel and centred on the vertical diametrical plane. The specimen was predisposed by repeatedly applying a formula waveform load absent impact for a brief period of time that allowed for measurement of uniform deformation. A peak load of 1000 N and a test pulse count of five were achieved with repeated loading pulse widths of 100 ms and a rest duration of 900 ms. Measuring and recording system has sensors for both monitoring horizontal deformation. Linear variable differential transducers were used to measure horizontal deformation (LVDTs). On horizontal diameter of the specimen, LVDTs were placed at mid-height opposite each other.

Photo 3.10: Apparatus for Resilient Modulus Test

3.3.4 X-ray diffractometer analysis

By using the X-Ray Diffraction (XRD) technique, the mineral phases that are present in the collected ferrochrome slag are detected. Rietveld refinement techniques were employed in conjunction with the X-ray diffraction method to perform quantitative estimations of the mineralogical composition and qualitative identification of the mineral phases on the samples. The samples were mostly placed into possible mechanism for X-ray diffraction examination after being dried at 110°C for 24 hours. Powders were initially subjected to X-ray powder diffraction for qualitative identification of mineral phases. A single crystal graphite monochromatic and a Cu K radiation source are used in a Philips diffractometer to analyse the sample. All measurements were made with an angular range of 10-70° of 2 value (where seems to be the glancing angle of the X-ray beam) in steps of 0.1°. The XRD setup utilised in this study is shown in photo 3.11.

Photo 3.11: XRD model for the mineralogical analysis

3.4 Design of Experiment (DoE)

A Mix design process was expanded utilising a range of statistical techniques that incorporated varying strength qualities, mixing temperatures, and RAP and Slag ingredient percentages. For mixed design, the design of experiments (DOE) data collecting and analysis tool was employed, where the many processes involved in execution were used.

The factors and levels are chosen first, followed by the response variables. Following that, the experiment is repeated, and a model is built to forecast the response variable based on the input factors. The optimum parameter combinations are now identified and chosen using the desirability technique, and trial implementation is used to check the results. This process is known as statistics of variance (ANOVA), and it is used to assess how well the developed model performs.

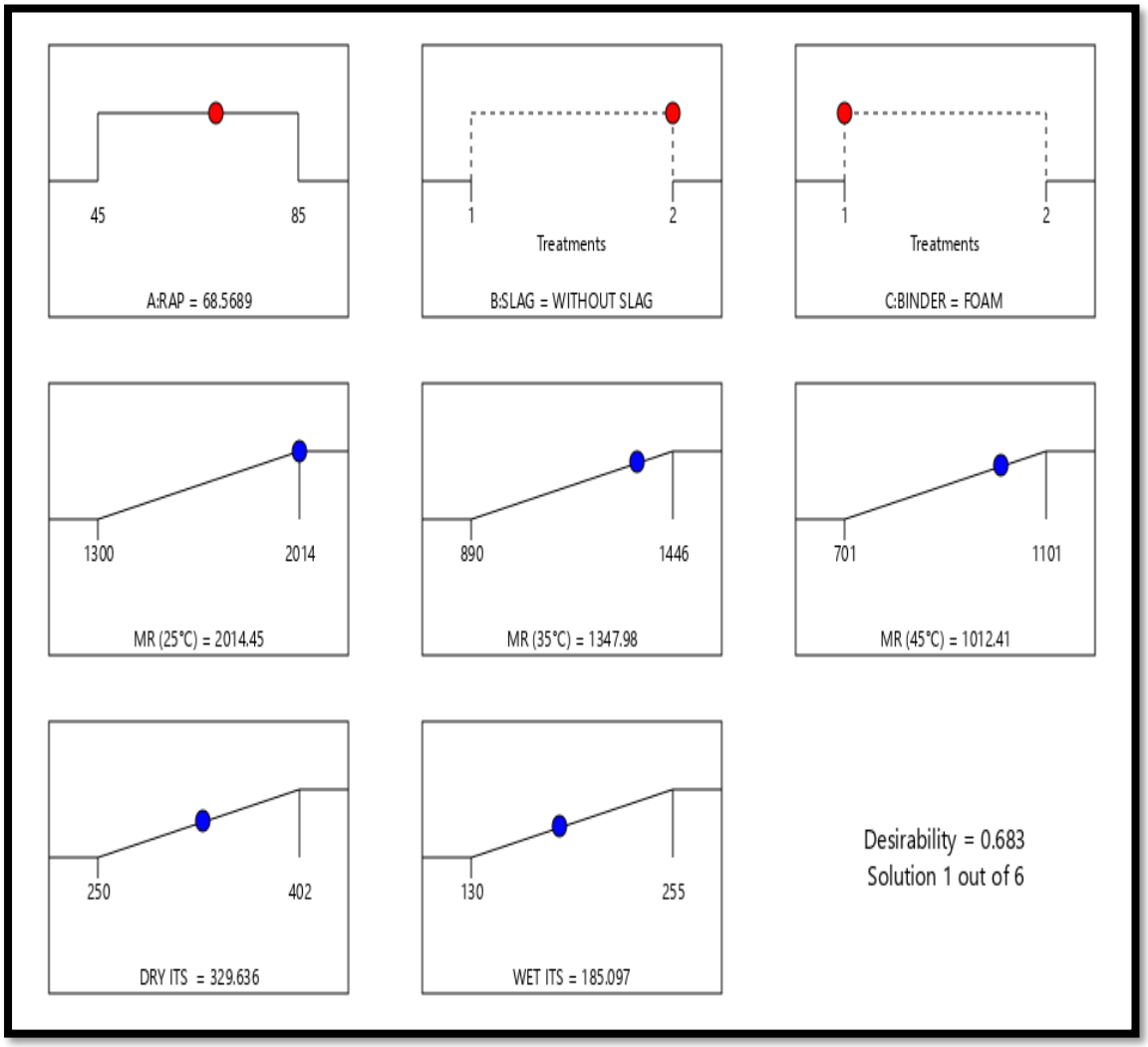

Photo 3.12: Optimization results in Design Expert Software

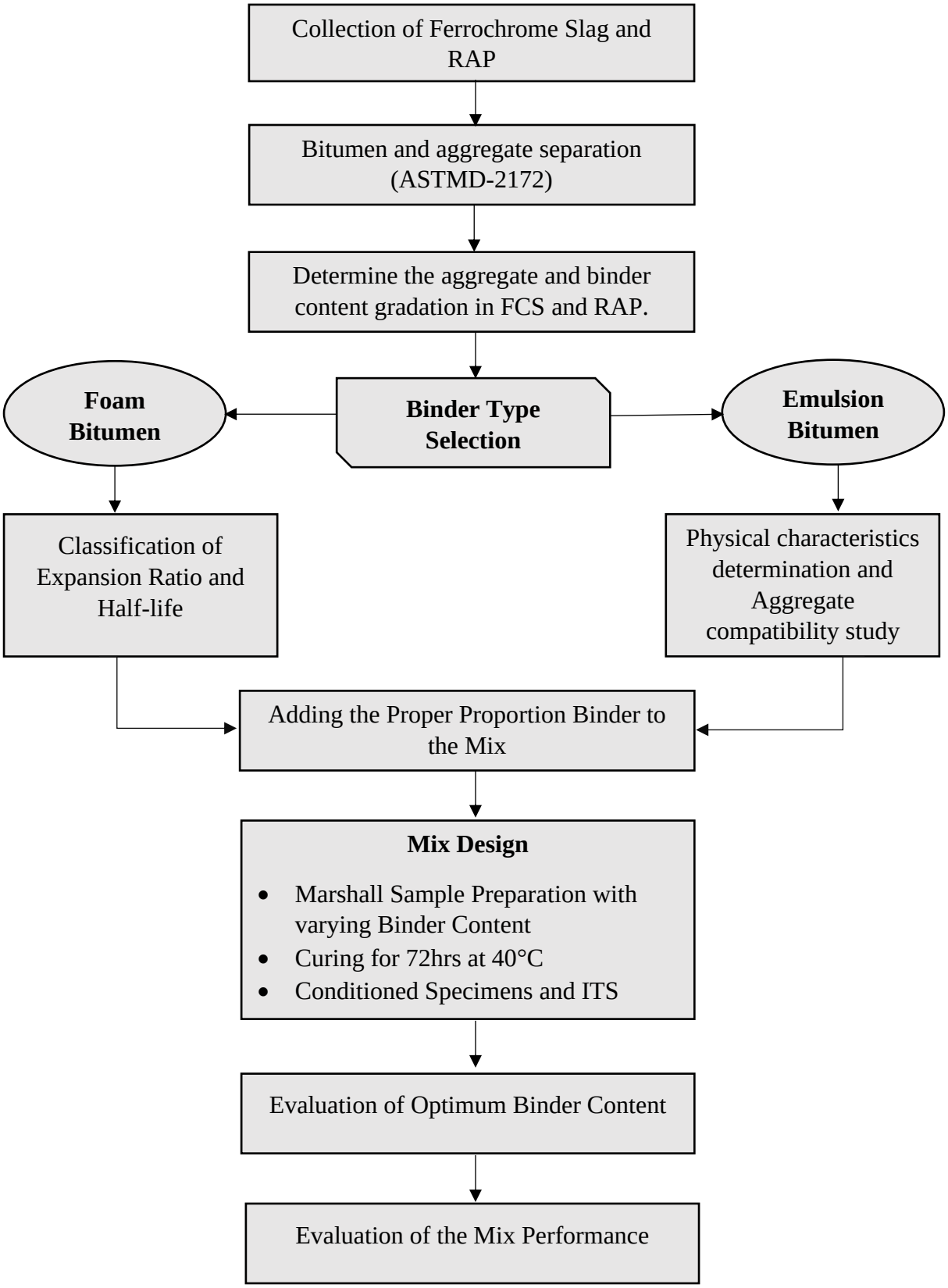

Figure 3.6: Flow chart for proposed methodology for laboratory evaluation of mixes

CHAPTER 4

MIXTURE DESIGN

This chapter discusses the approach used by various researchers to investigate and find useful foamed bitumen and emulsion as a binder in recycled mixtures. Additionally, a number of organisations have created Guidelines for Mix Design of Cold Recycled Asphalt Mixtures, which are founded on laboratory testing, empirical formulas, or prior experience with projects of a similar nature *(Wirtgen. 2012, Muthen, 1998; Austroads, 2006; Namutebi et al. 201, Ebels and Jenkins, 2007; TG 2, 2009).* In essence, these design methodologies consider the optimal dosage of total fluid volume and binder content. The following section describes the mixed design method used in this study.

Three different RAP percentages of VG-10 bitumen were used to make mix samples variations (45 percent RAP, 65 percent RAP, and 85 percent RAP) and two different ferrochrome slag content materials (with Slag & without Slag) with two different binder contents (Foam bitumen mix & Emulsion).

Table 4.1: 12 Combinations used in this study

Binder	S.No.	RAP	Aggregate	Slag
Foam Bitumen	1	85%	15%	0%
	2	65%	40%	0%
	3	45%	55%	0%
	4	85%	3%	12%
	5	65%	15%	25%
	6	45%	15%	40%
Emulsion	7	85%	15%	0%
	8	65%	40%	0%
	9	45%	55%	0%
	10	85%	3%	12%
	11	65%	15%	25%
	12	45%	15%	40%

4.1 Aggregate Gradations

4.1.1 Design of Mix with 45% RAP and Natural Aggregate

Table 4.2 shows the individual gradation of component aggregate and the proportioning achieved. Fig. 4.1 depicts the designed gradation as well as the specified limits.

Table 4.2: Combined aggregate gradation for 45% RAP

Sieve Size (mm)	**Grading of RAP Material (X)**	**Percentage Passing of Aggregates**				**Combined Gradation X: Y 45:55**	**Specified Limit as per IRC:37, 2012 Specifications**
		Nominal Size of Aggregates (Y)					
		10 mm	**20 mm**	**Stone Dust**	**Cement**		
45	100.00	100.00	100.00	100.00	100.00	**100**	100
37.5	100.00	100.00	100.00	100.00	100.00	**99**	87-100
26.6	98.19	100.00	100.00	100.00	100.00	**98**	77-100
19	86.36	100.00	96.84	100.00	100.00	**93**	66-99
13.2	70.96	99.85	16.44	100.00	100.00	**78**	67-87
4.75	35.17	0.57	0.13	100.00	100.00	**40**	33-50
2.36	24.29	0.22	0.13	93.41	100.00	**33**	25-47
0.6	9.62	0.22	0.13	57.45	100.00	**18**	12-27
0.3	4.29	0.22	0.13	38.52	99.80	**11**	8-21
0.075	0.26	0.22	0.13	10.26	90.40	**3**	2-9
Blend Proportion by weight	**45**	**20**	**10**	**24**	**1**	**100**	

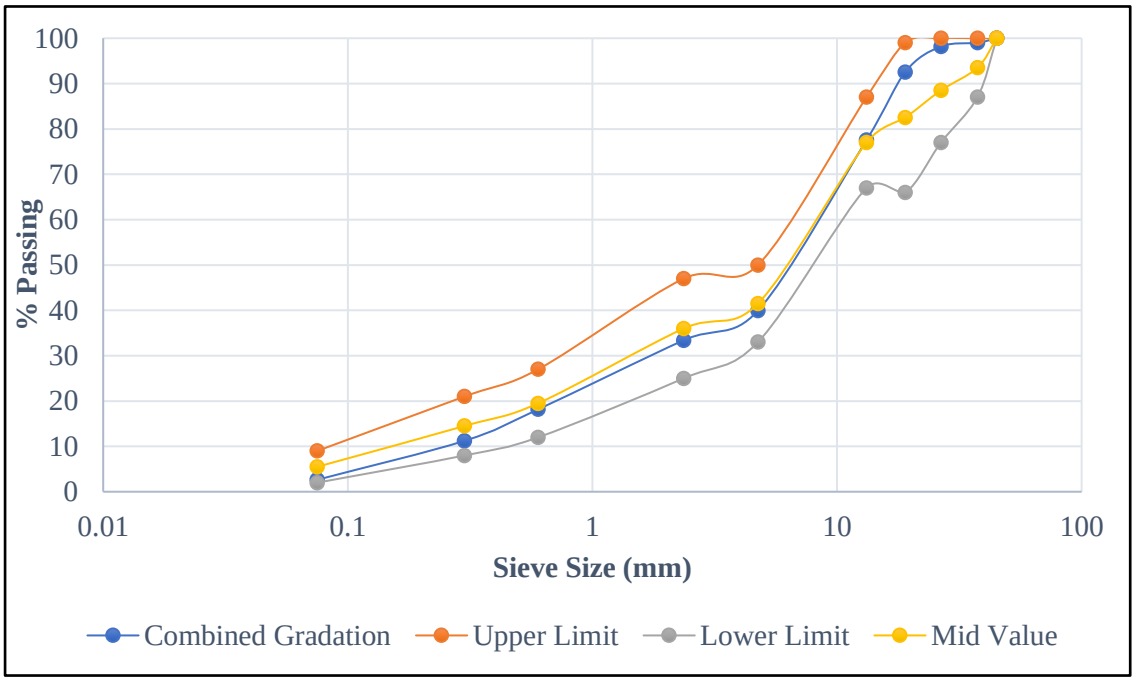

Fig. 4.1: Aggregate gradation adopted for 45% RAP in mix

4.1.2 Design of Mix with 65% RAP and Natural Aggregate

Table 4.3 shows the individual gradation of component aggregate and the proportioning achieved. Fig. 4.2 depicts the designed gradation as well as the specified limits.

Table 4.3: Combined aggregate gradation for 65% RAP

Sieve Size (mm)	Grading of RAP Material (X)	Percentage Passing of Aggregates				Combined Gradation X: Y 65:35	Specified Limit as per IRC:37, 2012 Specifications
		Nominal Size of Aggregates (Y)					
		10 mm	20 mm	Stone Dust	Cement		
45	100.00	100.00	100.00	100.00	100.00	**100**	100
37.5	100.00	100.00	100.00	100.00	100.00	**99**	87-100
26.6	98.19	100.00	100.00	100.00	100.00	**98**	77-100
19	86.36	100.00	96.84	100.00	100.00	**91**	66-99
13.2	70.96	99.85	16.44	100.00	100.00	**78**	67-87
4.75	35.17	0.57	0.13	100.00	100.00	**46**	33-50
2.36	24.29	0.22	0.13	93.41	100.00	**38**	25-47
0.6	9.62	0.22	0.13	57.45	100.00	**20**	12-27
0.3	4.29	0.22	0.13	38.52	99.80	**12**	8-21
0.075	0.26	0.22	0.13	10.26	90.40	**3**	2-9
Blend Proportion by weight	**65**	**4**	**10**	**20**	**1**	**100**	

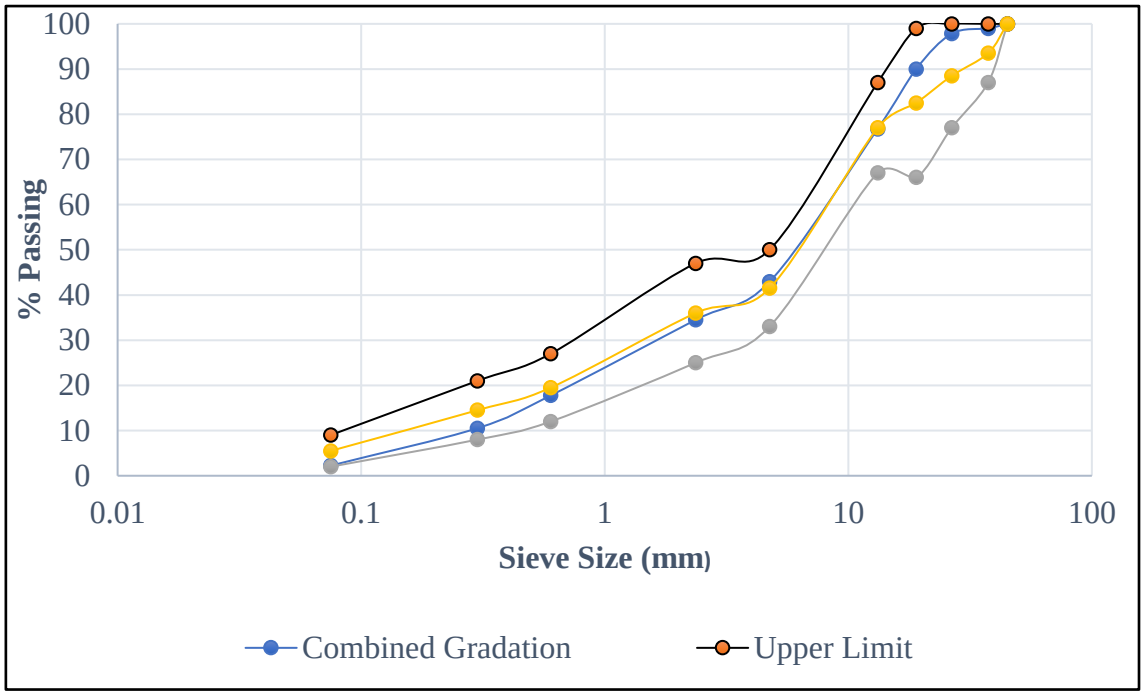

Fig. 4.2: Aggregate gradation adopted for 65% RAP in mix

4.1.3 Design of Mix with 85% RAP and Natural Aggregate

Table 4.4 shows the individual gradation of component aggregate and the proportioning achieved. Fig. 4.3 depicts the designed gradation as well as the specified limits.

Table 4.4: Combined aggregate gradation for 85% RAP

Sieve Size (mm)	Grading of RAP Material (X)	Percentage Passing of Aggregates				Combined Gradation X: Y 85:15	Specified Limit as per IRC:37, 2012 Specifications
		Nominal Size of Aggregates (Y)					
		10 mm	20 mm	Stone Dust	Cement		
45	100.00	100.00	100.00	100.00	100.00	**100**	100
37.5	100.00	100.00	100.00	100.00	100.00	**99**	87-100
26.6	98.19	100.00	100.00	100.00	100.00	**97**	77-100
19	86.36	100.00	96.84	100.00	100.00	**87**	66-99
13.2	70.96	99.85	16.44	100.00	100.00	**74**	67-87
4.75	35.17	0.57	0.13	100.00	100.00	**44**	33-50
2.36	24.29	0.22	0.13	93.41	100.00	**34**	25-47
0.6	9.62	0.22	0.13	57.45	100.00	**16**	12-27
0.3	4.29	0.22	0.13	38.52	99.80	**9**	8-21
0.075	0.26	0.22	0.13	10.26	90.40	**2**	2-9
Blend Proportion by weight	**85**	**0**	**0**	**14**	**1**	**100**	

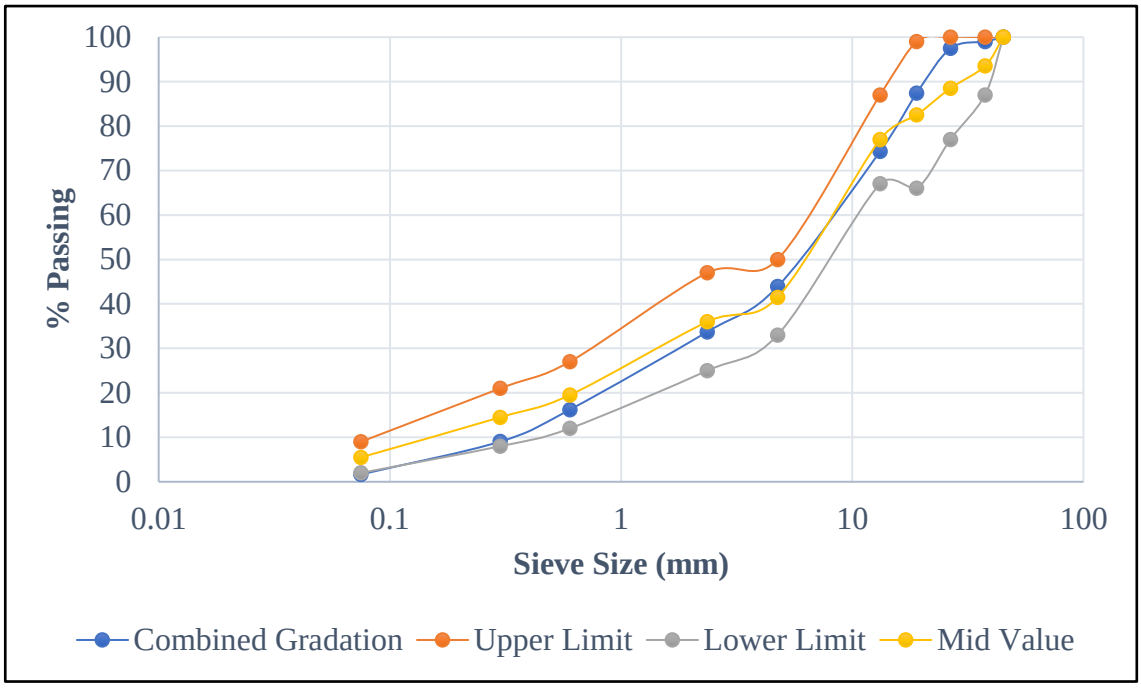

Fig. 4.3: Aggregate gradation adopted for 85% RAP in mix

4.1.4 Design of Cold Mix with 45% RAP and Ferrochrome Slag

Table 4.5 shows the individual gradation of component aggregate and the proportioning achieved. Fig. 4.4 depicts the designed gradation as well as the specified limits.

Table 4.5: Combined aggregate gradation for 45% RAP and ferrochrome slag

Sieve Size (mm)	Grading of RAP Material (X)	Percentage Passing of Aggregates				FC Slag (4.75mm)	FC Slag (finer Agg.)	Combined Gradation X: Y 45:55	Specified Limit as per IRC:37, 2012 Specifications
		Nominal Size of Aggregates (Y)							
		10 mm	20 mm	Stone Dust	Cement				
45	100.00	100.00	100.00	100.00	100.00	100	100	**100**	100
37.5	100.00	100.00	100.00	100.00	100.00	100	100	**100**	87-100
26.6	98.19	100.00	100.00	100.00	100.00	100	100	**99**	77-100
19	86.36	100.00	96.84	100.00	100.00	100	100	**94**	66-99
13.2	70.96	99.85	16.44	100.00	100.00	100	100	**79**	67-87
4.75	35.17	0.57	0.13	100.00	100.00	79.21	100	**49**	33-50
2.36	24.29	0.22	0.13	93.41	100.00	73.96	94.44	**42**	25-47
0.6	9.62	0.22	0.13	57.45	100.00	31.98	43.98	**19**	12-27
0.3	4.29	0.22	0.13	38.52	99.80	11.63	18.4	**9**	8-21
0.075	0.26	0.22	0.13	10.26	90.40	2.92	4.2	**2**	2-9
Blend Proportion by weight	**45**	**10**	**4**	**0**	**1**	**8**	**32**	**100**	

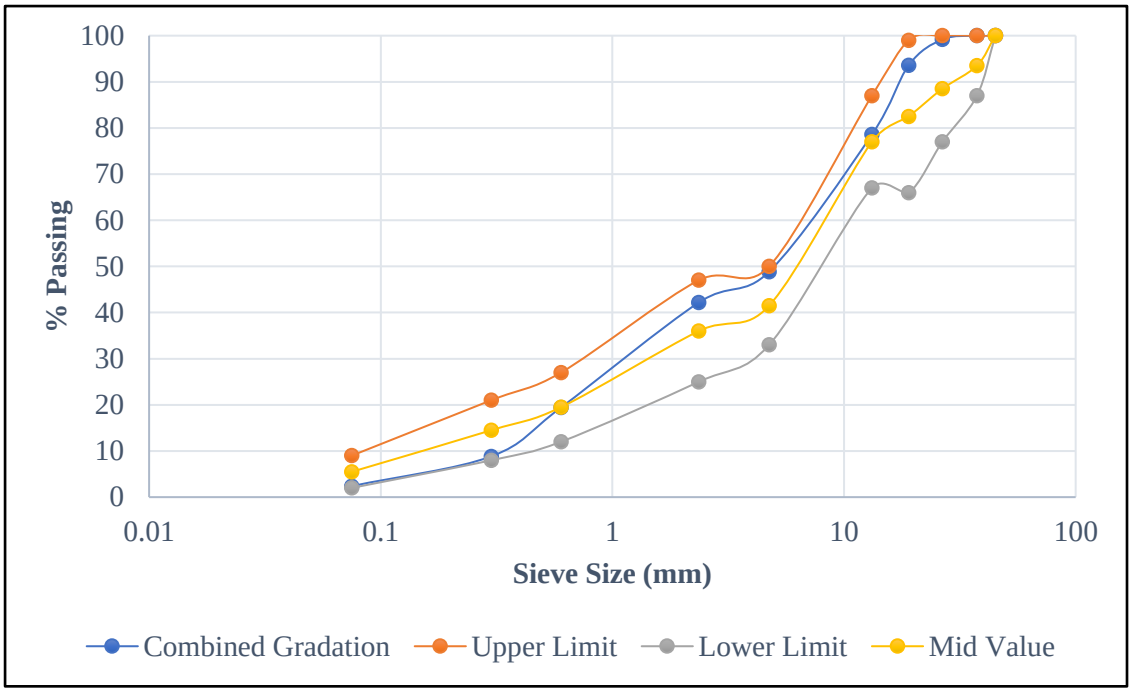

Fig. 4.4: Aggregate gradation adopted for 45% RAP in mix

4.1.5 Design of Mix with 65% RAP and Ferrochrome Slag

Table 4.6 shows the individual gradation of component aggregate and the proportioning achieved. Fig. 4.5 depicts the designed gradation as well as the specified limits.

Table 4.6: Combined aggregate gradation for 65% RAP and ferrochrome slag

Sieve Size (mm)	Grading of RAP Material (X)	Percentage Passing of Aggregates				FC Slag (4.75mm)	FC Slag (finer Agg.)	Combined Gradation X: Y 45:55	Specified Limit as per IRC:37, 2012 Specifications
		Nominal Size of Aggregates (Y)							
		10 mm	20 mm	Stone Dust	Cement				
45	100.00	100.00	100.00	100.00	100.00	100	100	**100**	100
37.5	100.00	100.00	100.00	100.00	100.00	100	100	**100**	87-100
26.6	98.19	100.00	100.00	100.00	100.00	100	100	**99**	77-100
19	86.36	100.00	96.84	100.00	100.00	100	100	**92**	66-99
13.2	70.96	99.85	16.44	100.00	100.00	100	100	**83**	67-87
4.75	35.17	0.57	0.13	100.00	100.00	79.21	100	**47**	33-50
2.36	24.29	0.22	0.13	93.41	100.00	73.96	94.44	**39**	25-47
0.6	9.62	0.22	0.13	57.45	100.00	31.98	43.98	**18**	12-27
0.3	4.29	0.22	0.13	38.52	99.80	11.63	18.4	**8**	8-21
0.075	0.26	0.22	0.13	10.26	90.40	2.92	4.2	**2**	2-9
Blend Proportion by weight	**65**	**9**	**0**	**0**	**1**	**0**	**25**	**100**	

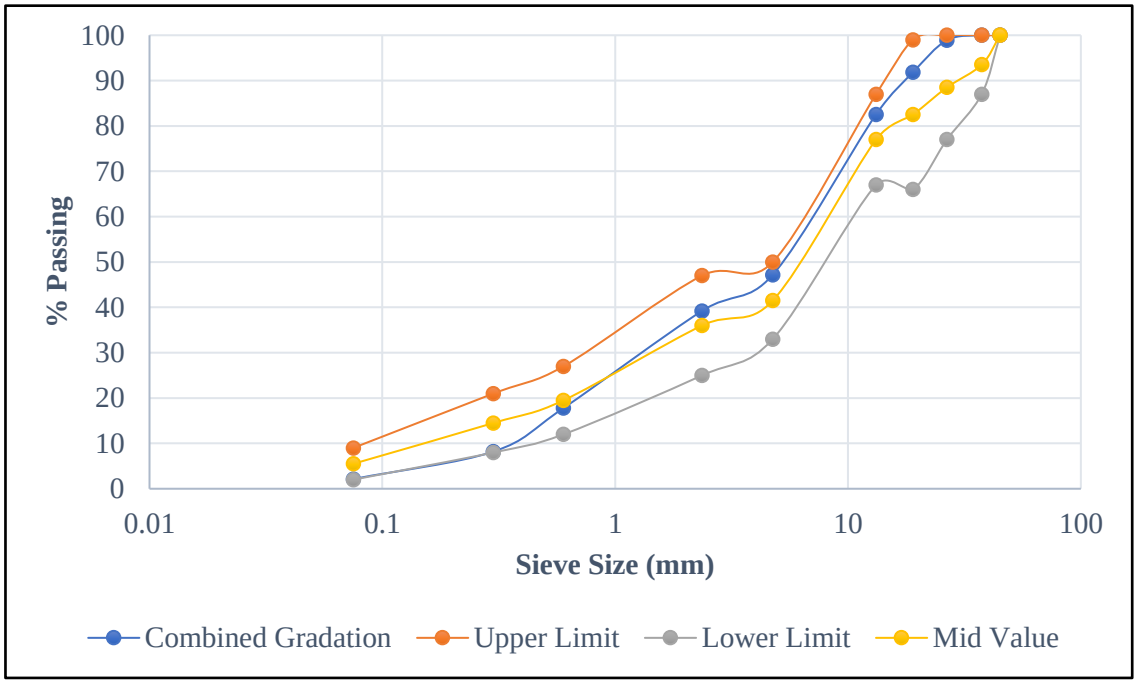

Fig. 4.5: Aggregate gradation adopted for 65% RAP and ferrochrome slag in mix

4.1.6 Design of Cold Mix with 85% RAP and Ferrochrome Slag

Table 4.7 shows the individual gradation of component aggregate and the proportioning achieved. Fig. 4.6 depicts the designed gradation as well as the specified limits.

Table 4.7: Combined aggregate gradation for 85% RAP and ferrochrome slag

Sieve Size (mm)	Grading of RAP Material (X)	Percentage Passing of Aggregates				FC Slag (4.75mm)	FC Slag (finer Agg.)	Combined Gradation X: Y 45:55	Specified Limit as per IRC:37, 2012 Specifications
		Nominal Size of Aggregates (Y)							
		10 mm	20 mm	Stone Dust	Cement				
45	100.00	100.00	100.00	100.00	100.00	100	100	**100**	100
37.5	100.00	100.00	100.00	100.00	100.00	100	100	**100**	87-100
26.6	98.19	100.00	100.00	100.00	100.00	100	100	**98**	77-100
19	86.36	100.00	96.84	100.00	100.00	100	100	**88**	66-99
13.2	70.96	99.85	16.44	100.00	100.00	100	100	**75**	67-87
4.75	35.17	0.57	0.13	100.00	100.00	79.21	100	**45**	33-50
2.36	24.29	0.22	0.13	93.41	100.00	73.96	94.44	**35**	25-47
0.6	9.62	0.22	0.13	57.45	100.00	31.98	43.98	**16**	12-27
0.3	4.29	0.22	0.13	38.52	99.80	11.63	18.4	**8**	8-21
0.075	0.26	0.22	0.13	10.26	90.40	2.92	4.2	**2**	2-9
Blend Proportion by weight	**85**	**0**	**0**	**2**	**1**	**0**	**12**	**100**	

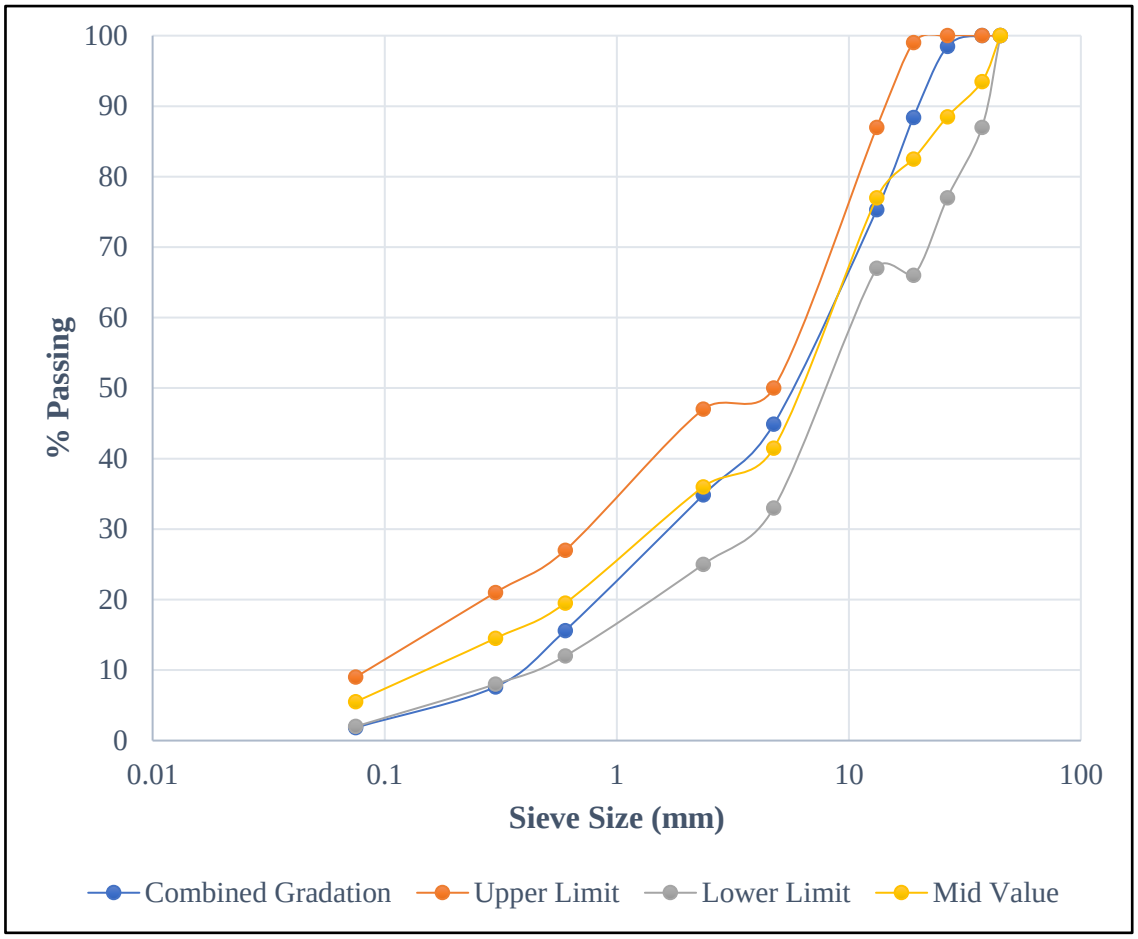

Fig. 4.6: Aggregate gradation adopted for 85% RAP and ferrochrome slag in mix

4.2 Cold Mix with Foam Bitumen

4.2.1 Maximum Dry Density (MDD) and Optimum Moisture Content (OMC)

The Modified Proctor Test (AASHTO T180) is used to optimize the water content in the Foamed Bitumen Mixes. Dry density is calculated by altering the moisture content in cold mixtures, and Maximum Dry Density (MDD) is attained at Optimal Moisture Content (OMC). When mixing and compaction of FBM, one of the critical factors for mix design is moisture content (He et al, 2008). MDD was observed to diminish when the RAP % increased. This is conceivable due to the existence of elongated and flaky aggregate in the RAP material, as well as the RAP material's poor physical qualities during compaction. These findings are also consistent with previous research (Kar et al., 2018). The test value obtained are shown in Table 4.8. for RAP and natural aggregate and in Table 4.9. for RAP and ferrochrome slag.

Table 4.8: Compaction results for different variations of RAP and natural aggregate

Mix	Dry Density (kg/cc)	Optimum Moisture Content (%)
85% RAP + NA	**2.09**	**5.8**
65% RAP + NA	**2.2**	**5.5**
45% RAP + NA	**2.26**	**4.8**

,

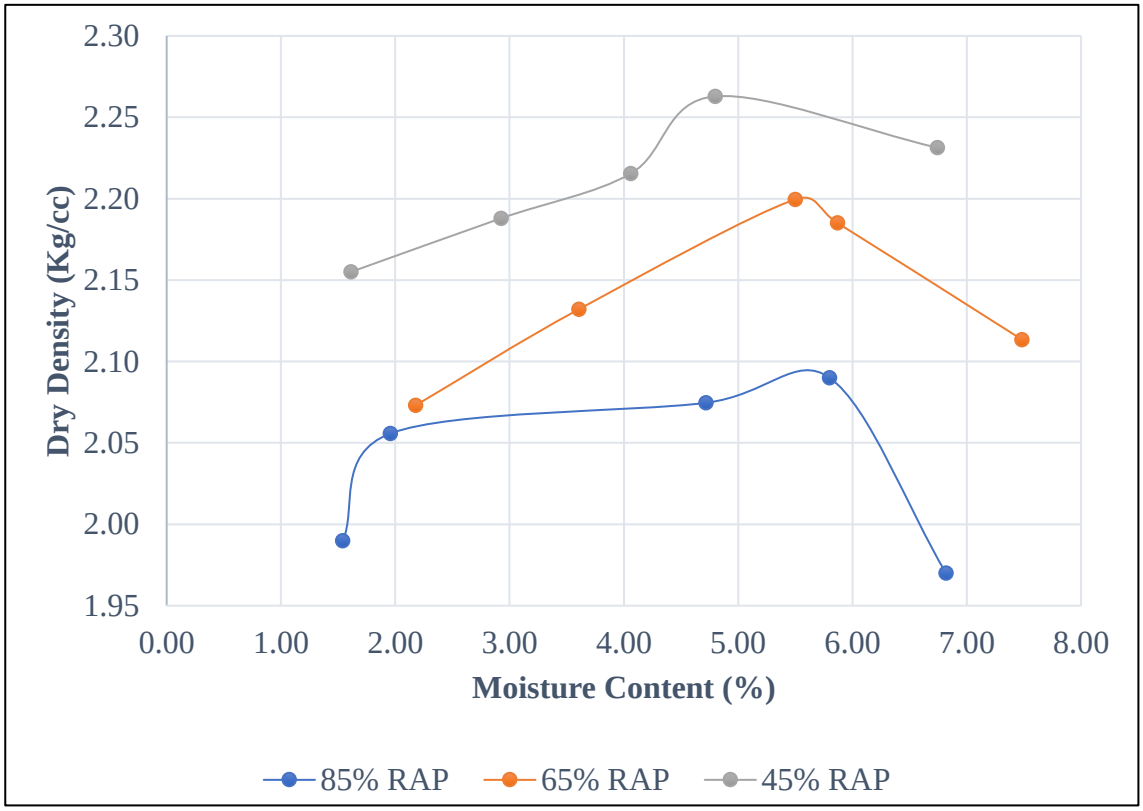

Fig. 4.7: Dry Density – Fluid content relation for RAP and natural agg. mix

Table 4.9: Compaction results for different variations of RAP and ferrochrome slag

Mix	Dry Density (kg/cc)	Optimum Moisture Content (%)
85% RAP + FCS	**2.04**	**6.8**
65% RAP + FCS	**2.07**	**6.6**
45% RAP + FCS	**2.10**	**6.2**

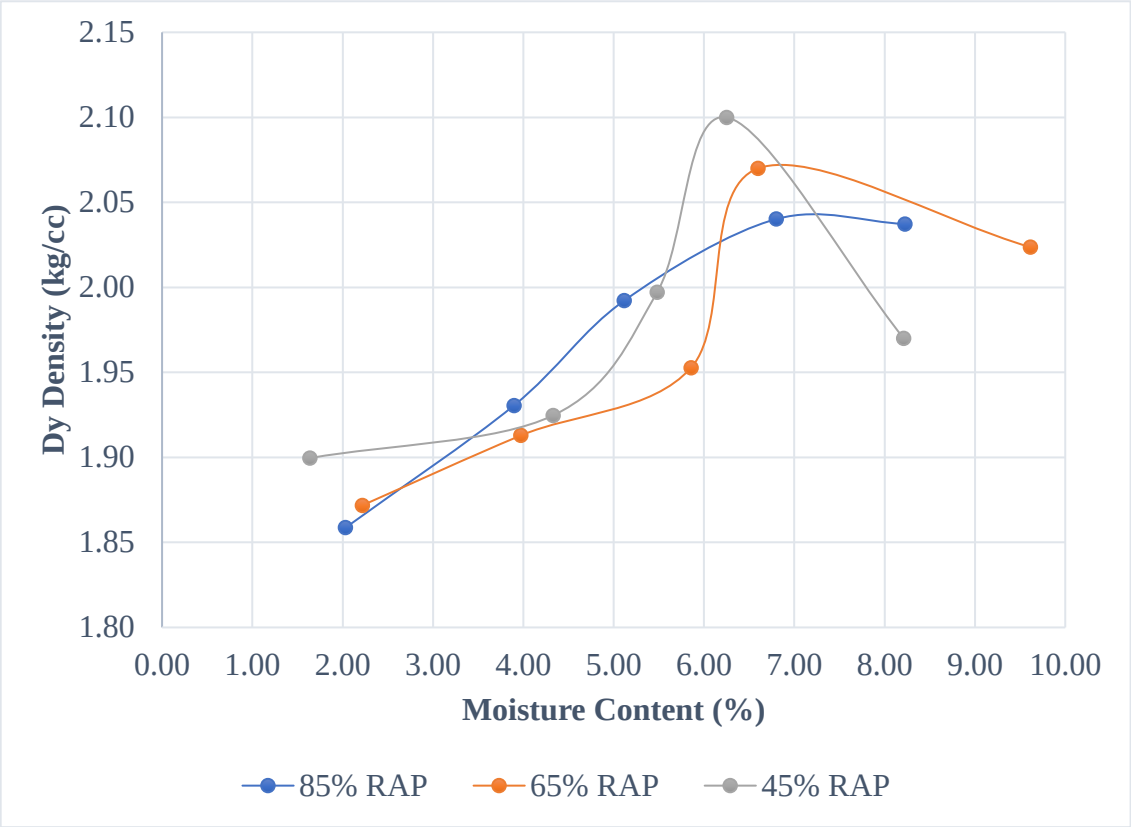

Fig. 4.8: Dry Density – Fluid content relation for RAP and ferrochrome slag mix

The fineness of the mix (materials passing through with a 4.75mm sieve) is proportional to the OMC necessary to attain MDD. It may be claimed that the gaps generated by bigger particles as RAP percentages grow are filled with water rather than finer particles. This explains why greater RAP material mixes have lower density and require a larger water concentration to generate MDD, as seen in (Fig. 4.7 and Fig. 4.8).

4.2.2 Optimization of Foam Bitumen

As previously established in Chapter 3, the foaming parameters were optimized using the criteria given in IRC: 120.2015 as well as TG-2 (2009). The VG-10 binder's optimal binder temperature and foaming water concentration were determined to be 150°C and 6.5 percent, respectively. The optimal foamed bitumen percentage was discovered to be 2.5 percent by weight of aggregates in all RAP combinations.

4.2.3 Preparation of Samples

Foam Bitumen Mix (FBM) samples was made at 150°C using VG-10 bitumen and various percentage changes of RAP components (45 percent, 65 percent, & 85 percent). About 10kg of each samples mix (blended aggregates) being weighed, and 1% cement was used as a filler to aid in bitumen dispersion into the mix. Adding more than 1% cement may result in increased

strength as well as fracture energy, which may cause fatigue damage if exposed to extreme heat (Prachi et al, 2019). The foamed bitumen was then created at the optimal level when it comes of foaming temperature and foaming water content, with a 2.5 percent foam binder added. It was then completely mixed with each specimen's OMC using the WLM Mixer (Photo 4.1)

Photo 4.1: WLM Mixer

4.2.4 Compaction

At the mix design stage, a Marshall compactor is used to compact specimens according to ASTM D 6926 "Preparation of Bituminous Mixtures Using Marshall Apparatus," as shown in Photo 4.2. At the anticipated compaction temperature, each sample is crushed using a Marshall hammer, a machine that applies pressure toward a sample through one tamper foot. The hammers are controlled by a computer. The compactor's most important parameters are:

Sample size is a cylinder with a 102 mm (4 inch) diameter and 64 mm (2.5 inch) height (improvements can be made for changed sample heights). 98.4 mm (3.875 inches) in diameter, 76 cm2 in area, and a flat, circular shape (11.8 in2). 457.2 mm of compaction pressure (18 inches) Hammer assembly free-fall drop distance at a slipping weight of 4536 g (10 lb).

Typically, there are 75 blows on each side, based on anticipated volume of traffic. The sample is struck on top by the tamper foot, which nearly completely surrounds the top of the sample. After a predetermined number of strikes, sample is replaced, and procedure is repeated. AASHTO T 245: Bituminous Mixtures' Resistant to Plastic Flow The protocol for sample preparation for the Marshall technique is included in Using the Marshall Apparatus.

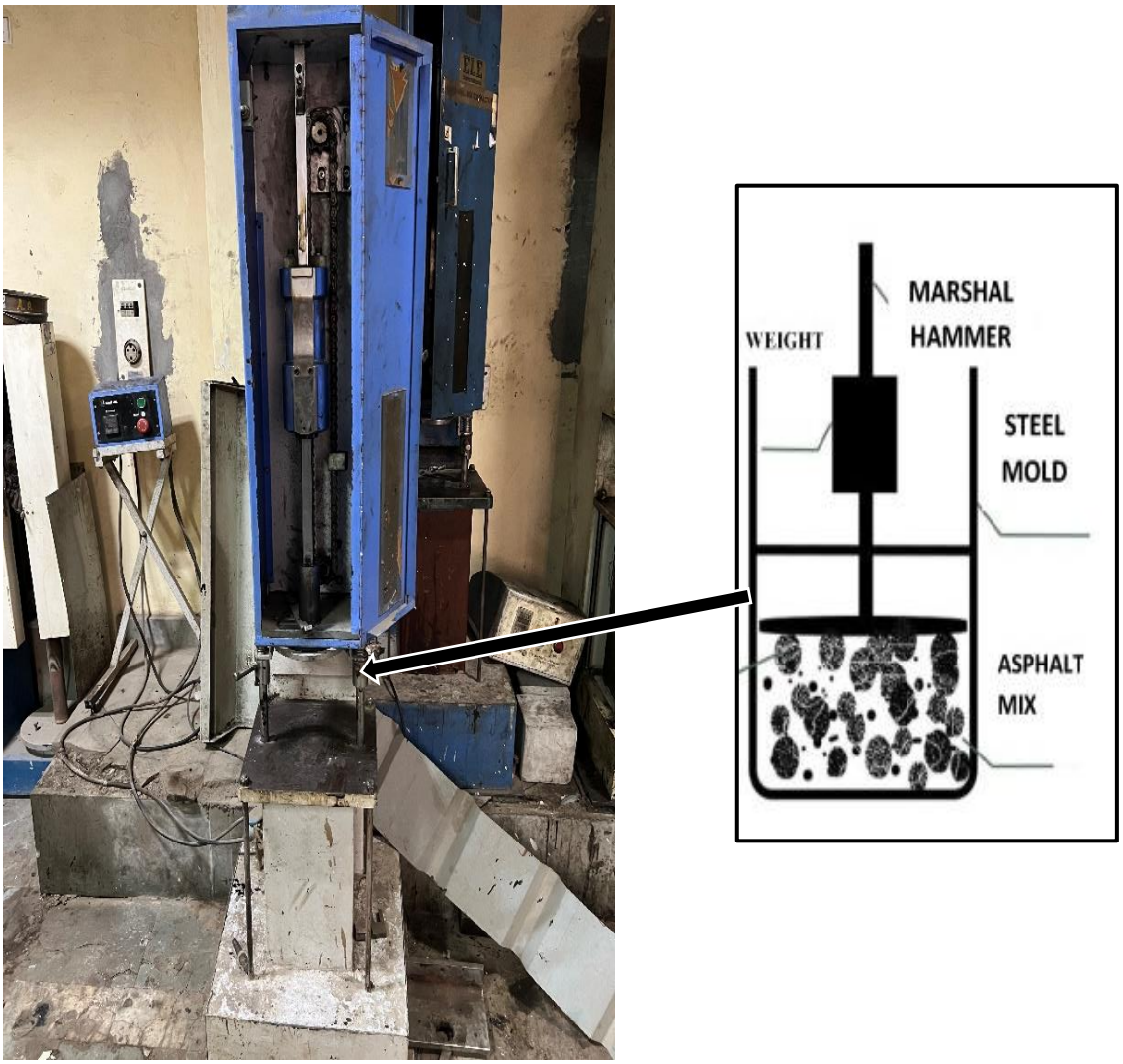

Photo 4.2: Marshall compactor for compaction specimen at mix design stage.

4.2.5 Curing

After compaction, the samples were air-dried for 24 hours and then, later on, were kept in oven for 3 days at 40°C and was also allowed to rest for an additional 4 hours before carrying out any tests on them. To prepare samples at higher mixing temperatures (60°C and 90°C), the specimen mix was initially pre-heated in the oven at 60°C and 90°C temperature for 2 hours.

(A)

(B)

Photo 4.3: (A) Sample Kept for Curing for 3 days and (B) Sample after Curing

4.3 Cold Mix with Bitumen Emulsion

4.3.1 Estimation of Total Fluid Content (TFC)

The following formula should be used to calculate dry density at each fluid content in E.q. 4.1

$$D_{dd} = (D_{bulk}) / (1 + FC) \quad \text{(E.q. 4.1)}$$

Where, D_{dd} = Dry density (kg/m3),

D_{bulk} = Bulk density (kg/m3),

FC = Fluid content (dry weight of aggregates).

To calculate the Total Fluid Content (FC), samples were created while maintaining the emulsion Constant content by aggregate mass (as numerically determined, E.q. 4.1). The pre-wetting water content was gradually raised by the mass of the aggregate, beginning with a total fluid content of 4.0 percent and finishing at 6 percent. Then, as illustrated below, a plot of dry density vs. fluid content is created, and the maximum dry density and matching optimal fluid content are obtained. TFC of RAP and Natural Aggregate was determined to be 4.5 percent, 4.5 percent, and 5 percent by weight of aggregates in 45 percent, 65 percent, and 85 percent RAP, respectively, using the aforesaid parameters, as shown in Fig. 4.9. As illustrated in Fig. 4.10, the TFC of RAP and ferrochrome slag was determined to be 4.5 percent, 4.5 percent, and 4.5 percent by weight of aggregates in 45 percent, 65 percent, and 85 percent RAP, respectively. As indicated in the diagram below, a plot of dry density vs. fluid content is made, and the maximum dry density and associated optimum fluid content are determined. The RAP mixes must be compacted to their maximum density, which necessitates use of optimal fluid content. (IRC 37:2012).

Table 4.10: Determination of optimum fluid content & optimum emulsion content

Mix	Optimum Fluid Content	Optimum Emulsion Content
85% RAP + NA	5%	3.5%
85% RAP + FCS	4.5%	3.5%
65% RAP + NA	4.5%	3.5%
65% RAP + FCS	4.5%	3.5%
45% RAP + NA	4.5%	3.5%
45% RAP + FCS	4.5%	3.5%

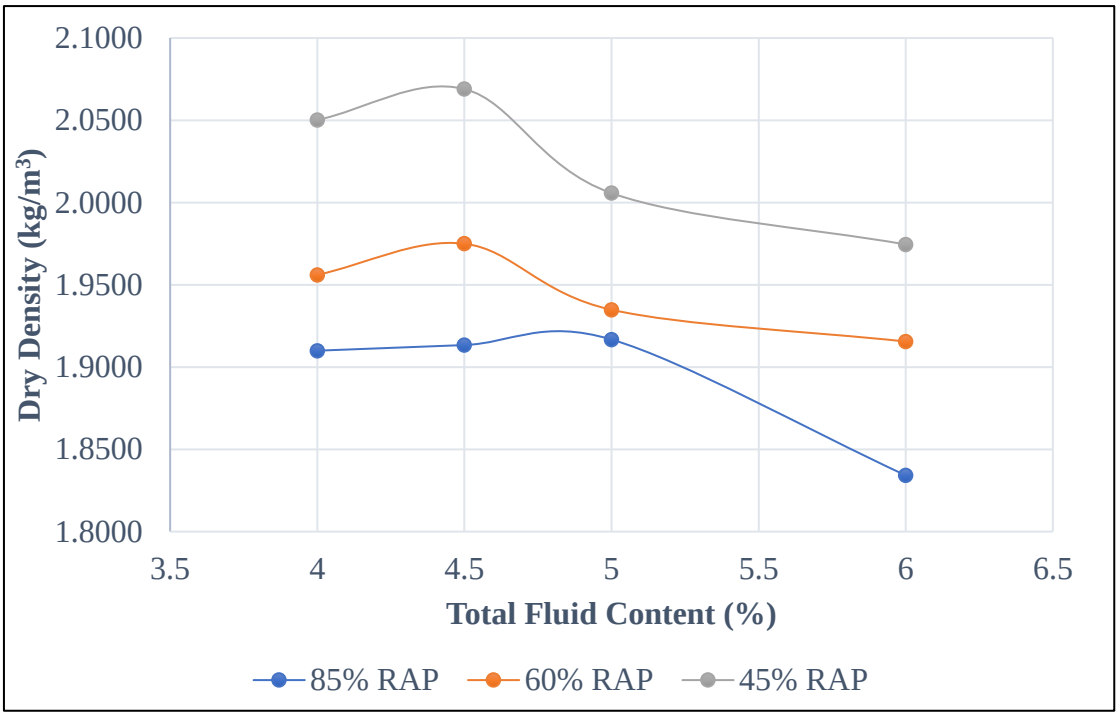

Fig. 4.9: Dry Density-Fluid content relation for RAP and natural aggregate mix

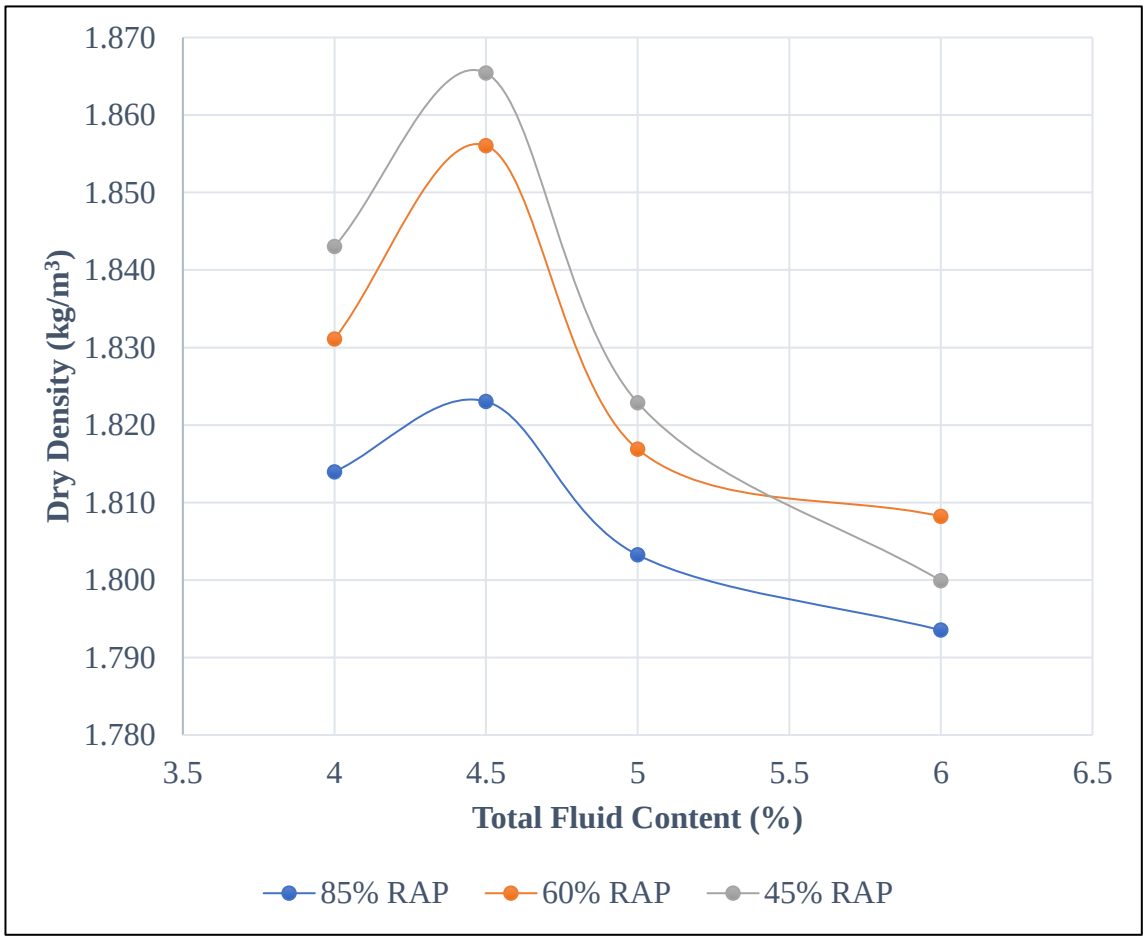

Fig. 4.10: Dry Density-Fluid content relation for RAP and ferrochrome slag mix

4.3.2 Estimation of Optimum Emulsion Content (OEC)

The approach used to optimise the binder content involves holding the TFC continual while altering content of emulsion at 0.5 percent intervals starting at 3 percent and finishing at 4 percent, yielding a total of three levels of observations as demonstrated in traditional mixes. The acquired mechanical characteristics, such as dry ITS, are graphed. Using the characteristics listed above, the OEC of RAP and natural aggregate was calculated to be 3.5 percent, 3.5 percent, and 3.5 percent by weight of aggregates comprising 45 percent, 65 percent, and 85 percent RAP, as shown in Fig. 4.11. As illustrated in Fig. 4.12, the OEC of RAP and ferrochrome slag was determined to be 3.5 percent, 3.5 percent, and 3.5 percent by weight of aggregates comprising 45 percent, 65 percent, and 85 percent RAP, respectively. From the results obtained 5% TFC, 3.5% emulsion content, and 1.5% of water content are used in a mix with 85% RAP.

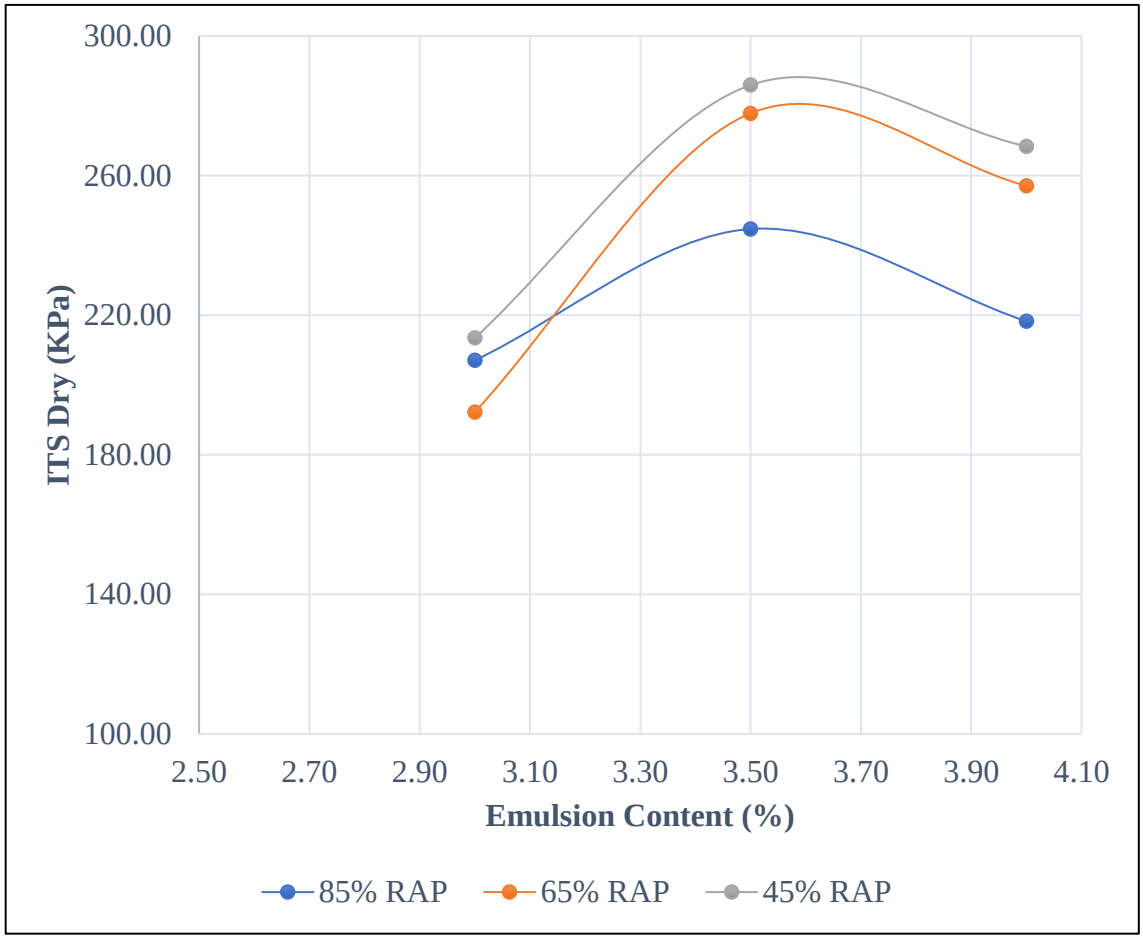

Fig. 4.11: ITS_{dry}-Emulsion content for RAP and natural aggregate mix

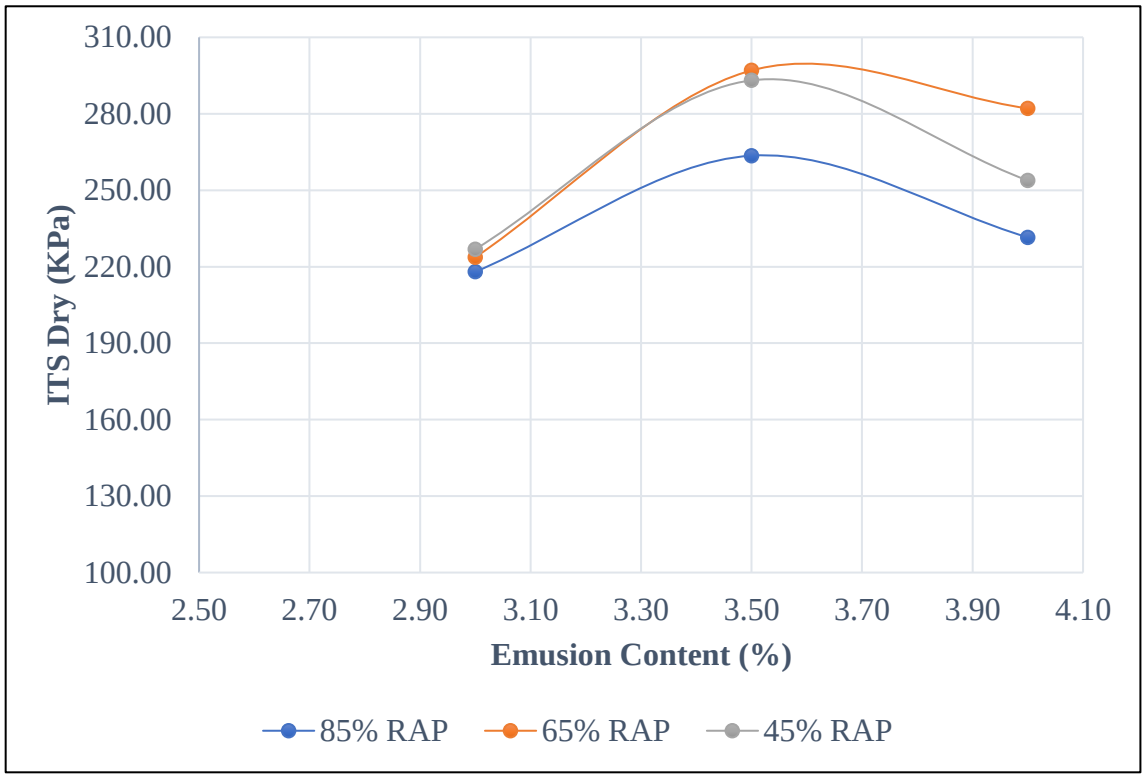

Fig. 4.12: ITS_{dry}-Emulsion content for RAP and ferrochrome slag mix

4.3.3 Preparation of Samples

To create a homogeneous mix, aggregate, RAP, FCS, emulsion, and stone dust were combined. Cement was then added as filler. Dry samples were combined with the necessary amount of binder and emulsion, and the mixture was then poured into 100 mm Marshall moulds. Mixture might not be cool while hammering because the mould were heated and oil-coated before usage. Hammering was done after inserting the mould.

A typical hammer was used for hammering. Oiling the inside face of the mould and the bottom of the hammer before inserting the sample was done to prevent sample sticking towards the mould and hammer. The fitting was then covered with a sheet of paper with an identical dimension to the mould. The specimen was then subjected to 75 blows on every side in order to condense it. After being hammered, the sample was removed from the mould. Name sticks indicating the sample's binder content, sample size, and type of additives are adhered to the sample EMULSION so that it may be identified afterwards. The sample was then allowed to cool until it reached room temperature.

Photo 4.4: View of after mixing of sample

(A) **(B)**

Photo 4.5: (A) SS2 Bitumen Emulsion and (B) Sample after compaction

CHAPTER 5

DESIGN of EXPERIMENT APPROACH

This chapter examines the statistical technique used for the design of Foam Bitumen Mix and Bitumen Emulsions, as well as the construction of the model, which includes three factors: mixing Slag content, binder content, and RAP material content. The experimental examination, which includes laboratory research and optimization techniques also the prediction of models, and determination of the effectiveness of the model through statistical ANOVA analysis, is provided. Final step is using a response surface design matrix, an experimentation with a factorial design can be done to determine the input parameters and operating rate. To optimize the input parameters, the resilient modulus (MR) at three distinct temperatures (25°C, 35°C, and 45°C) dry and wet indirect tensile strength characteristics were also taken into account. The flow chart and Figure 5.1 show a summary of the various steps taken during the mix design.

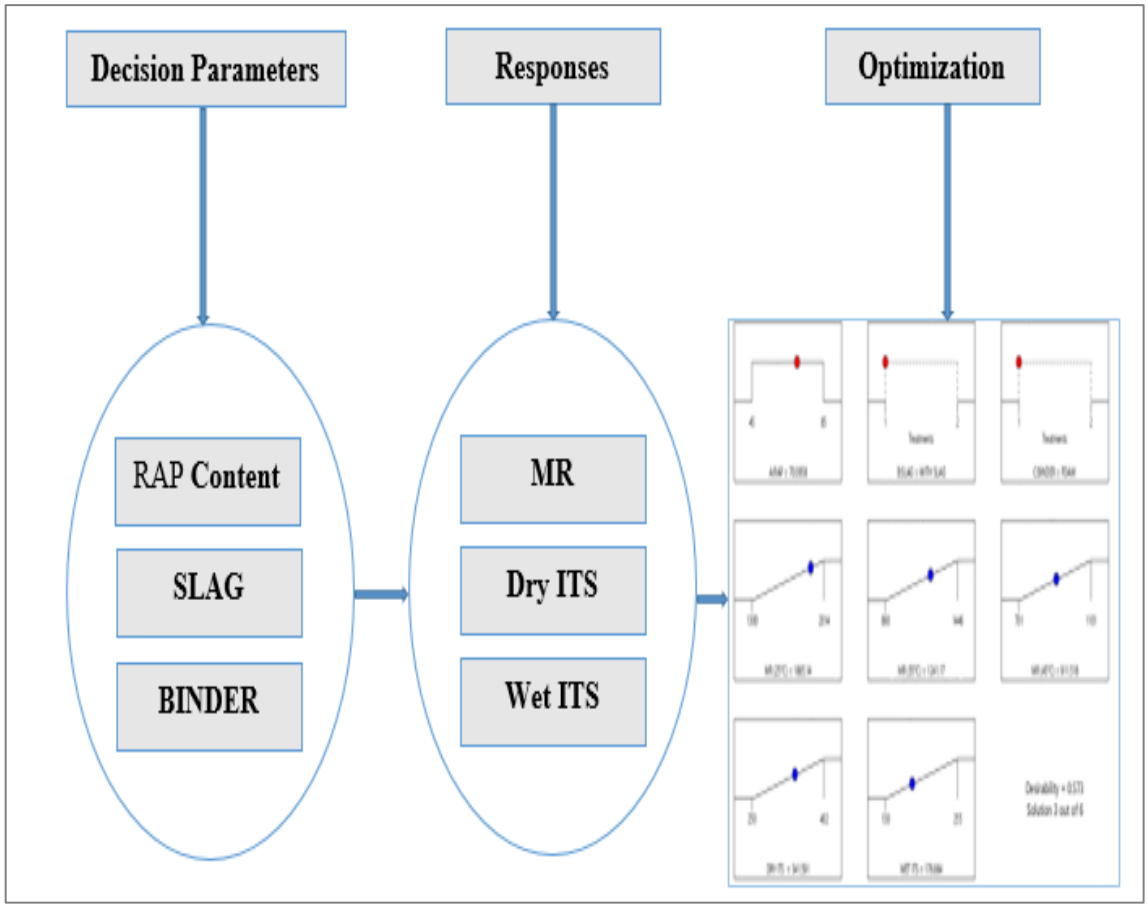

Fig. 5.1. Flow Chart of DoE Approach

5.1 Design of Experiment using RSM

DOE were carried out utilising the response surface methodology (RSM) statistical assessment approach to evaluate the link between their responses and independent variables. DoE software (Design-Expert version 13) was utilised in this investigation for designing, mathematical analysis, optimization, and statistical analysis of process conditions at two levels with three criteria (2^3). Three independent factors were examined: binder content (Foam Bitumen and Emulsion), RAP material percentage varying from 45 to 85 percent, and Slag content (with or without slag). Since the samples were produced, the ambient temperature has been taken into account. The responses (dependent variables) investigated were MR, dry ITS, also moist ITS. The research were carried to investigate the outcome of independent factors on ultimate strength of mix design. The levels as well as range of actual values of the independent variables were determined after testing and are displayed in Table 5.1.

To eliminate systematic bias, 18 laboratory tests were done with triplicates and in a randomized order which is presented in Table 5.1. ANOVA was afterward utilized to evaluate the interaction of the various components as well as the effect of individual parameters. The proposed regression model was utilized to get ideal condition for the responses of three parameters, shown in equation 5.1 (Montgomery, 2012)

$$Y = \beta_0 + \sum^k \beta_j x_j + \sum^k \beta_{jj} x_j^2 + \sum^k \beta_{ij} x_j x_i + e_i \quad (5.1)$$

Where, Y is the response, x_i and x_j are the input parameters,

β is the regression coefficient,

k is the number of parameters included in the experiment and

e is the random error.

5.2 Optimization based on Desirability Function

The software uses model equations derived using RM and the desire function to determine optimal circumstances based on the data provided. The desirability function was first created by Harrington (1965), then Derringer and Such (1980) furthered the technique's development. One of the most widely used techniques for instantaneous multiple response optimization is this one. A value between 0 to 1 is obtained for each solution where O indicates low desirability and 1 indicates high desirability.

Table 5.1: Layout of design of experiment

	Factor 1	Factor 2	Factor 3	Response 1	Response 2	Response 3	Response 4	Response 5
Run	**A:RAP (%)**	**B: SLAG**	**C: BINDER**	**MR (25°C) MPa**	**MR (35°C) MPa**	**MR (45°C) MPa**	**DRY ITS kPa**	**WET ITS kPa**
1	85	WITH SLAG	FOAM	1750	1040	701	370	195
2	65	WITH SLAG	FOAM	1880	1321	1005	305	165
3	85	WITHOUT SLAG	EMULSION	1465	912	788	402	255
4	45	WITH SLAG	FOAM	1803	1240	844	258	133
5	85	WITHOUT SLAG	FOAM	1891	1103	765	383	225
6	85	WITH SLAG	EMULSION	1402	899	744	390	235
7	65	WITHOUT SLAG	EMULSION	1695	1074	859	368	205
8	65	WITHOUT SLAG	FOAM	2014	1446	1101	311	190
9	45	WITHOUT SLAG	EMULSION	1505	1001	803	310	176
10	65	WITH SLAG	EMULSION	1558	1005	877	345	180
11	85	WITH SLAG	FOAM	1740	1030	710	375	185
12	65	WITHOUT SLAG	FOAM	1990	1338	986	285	130
13	45	WITH SLAG	EMULSION	1544	944	809	300	133
14	65	WITH SLAG	FOAM	1870	1310	990	300	160
15	85	WITHOUT SLAG	EMULSION	1455	900	790	250	143
16	65	WITHOUT SLAG	FOAM	2000	1438	1096	300	180
17	65	WITHOUT SLAG	EMULSION	1685	1067	850	360	200
18	85	WITH SLAG	EMULSION	1300	890	750	395	240

5.3 Development of Model

Various variants (quadratic, linear, cubic, and three-factor interactions) have been constructed using RSM for prediction purposes, and it was found that the quadratic model performed the best, having a higher determination coefficient than the other models. It was also shown that quadratic model offered the optimum match for reducing bitumen content in cold and recycled mix technologies (Nassar et al. 2016; Hamzah et al., 2017). As a result, utilising RSM in equation 5.2, a quadratic model for prediction was examined. ANOVA was then used to determine which input variable had the biggest influence on the outcome.

$$Y = \beta_0 + \sum^k \beta_j x_j + \sum^k \beta_{jj} x_j^2 + \sum^k \beta_{ij} x_j x_i + e_i \quad (5.2)$$

In Table 5.2, the ANOVA result for the model outputs is displayed. The outcome demonstrates that the model's F-values for MR at 25°C, 35°C, 45°C, dry ITS, and wet ITS, respectively, are 84.61, 86.46, 89.94, 52.18, and 21.71, with p-values (0.05) for each. A p-value larger than 0.1 often implies that the model terms were negligible (Montgomery, 2012). The models' low p-values also imply that there is just a 0.01 percent possibility that a model F-value of this size may arise due to noise. The ANOVA findings demonstrate that all of the primary factors (Slag content, binder content, and RAP material content) in FBM and EBM mix design have a substantial influence on the ITS and MR. In order to enhance the models, insignificant factors with little significance (P >0.1) were removed from the analysis. According to ANOVA for both models (MR and ITS). In relations of the important influencing factors, the final regression models developed are stated in the subsequent second-order polynomial equations:

$$MR\ (25^{\circ}C) = 1786.37 + 31.17\ x_1 + 48.04\ x_2 + 170.95\ x_3 + 23.40\ x_1^2 + 32.45\ x_2^2 \quad (5.3)$$

$$MR\ (35^{\circ}C) = 1190.87 + 79.81\ x_1 + 34.92\ x_2 + 136.90\ x_3 + 48.06\ x_2^2 \quad (5.4)$$

$$MR\ (45^{\circ}C) = 946.75 + 52.95\ x_1 + 43.27\ x_3 + 45.41\ x_2^2 + 21.36\ x_3^2 \quad (5.5)$$

$$Dry\ ITS = 338.879 + 41.91\ x_1 + 28.04\ x_2 + 70.95\ x_3 + 23.40\ x_2^2 - 32.45\ x_3^2 \quad (5.6)$$

$$Wet\ ITS = 185.011 + 29.92\ x_1 + 18.04\ x_2 + 40.95\ x_3 + 73.40\ x_1^2 \quad (5.7)$$

where x_1 represents RAP content in percentage, x_2 represents SLAG content in categorical, and x_3 represents the Binder in categorical. According to the equations, all three input factors have a positive and substantial influence on MR and ITS. The Binder also has a negative parabolic effect on the dry ITS value, which means that when the input parameter is increased, the output

parameter initially lowers and subsequently grows. Likewise, only the foam bitumen content have substantial favourable influence on the wet ITS.

Table 5.2: ANOVA Variance analysis and the adequacy of quadratic model responses

MR (25°C)

Source	Sum of Squares	df	Mean Square	F-value	p-value
Model	8.180E+05	7	1.169E+05	84.61	< 0.0001
A-RAP	6966.18	1	6966.18	5.04	0.0485
B-SLAG	36321.16	1	36321.16	26.30	0.0004
C-BINDER	4.598E+05	1	4.598E+05	332.88	< 0.0001
AB	4880.44	1	4880.44	3.53	0.0896
AC	9389.04	1	9389.04	6.80	0.0262
BC	1489.23	1	1489.23	1.08	0.3236
A^2	51916.50	1	51916.50	37.59	0.0001
Residual	13811.97	10	1381.20		
Lack of Fit	8119.31	3	2706.44	3.33	0.0861
Pure Error	5692.67	7	813.24		
Cor Total	8.319E+05	17			

MR (35°C)

Source	Sum of Squares	df	Mean Square	F-value	p-value
Model	6.050E+05	7	86434.52	86.46	< 0.0001
A-RAP	45664.17	1	45664.17	45.68	< 0.0001
B-SLAG	19187.57	1	19187.57	19.19	0.0014
C-BINDER	2.949E+05	1	2.949E+05	295.01	< 0.0001
AB	2055.07	1	2055.07	2.06	0.1822
AC	20586.86	1	20586.86	20.59	0.0011
BC	3836.41	1	3836.41	3.84	0.0786
A^2	40258.41	1	40258.41	40.27	< 0.0001
Residual	9997.50	10	999.75		
Lack of Fit	2507.34	3	835.78	0.7811	0.5410
Pure Error	7490.17	7	1070.02		
Cor Total	6.150E+05	17			

MR (45°C)

Source	Sum of Squares	df	Mean Square	F-value	p-value
Model	2.417E+05	7	34534.41	13.94	0.0002
A-RAP	20104.90	1	20104.90	8.12	0.0173
B-SLAG	7946.82	1	7946.82	3.21	0.1035
C-BINDER	29471.38	1	29471.38	11.90	0.0062
AB	62.00	1	62.00	0.0250	0.8774
AC	18377.20	1	18377.20	7.42	0.0214
BC	7980.26	1	7980.26	3.22	0.1029
A^2	48336.18	1	48336.18	19.51	0.0013
Residual	24771.16	10	2477.12		
Lack of Fit	16107.66	3	5369.22	4.34	0.0502
Pure Error	8663.50	7	1237.64		
Cor Total	2.665E+05	17			

DRY ITS

Source	Sum of Squares	df	Mean Square	F-value	p-value
Model	23826.54	7	3403.79	52.18	< 0.0001
A-RAP	12593.09	1	12593.09	8.06	< 0.0001
B-SLAG	367.80	1	367.80	0.2353	0.0014
C-BINDER	4041.14	1	4041.14	2.59	0.0301
AB	1155.63	1	1155.63	0.7393	0.4100
AC	3057.56	1	3057.56	1.96	0.1922
BC	198.37	1	198.37	0.1269	0.7291
A^2	639.34	1	639.34	0.4090	0.5368
Residual	15631.07	10	1563.11		
Lack of Fit	3668.90	3	1222.97	0.7157	0.5732
Pure Error	11962.17	7	1708.88		
Cor Total	39457.61	17			

WET ITS

Source	Sum of Squares	df	Mean Square	F-value	p-value
Model	13144.43	7	1877.78	21.71	< 0.0001
A-RAP	6419.15	1	6419.15	5.84	< 0.0001
B-SLAG	314.37	1	314.37	0.2862	0.0014
C-BINDER	1765.05	1	1765.05	1.61	0.0501
AB	827.31	1	827.31	0.7532	0.4058
AC	0.0057	1	0.0057	5.221E-06	0.9982
BC	134.27	1	134.27	0.1222	0.7339
A^2	81.32	1	81.32	0.0740	0.7911
Residual	10983.57	10	1098.36		
Lack of Fit	2557.41	3	852.47	0.7082	0.5770
Pure Error	8426.17	7	1203.74		
Cor Total	24128.00	17			

5.4 Effect of RAP content, Binder, and Slag Content for ITS and MR

In fact, the ITS test is recognized as one of the best methods for measuring a mix's strength when subjected to strain. As a consequence, samples of ITS test were arranged by varying the concentrations of RAP, binder, and slag in order to investigate their impact on both dry and wet ITS (Fig. 5.2 and 5.3). As a result, the results demonstrate that as RAP concentration increases, dry ITS values with 2.5 percent Foam bitumen binder rise dramatically. However, in the situation of emulsion and foam bitumen, the dry ITS values in emulsion bitumen are greater when slag is present. The existence of binder in RAP material must have activated on increased slag content, leading to the creation of a thicker binder layer. A similar pattern was seen in the case of wet ITS. However, all of the mixes had wet ITS values of more than 100kPa, which met the code's minimum required limit (IRC 37, 2012). The drying of Portland cement as a filler is also one of the reasons for increased wet ITS. Furthermore, emulsion bitumen increases aggregate coating or creates a homogeneous weld on the aggregate and binder interface, leading to greater ITS values.

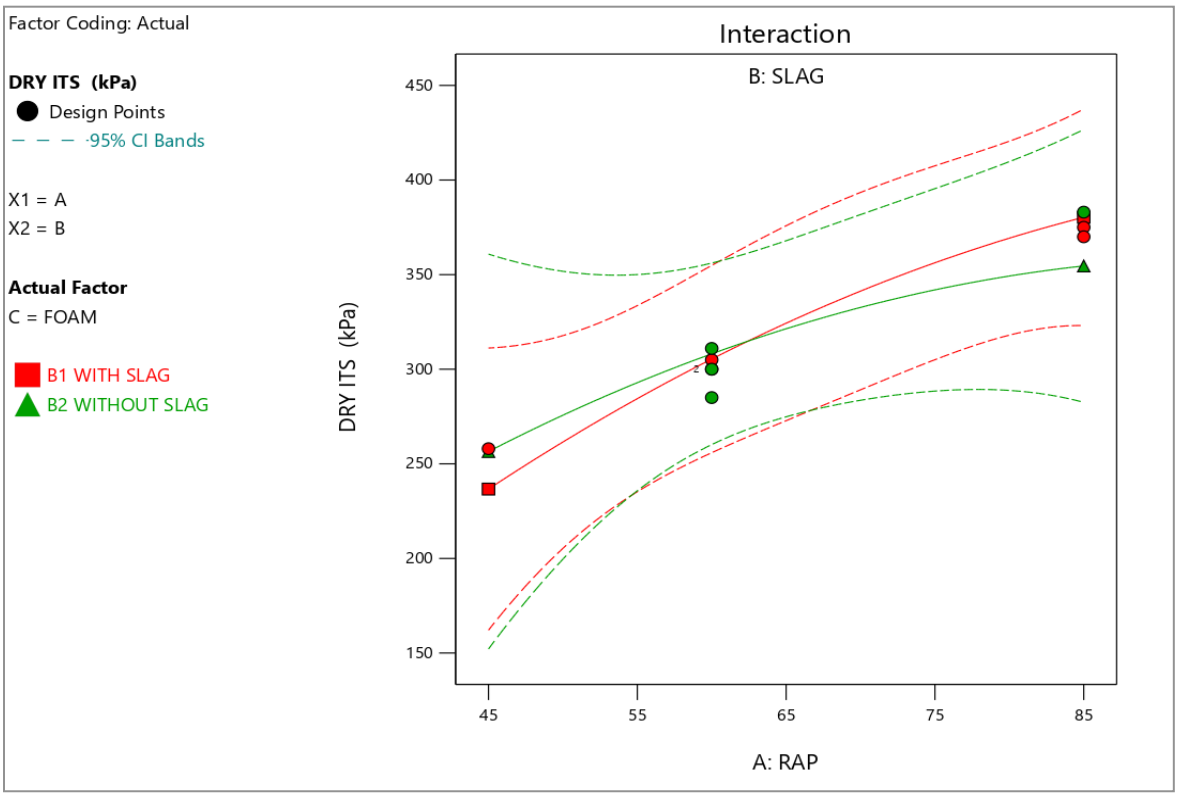
Factor Coding: Actual
DRY ITS (kPa)
Design Points
95% CI Bands
X1 = A
X2 = B
Actual Factor
C = FOAM
B1 WITH SLAG
B2 WITHOUT SLAG
Interaction
B: SLAG
DRY ITS (kPa)
450
400
350
300
250
200
150
45
55
65
75
85
A: RAP

(a)

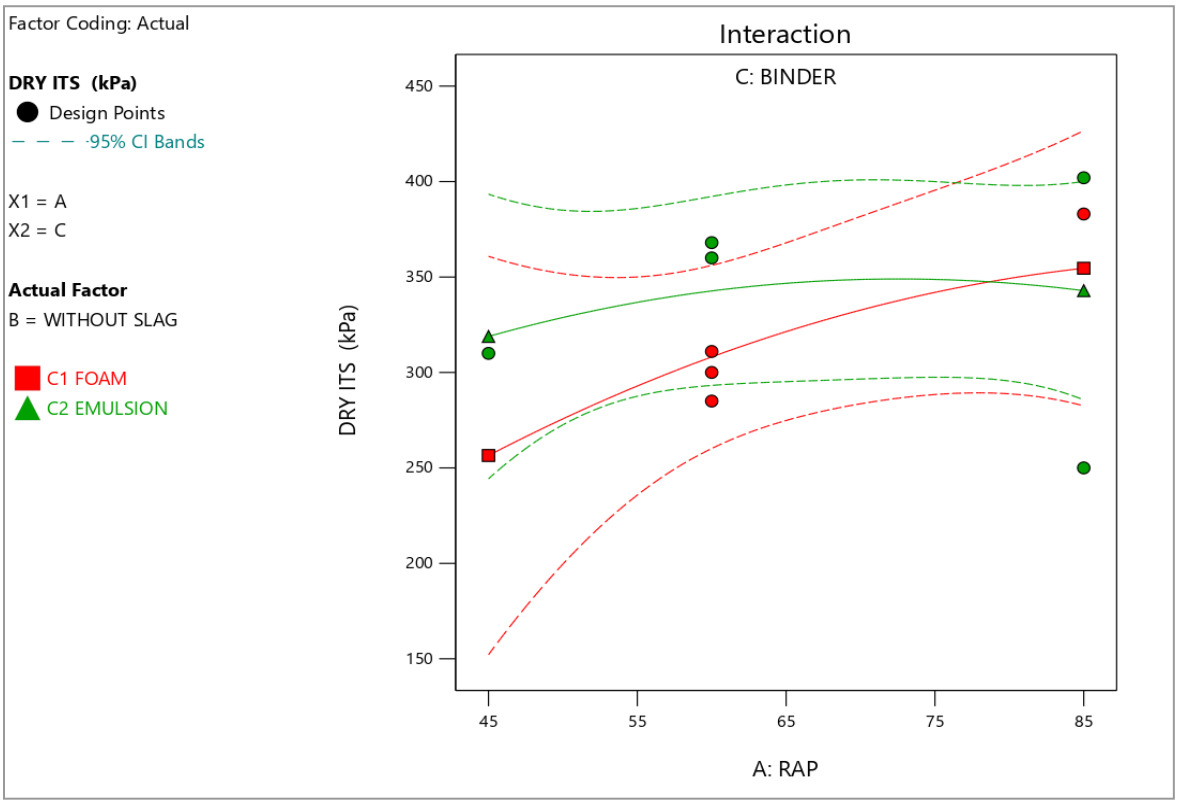
Factor Coding: Actual
DRY ITS (kPa)
Design Points
95% CI Bands
X1 = A
X2 = C
Actual Factor
B = WITHOUT SLAG
C1 FOAM
C2 EMULSION
Interaction
C: BINDER
DRY ITS (kPa)
450
400
350
300
250
200
150
45
55
65
75
85
A: RAP

(b)

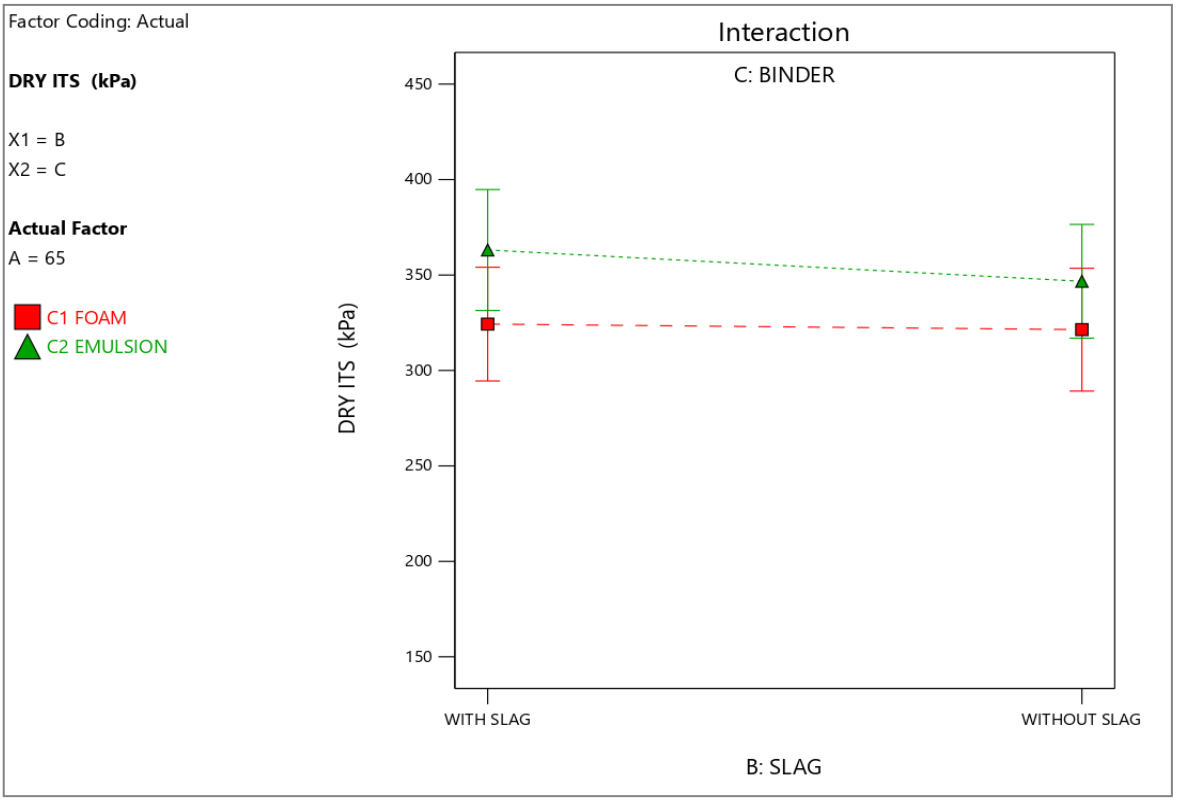

(c)

Fig 5.2: Variation of Dry ITS at different Actual Factors

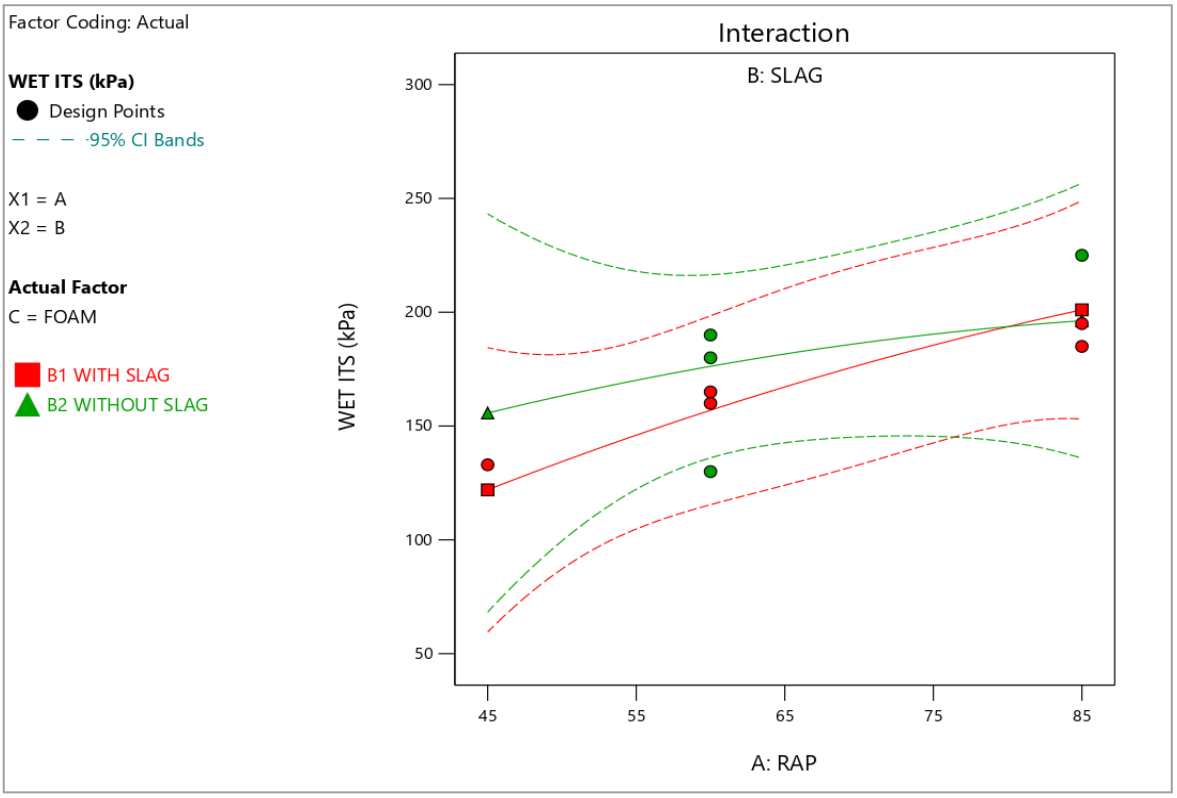

(a)

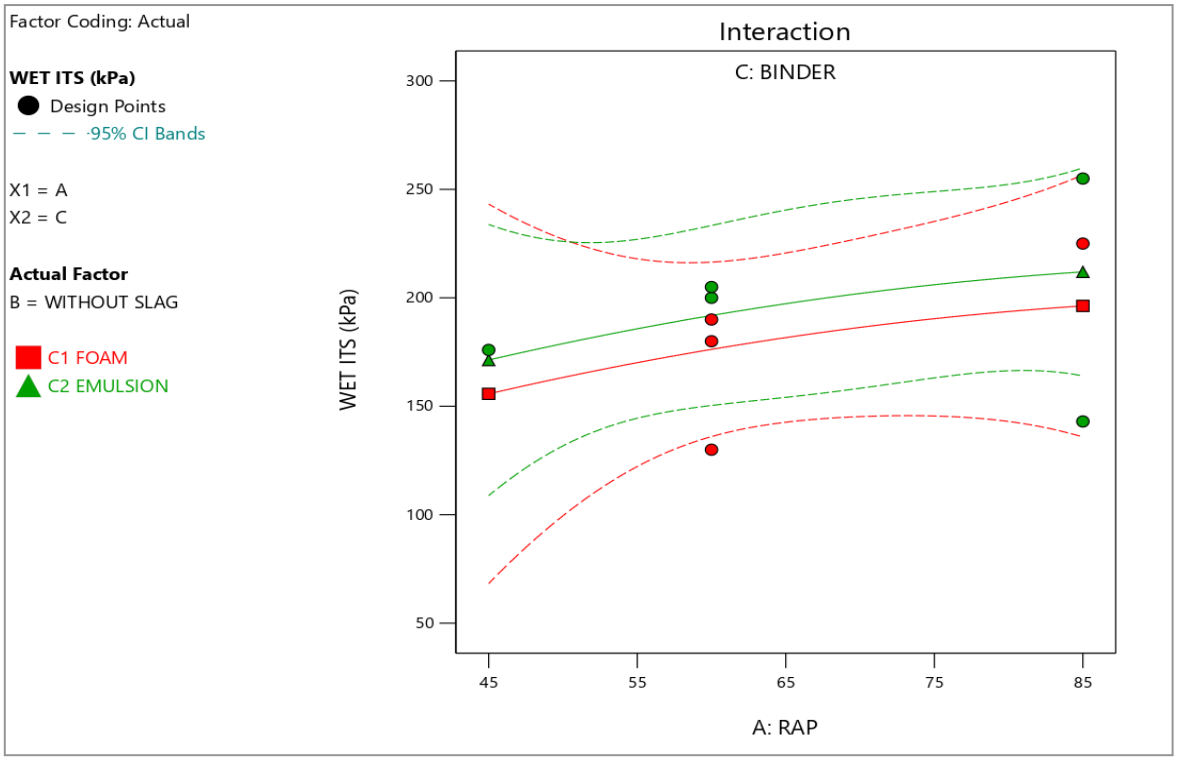

(b)

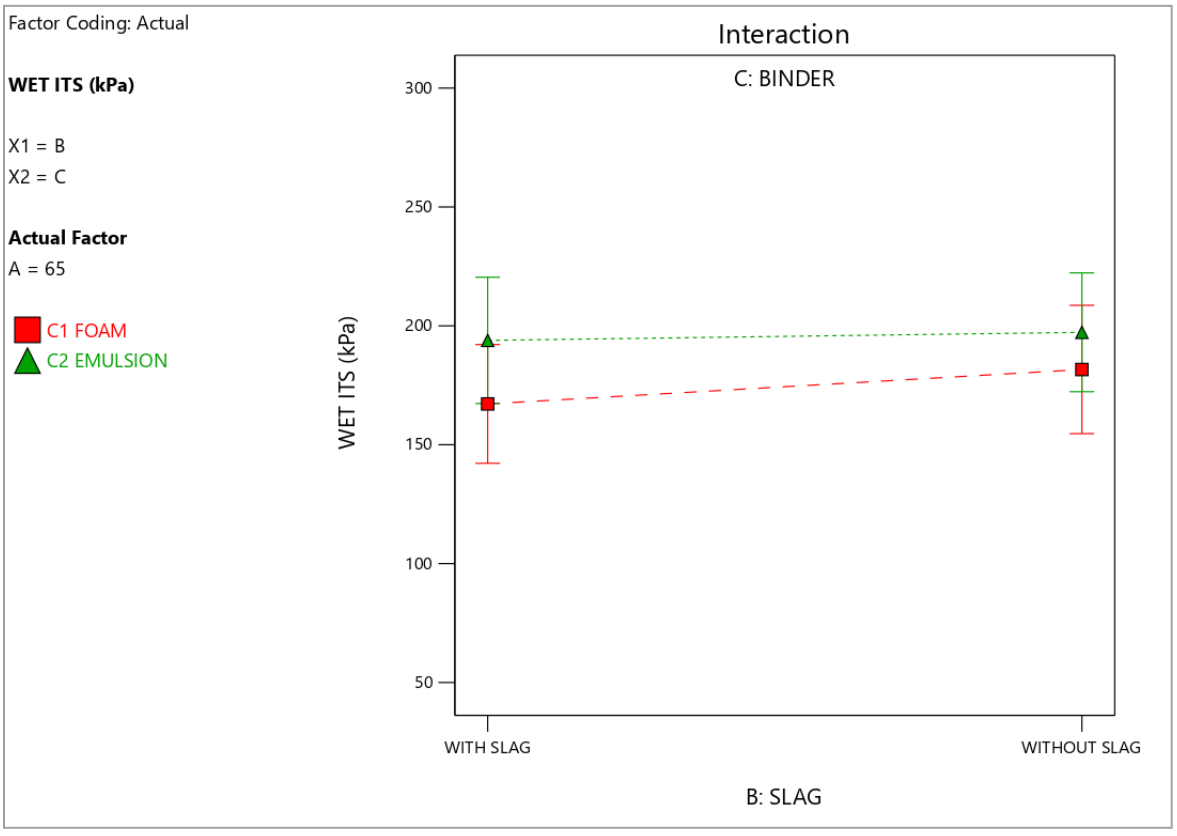

(c)

Fig 5.3: Variation of Wet ITS at different actual factors

Similarly, resilient modulus at temperatures at 25°C, 35°C, and 45°C was investigated through a model graph (Fig. 5.4, 5.5, and 5.6) in order to find out that the foam bitumen binder and with slag content has higher values of MR at different temperature. Thus, for specific binder and slag content, through increased RAP content, the MR values increase and then decrease from the peak however, at lower RAP content bitumen becomes inadequate and does not deliver proper lubrication throughout compaction. MR at 25°C, 35°C shows similar trend showing a plot which is close interaction in the pattern obtained between independent variables. However, MR at all temperatures was found to be higher at 65% RAP material content whereas the binder and slag content variation is almost the same. As per the response surface model, When the model graphs are linear, it suggests that the interaction effect is not substantial, but when the model graph has a significant amount of curvature, it suggests that the interaction effect is significant and huge.

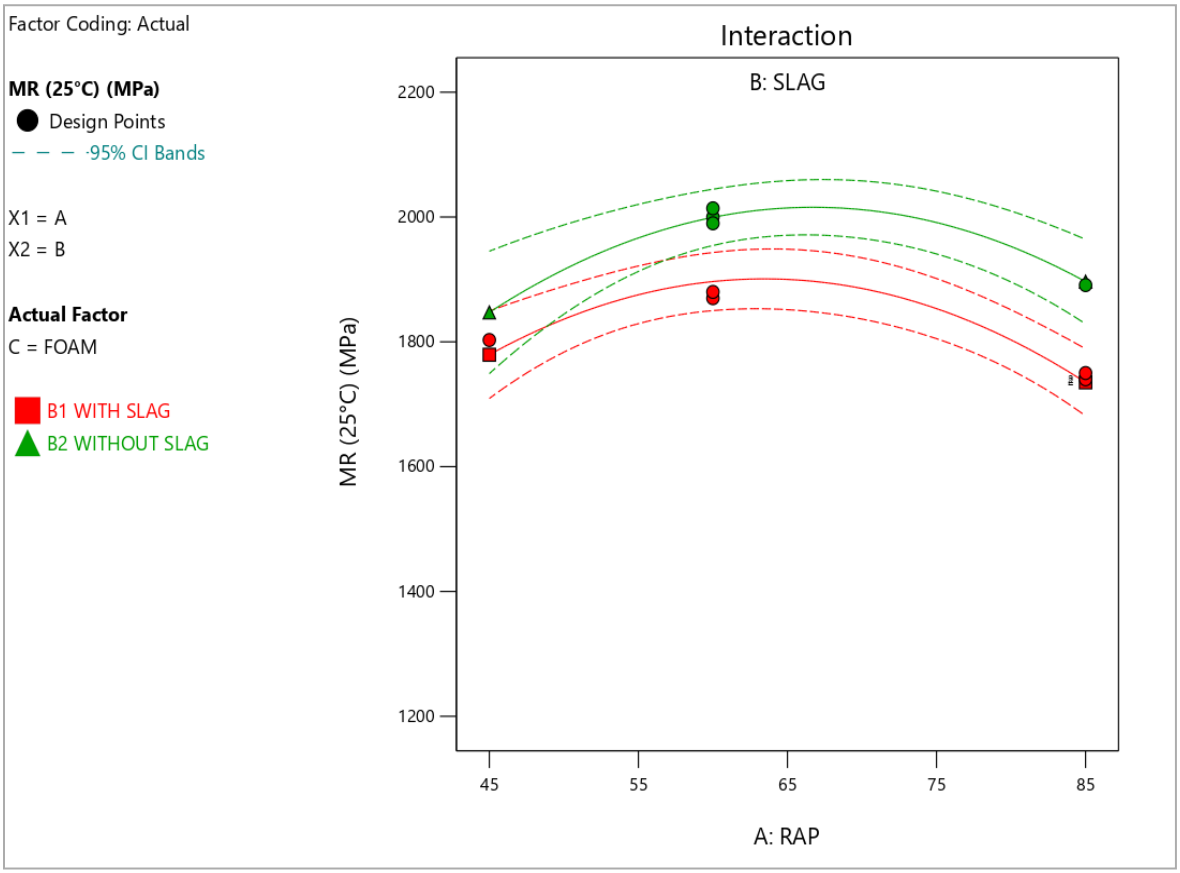

(a)

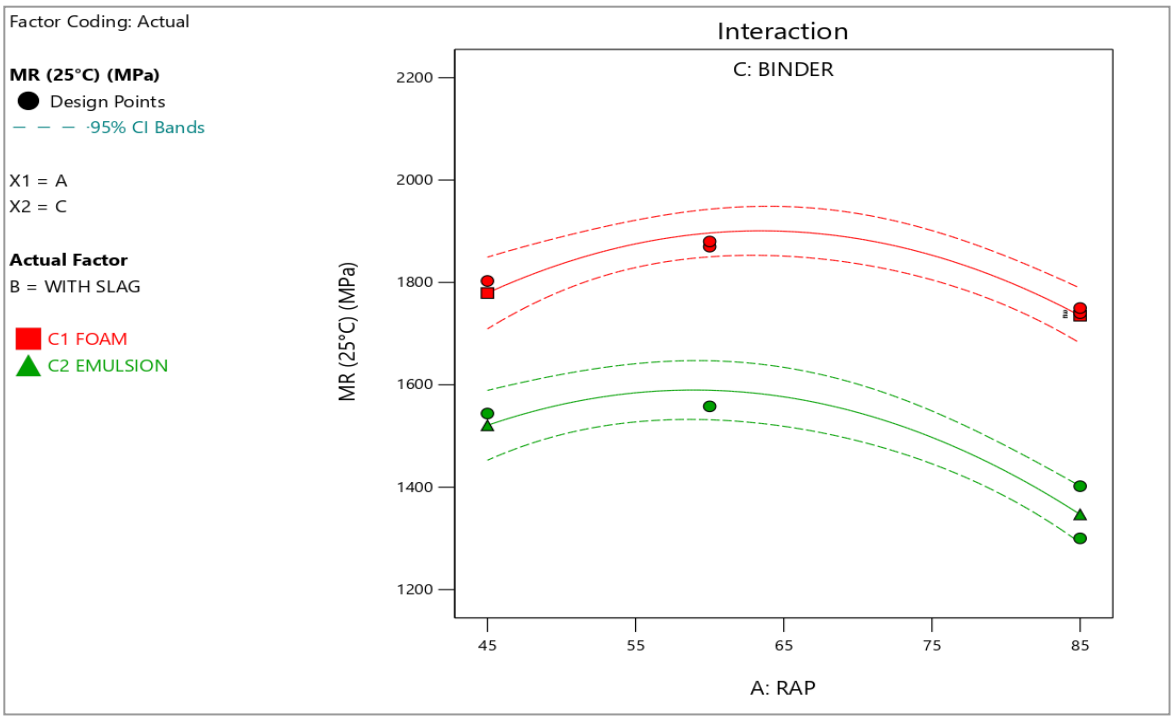

(b)

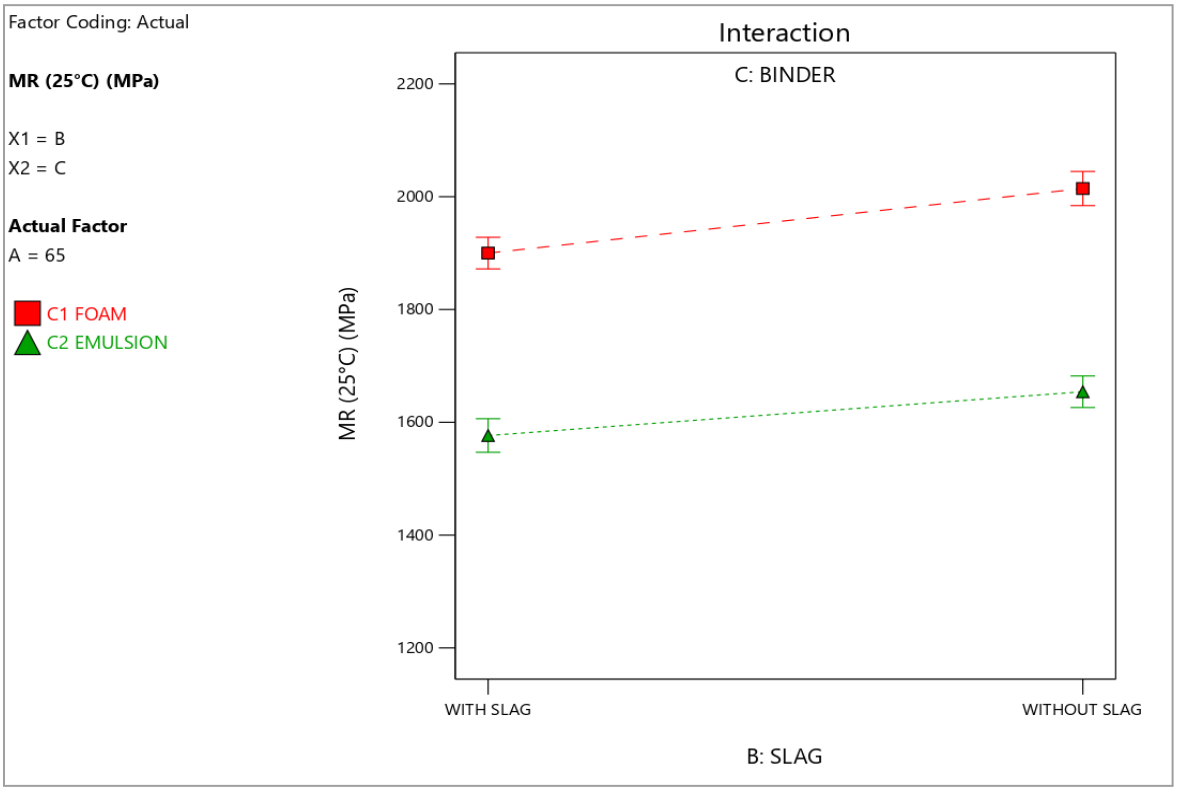

(c)

Fig 5.4: Variation of MR 25°C at different actual factors

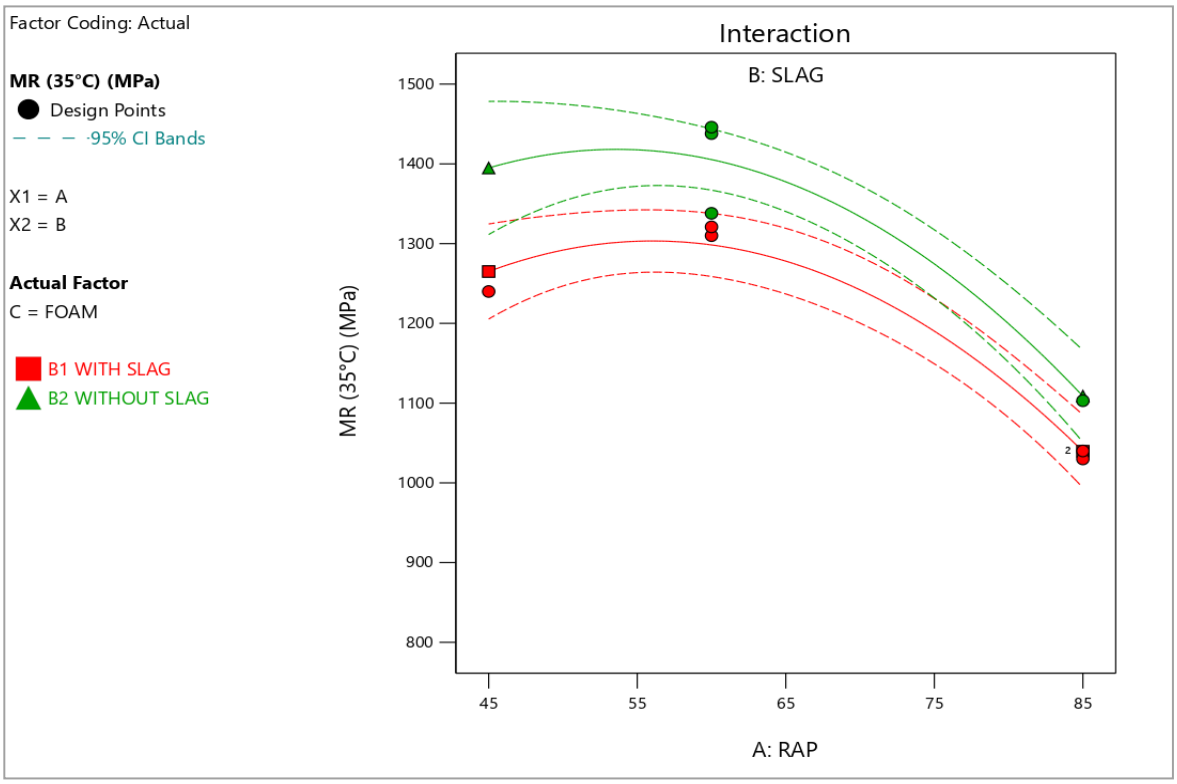
Factor Coding: Actual
MR (35°C) (MPa)
Design Points
95% CI Bands
X1 = A
X2 = B
Actual Factor
C = FOAM
B1 WITH SLAG
B2 WITHOUT SLAG
Interaction
B: SLAG
MR (35°C) (MPa)
1500
1400
1300
1200
1100
1000
900
800
45
55
65
75
85
A: RAP

(a)

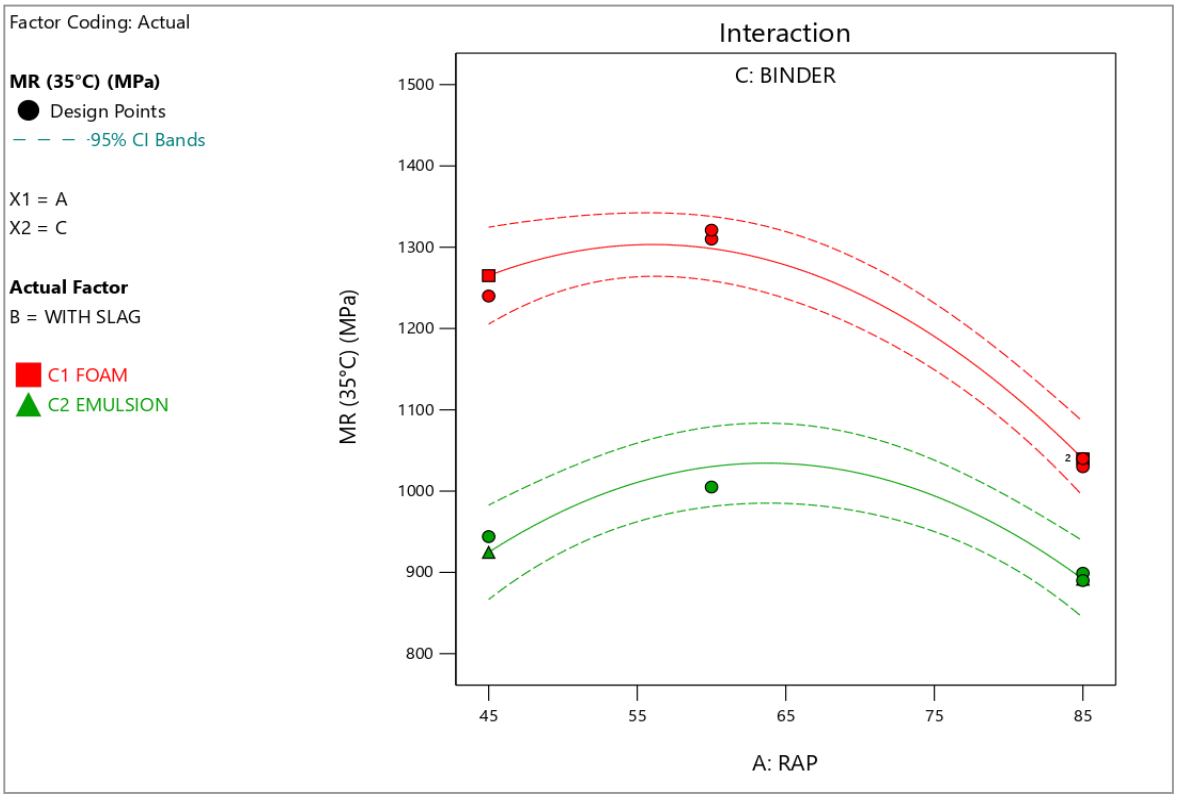
Factor Coding: Actual
MR (35°C) (MPa)
Design Points
95% CI Bands
X1 = A
X2 = C
Actual Factor
B = WITH SLAG
C1 FOAM
C2 EMULSION
Interaction
C: BINDER
MR (35°C) (MPa)
1500
1400
1300
1200
1100
1000
900
800
45
55
65
75
85
A: RAP

(b)

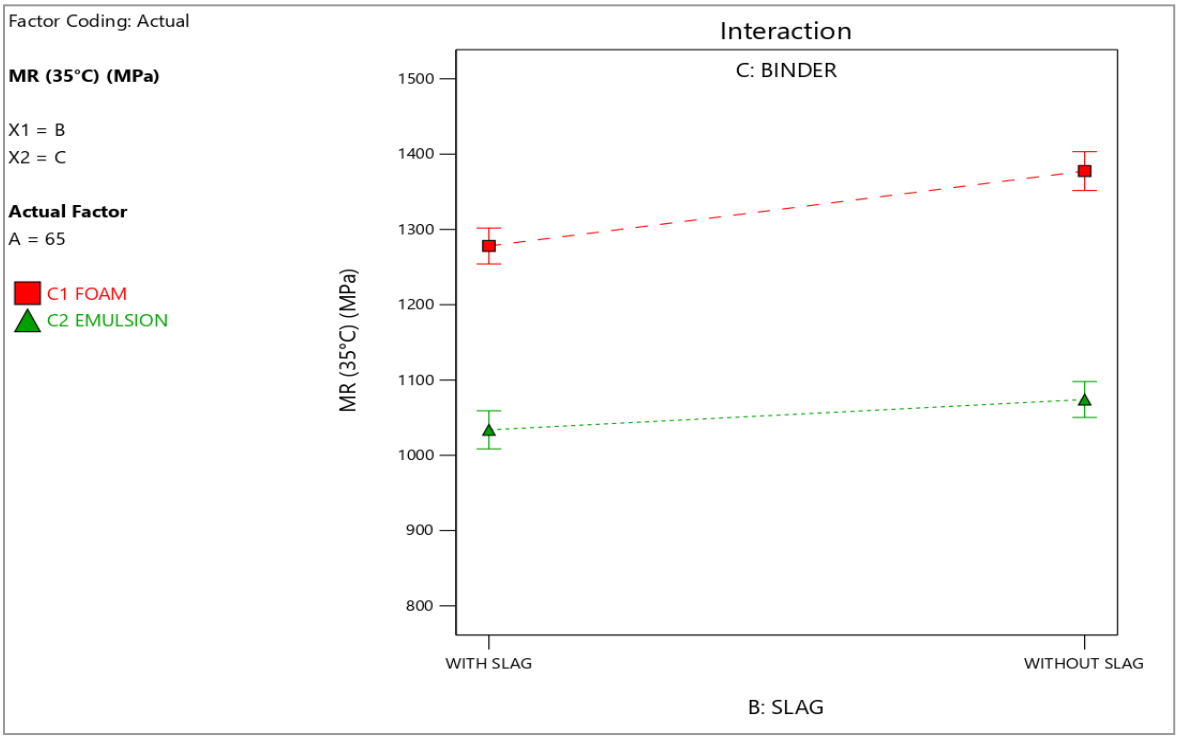

(c)

Fig 5.5: Variation of MR 35°C at different actual factors

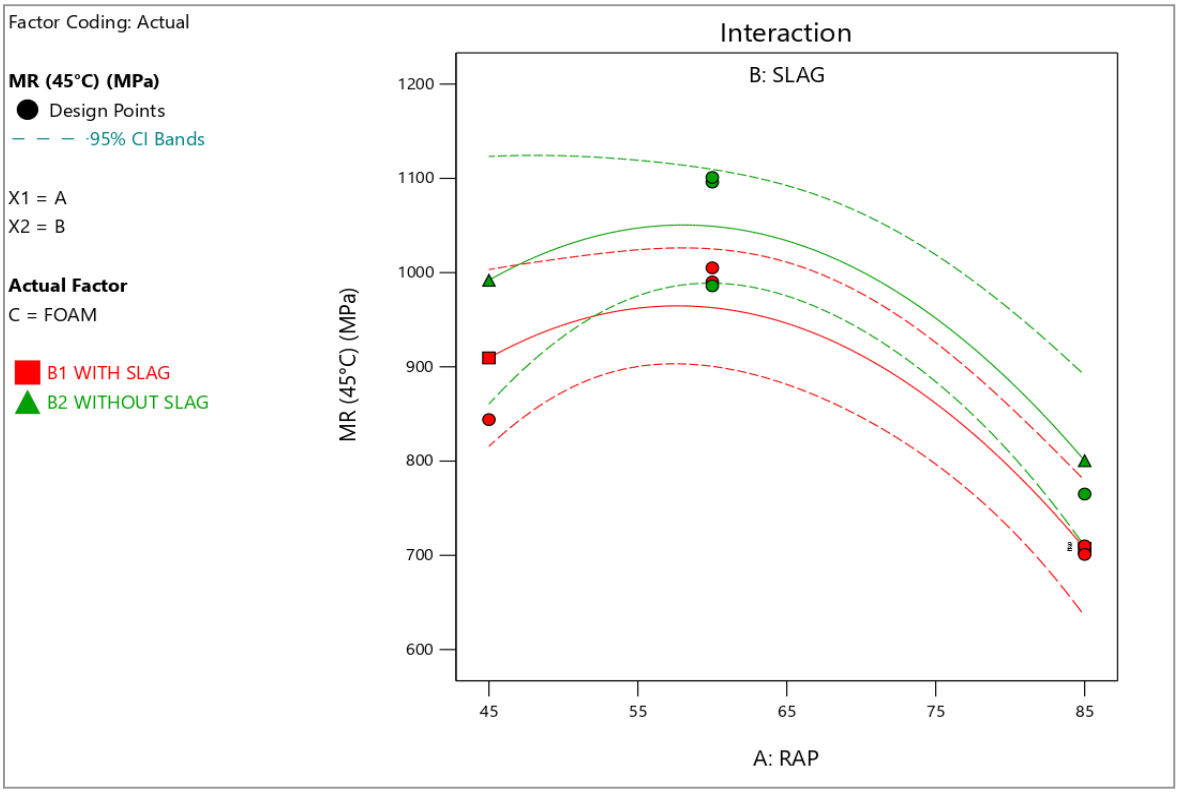

(a)

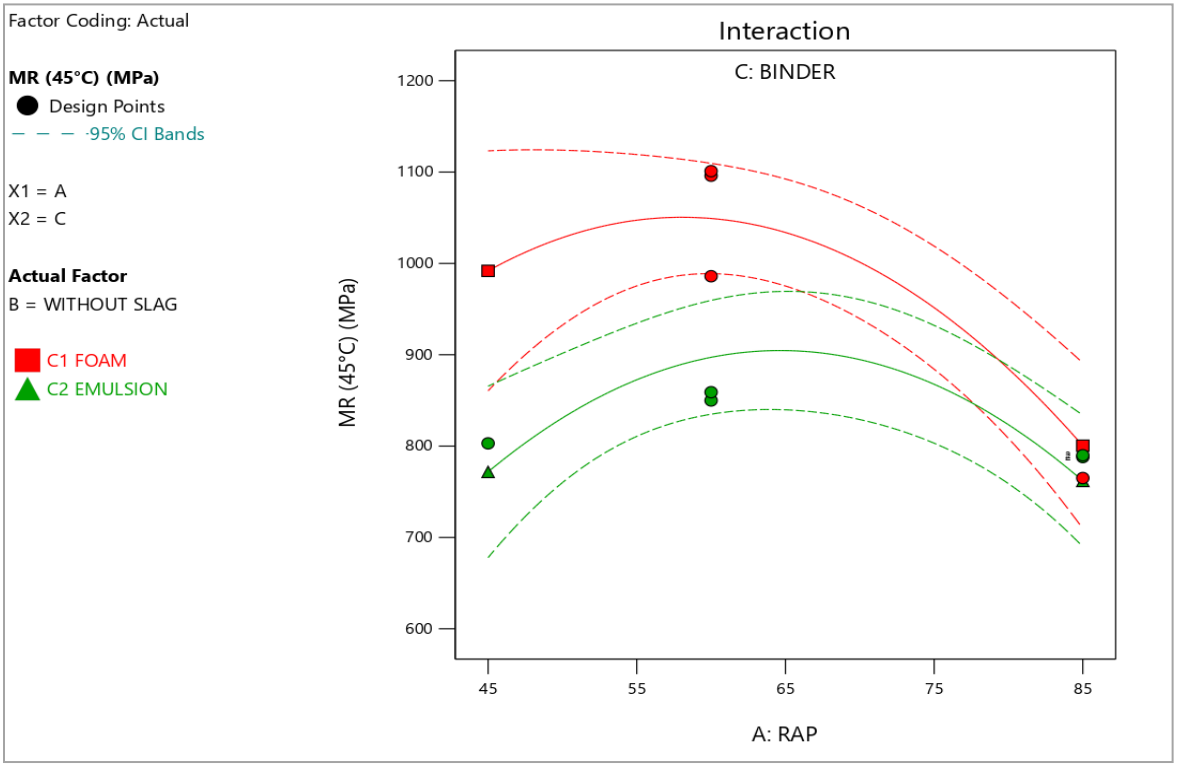

(b)

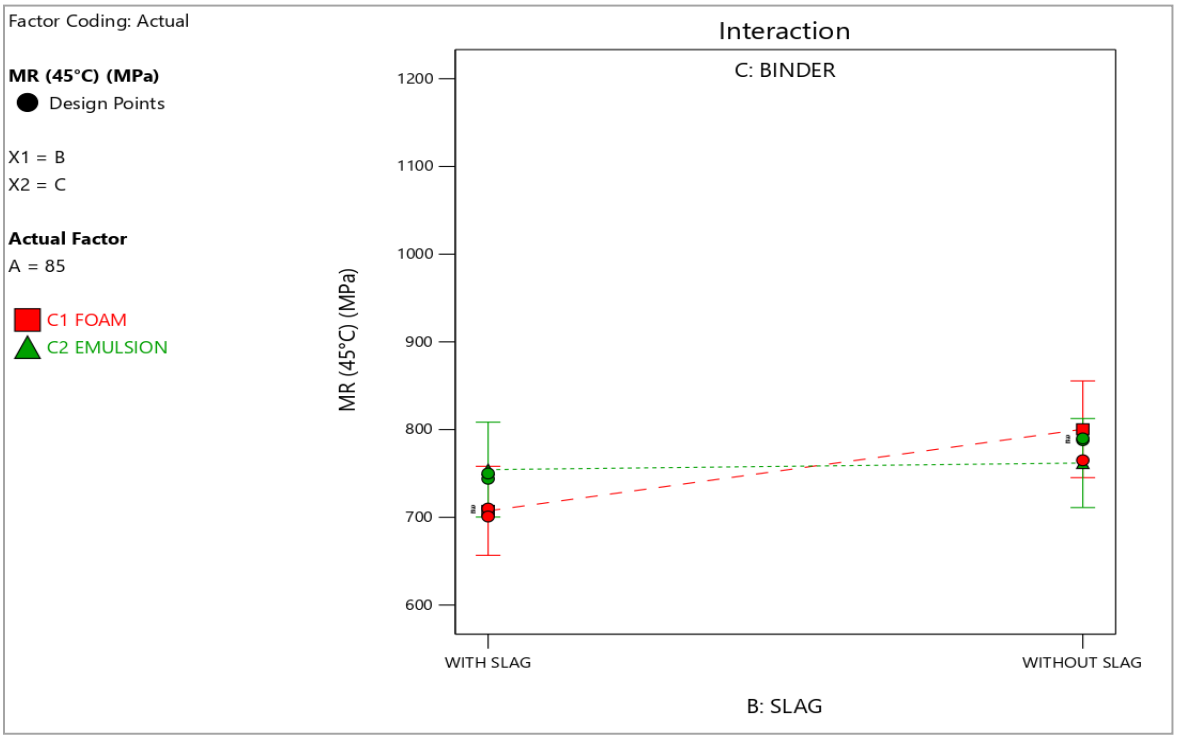

(c)

Fig 5.6: Variation of MR 45°C at different actual factors

5.5 Statistical Analysis of Response Variable Test Results

Statistical analysis ware performed to assess mix results in terms of prior tests performed in earlier stages. To forecast the answers, quadratic models were built. The created models' quality was assessed using R2, standard deviation, and appropriate precision (AP) for three-level factorial optimization. The specifics of three-level optimization are provided below.

R^2 values for dry ITS, wet ITS, MR at 25°C, MR at 35°C, and MR at 45°C were 0.9339, 0.9148, 0.9434, 0.9837, and 0.9071 for three factorial optimizations. The high R2 values, which are more than minimal threshold of 0.80 for a successful model fit, suggests the actual and projected values are in fair and desirable agreement (Montgomery, 2012; Noordin. 2004). As a result, for the ITS and MR, the projected R^2 agrees with the adjusted R^2 since the difference between the two values is smaller than 0.2. (Shown in Table 5.3).

An extra tool, incorporated within software, known as "Adequate Precision," was utilised to analyse the produced model (AP). The experimental signal-to-noise ratio is measured using AP. It compares the projected value range at each design point to the mean prediction error. For forecasting reaction inside the space examined by the experiment, models with AP larger than 4 are preferred. The AP values of the models in this example were 15.51, 14.79, 26.34, 24.37, and 20.30 for dry ITS, wet ITS, MR at 25°C, MR at 35°C, and MR at 45°C, respectively. Thus these are larger than 4, indicating that model can be utilised to navigate the DOE-defined space. R^2 values and AP obtained for all grade of bitumen binders are presented in Table 5.3.

Table 5.3: Statistical results for three level factorial optimizations

Responses	R^2	adjusted R^2	Adequate Precision (AP)
Dry ITS	0.9339	0.8939	15.51
Wet ITS	0.9148	0.8540	14.79
MR at 25°C	0.9434	0.9034	26.34
MR at 35°C	0.9837	0.9037	24.37
MR at 35°C	0.9071	0.8671	20.30

5.6 Desirability Approach for Optimization

The programme also determines the maximum attractiveness for a lot of replies at the same time. As a result, the desirability approach to optimization issues seeks the most desirable solution. An optimal objective function is utilised when there are several response variables. The weighted average of the various desirability functions is the overall desirability function. As a result, the desired performance reaction was set to maximum in order to attain a longer service life with its performance.

The optimal combination ranges of the independent factors were chosen in order to optimize the result of the performance qualities in order to satisfy the intended optimization goal (criteria) (Table 5.4). Additional laboratory tests were conducted to verify the experimental and anticipated results for optimal mix design proportions produced by the RSM model utilising 65% RAP content. Since the percent error difference is minimal, it was noticed that the experimental findings were rather near to the expected results, demonstrating that the parameter estimates for generated models are pretty consistent with the experimental.

Table 5.4: Optimization criteria

Parameter	Unit	Desired Goal	Lower Limit	Upper Limt
RAP Content	%	Maximize	45	85
Binder Content	-	Categorical	Foam Bitumen	Bitumen Emulsion
Slag Content	-	Categorical	With Slag	Without Slag
Dry ITS	kPa	Maximize	-	-
Wet ITS	kPa	Maximize	-	-
MR at 25°C	MPa	Maximize	-	-
MR at 35°C	MPa	Maximize	-	-
MR at 45°C	MPa	Maximize	-	-

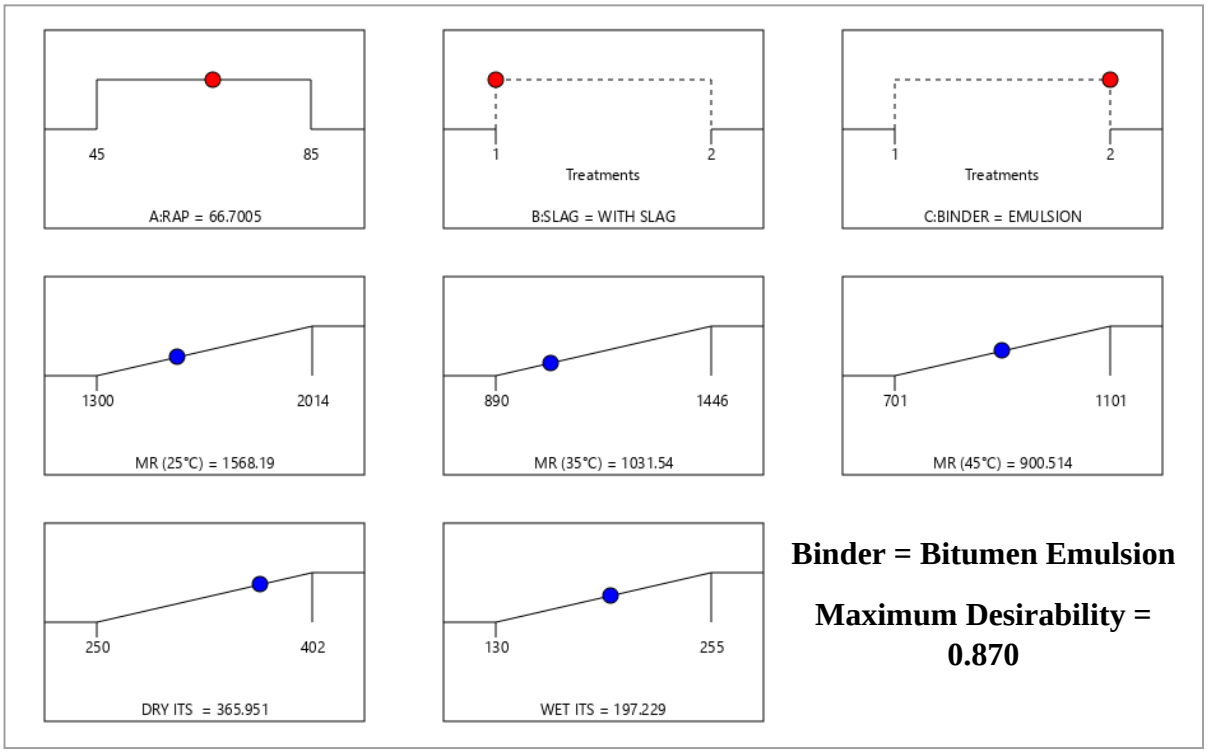

(a)

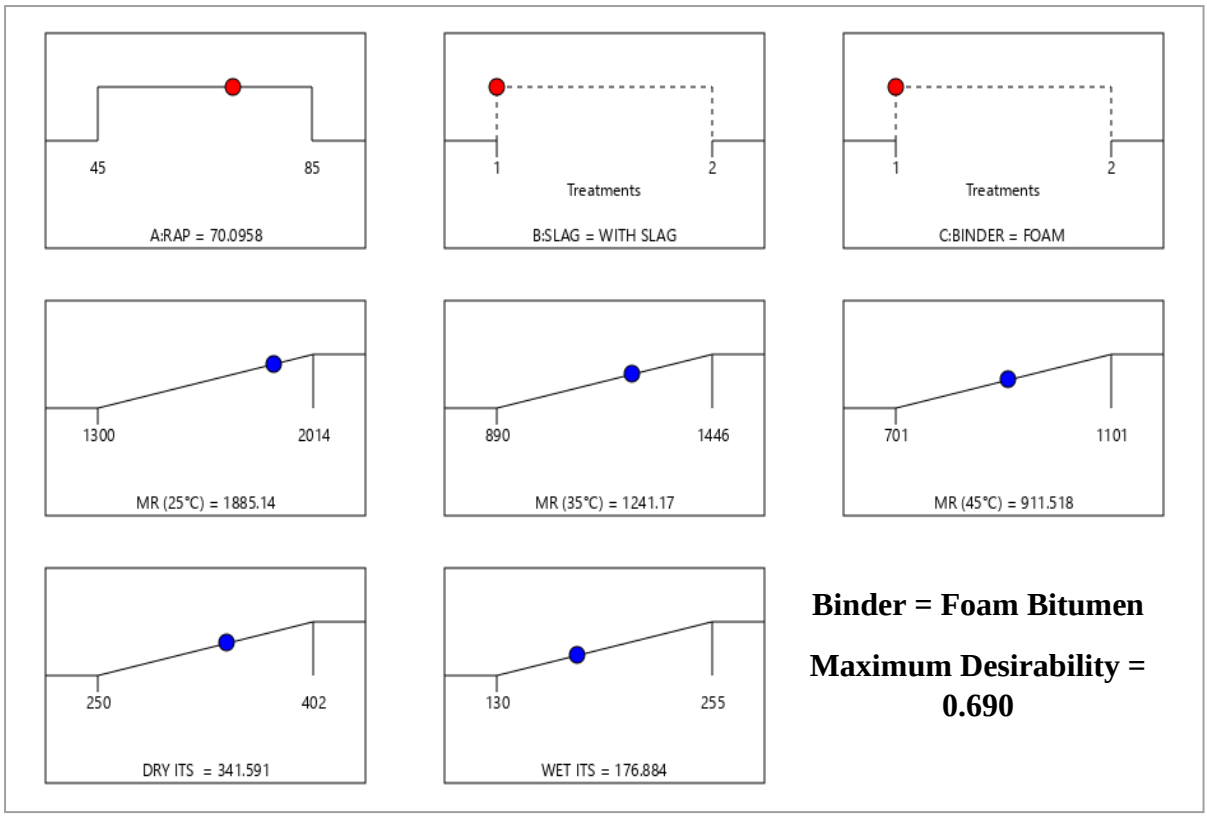

(b)

Fig. 5.7: Numerical optimization of design mixture

CHAPTER 6

RESULT AND DISCUSSION

The current study employs number of laboratory tests to assess the strength of bituminous mixes. In this portion of the report, the findings of numerous tests are reviewed and presented.

6.1 Emulsion Bitumen Mix

6.1.1 Moisture Susceptibility

In an HMA mixture, moisture-induced weakening or loss of adhesion seen between both aggregate surface and binder is known as moisture susceptibility. In order to investigate moisture susceptibility of cold bituminous mixtures, Tensile Strength Ratio, Indirect Tensile Strength, and tests were accomplished on samples comprehending varying amounts of RAP. The results demonstrate that the maintained tensile strength ratios of cold mixtures including RAP outperformed standard mixes in terms of moisture resistance. This demonstrates that a combination with a larger proportion of RAP is less prone to stripping.

6.1.2 Indirect Tensile Strength

The ITS tests were performed in both dry and wet circumstances using marshall compacted samples generated at Optimum Emulsion Content. The samples were made with various RAP percentages (45%, 65%, and 85%) and slag content (with and without slag) using binder grades (VG-10) as shown in Tables 6.1. Figures 6.1 and 6.2 show the dry and wet ITS values, respectively. It was discovered that increasing RAP concentration resulted in a substantial rise in ITS values in both dry and wet environments.

Table 6.1: Dry ITS, Wet ITS, and TSR Test Results for Emulsion Binder

S.No.	RAP %	Slag Content	ITS Dry (kPa)	ITS Wet (kPa)	TSR (%)
1	**85%**	Without Slag	402	255	63
2	**65%**	Without Slag	368	205	55
3	**45%**	Without Slag	310	176	56
4	**85%**	With Slag	390	235	60
5	**65%**	With Slag	345	180	52
6	**45%**	With Slag	300	153	51

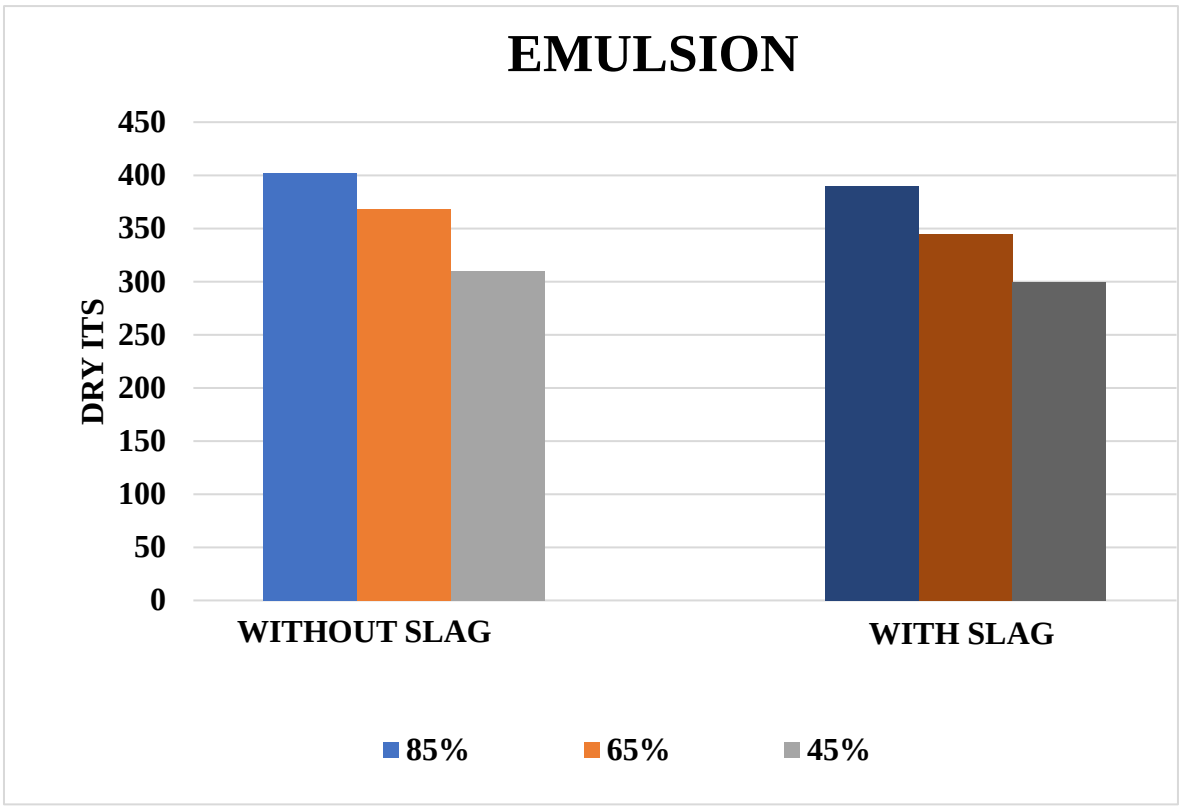

Fig 6.1: Variation of Dry ITS (kPa) with RAP content and slag content

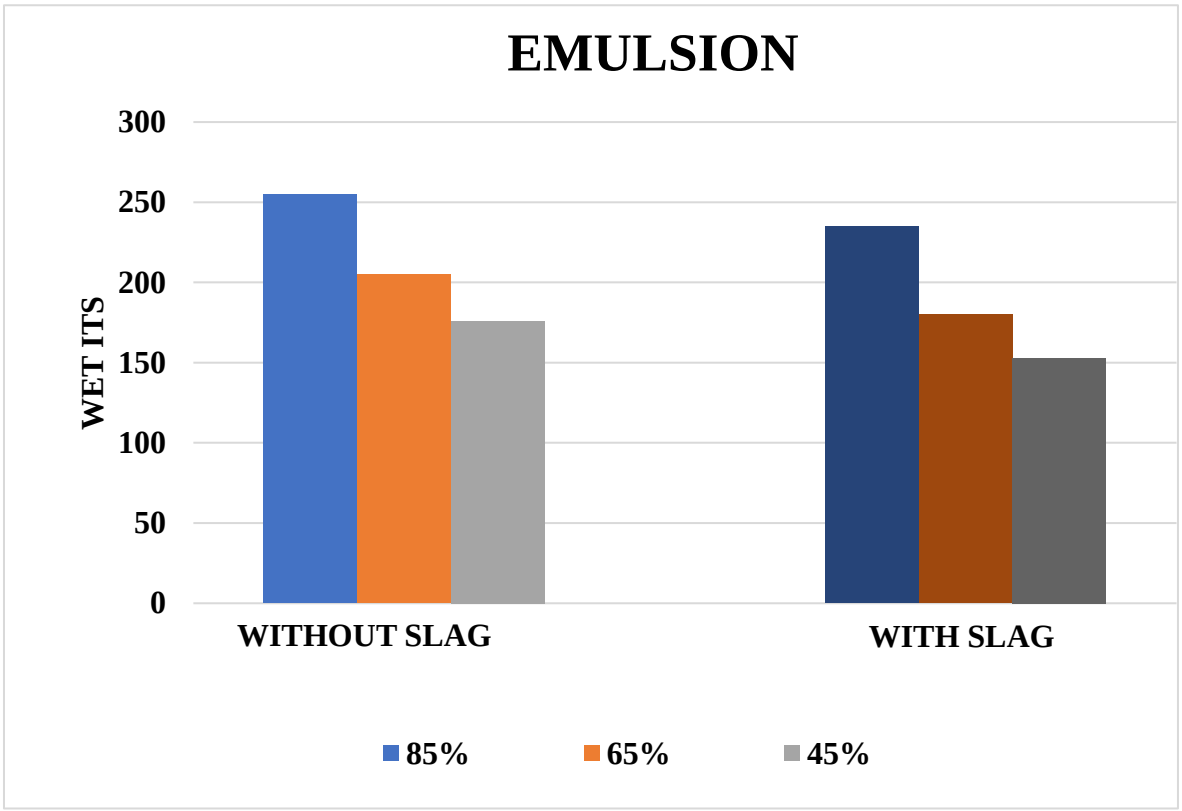

Fig 6.2: Variation of Wet ITS (kPa) with RAP content and slag content

6.1.3 Resilient Modulus Test

Figures 6.3, 6.4, and 6.5 show the fluctuation of resilient modulus with RAP % and Slag content for the VG-10 binder at 25°C, 35°C, and 45°C, respectively. Keeping all other factors fixed, 25°C had higher resilient modulus than 35°C and 45°C for all mixes. This finding suggests that the slag content of EBM has a considerable impact on the sample mix's resilient modulus. All EBM samples displayed increased resilience modulus with increasing RAP concentration and eventually decreased for a given binder grade. For all mixes, the maximum robust modulus was recorded at 65 percent RAP concentration. This can be due to softening of aged binder in 65 percent RAP combinations related to 45 percent RAP mixtures. The inclusion of an extra stiff binder (recovered binder) lowers the cohesion of the mix at 85 percent RAP content, resulting in a lower resilient modulus value. All combinations displayed improved resilience modulus with slag concentration for the specific grade of binder and RAP component.

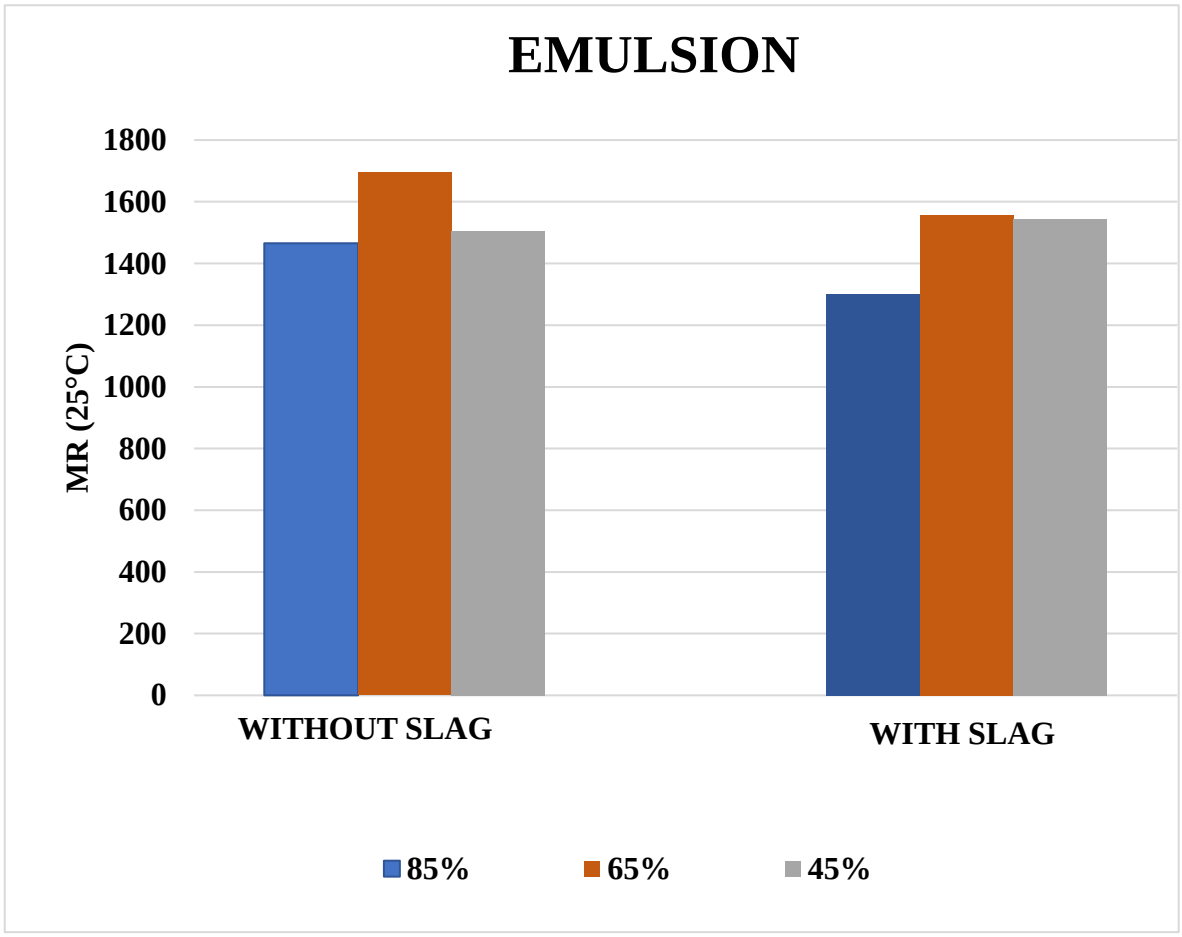

Fig 6.3: Variation of MR at 25°C (MPa) with RAP percentage and slag content

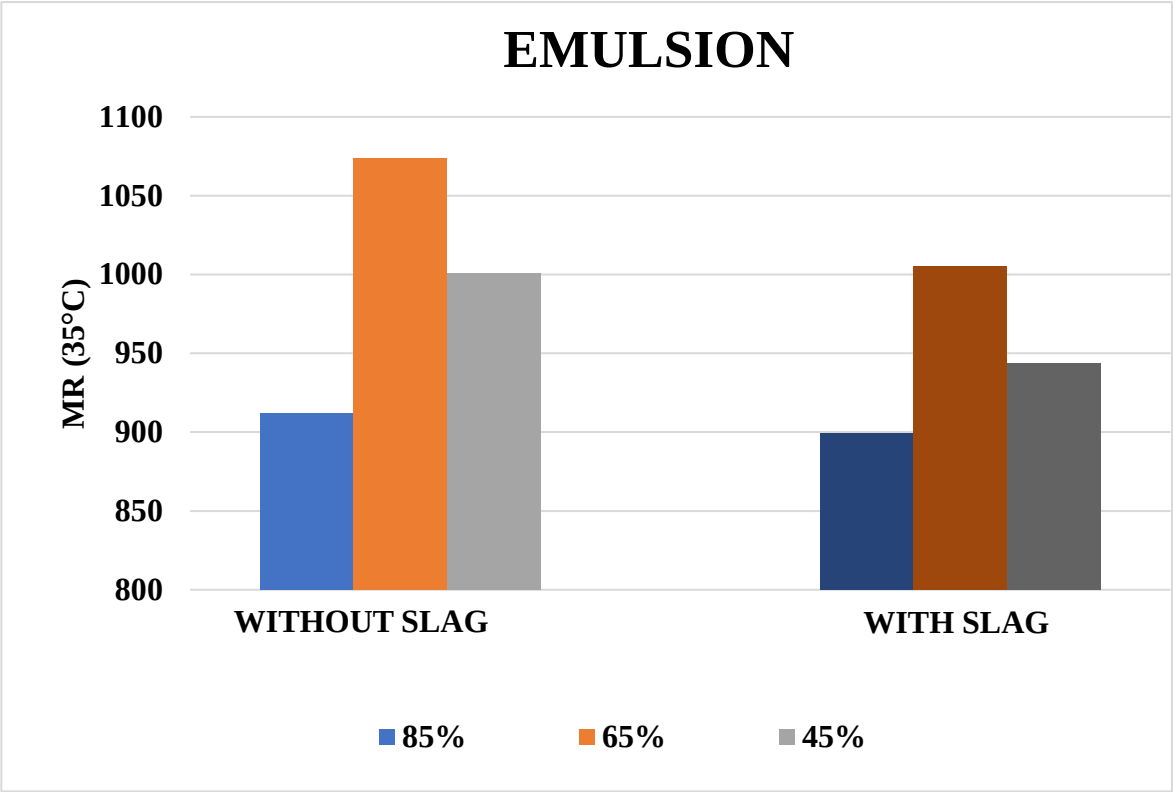

Fig 6.4: Variation of MR at 35°C (MPa) with RAP percentage and slag content

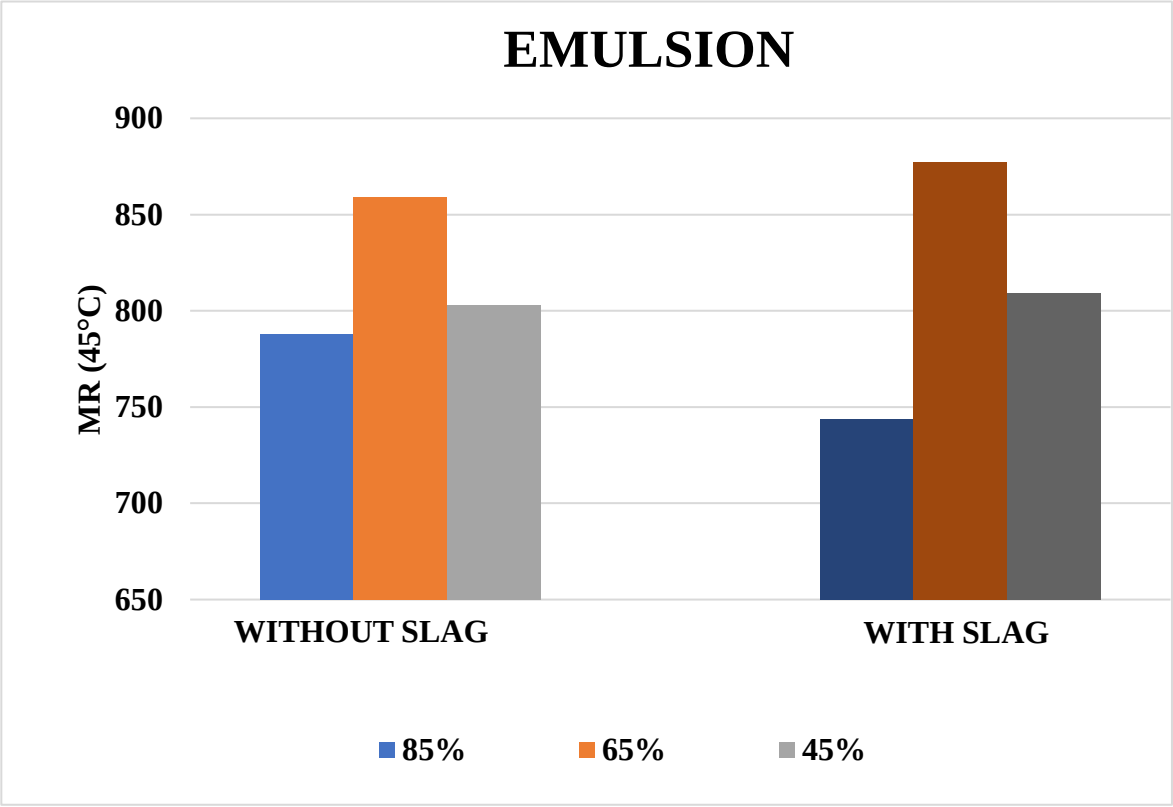

Fig 6.5: Variation of MR at 45°C (MPa) with RAP percentage and slag content

6.1.4 Tensile Strength Ratio

Considering EBM has a large low early strength, void content, a slow rate of strength growth, and a low binder concentration, its strength properties are greatly reliant on the moisture present. As a result, moisture susceptibility is an important element in determining EBM performance. The ITS tests were carried out on a marshall compactor, findings for dry ITS, wet ITS, and TSR values for VG 10 binder are already shown in Tables 6.1. The specification specifies 225 kPa and 100 kPa as the minimum acceptable values for dry and wet ITS, respectively (Asphalt Academy, 2020; IRC 37, 2012). Furthermore, the literature states that if the value falls lower to 100 kPa, the mix can be used by applying an active filler like as cement or lime (Asphalt Academy. 2020). According to the literature, in the case of EBM, a TSR value less than 40% suggests questionable material (Kushwaha and Swampy, 2019). Figure 6.6 depicts the fluctuation of TSR with RAP content and mixing temperature. In the current study, the TSR value for all mixes is greater than 50%, which is greater than the minimal criterion of 40%.

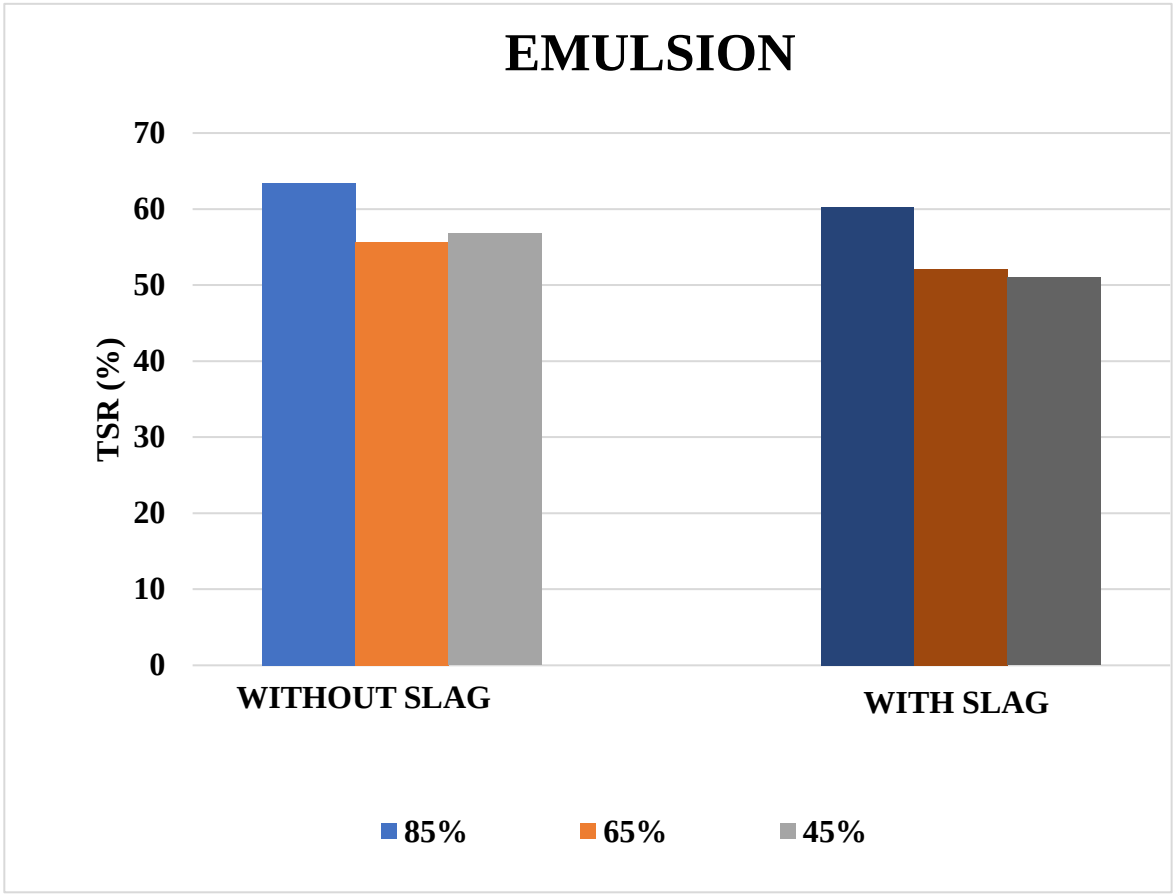

Fig 6.6: Variation of TSR with RAP percentage and slag content

6.2 Foam Bitumen Mix

6.2.1 Indirect Tensile Strength

The ITS tests was performed in both dry and wet circumstances using marshall compacted samples generated at Optimum Foam Bitumen Content. The samples were made with various RAP percentages (45%, 65%, and 85%) and slag content (with and without slag) using binder grades (VG-10) as shown in Tables 6.2. Figures 6.7 and 6.8 show the dry and wet ITS values, respectively. It was discovered that increasing RAP concentration resulted in substantial rise on ITS values in both dry and wet environments.

Table 6.2: Dry ITS, Wet ITS, and TSR Test results for emulsion binder

S.No.	RAP %	Slag Content	ITS Dry (kPa)	ITS Wet (kPa)	TSR (%)
1	**85%**	Without Slag	383	225	58
2	**65%**	Without Slag	311	190	61
3	**45%**	Without Slag	270	160	59
4	**85%**	With Slag	370	195	52
5	**65%**	With Slag	305	165	54
6	**45%**	With Slag	258	133	51

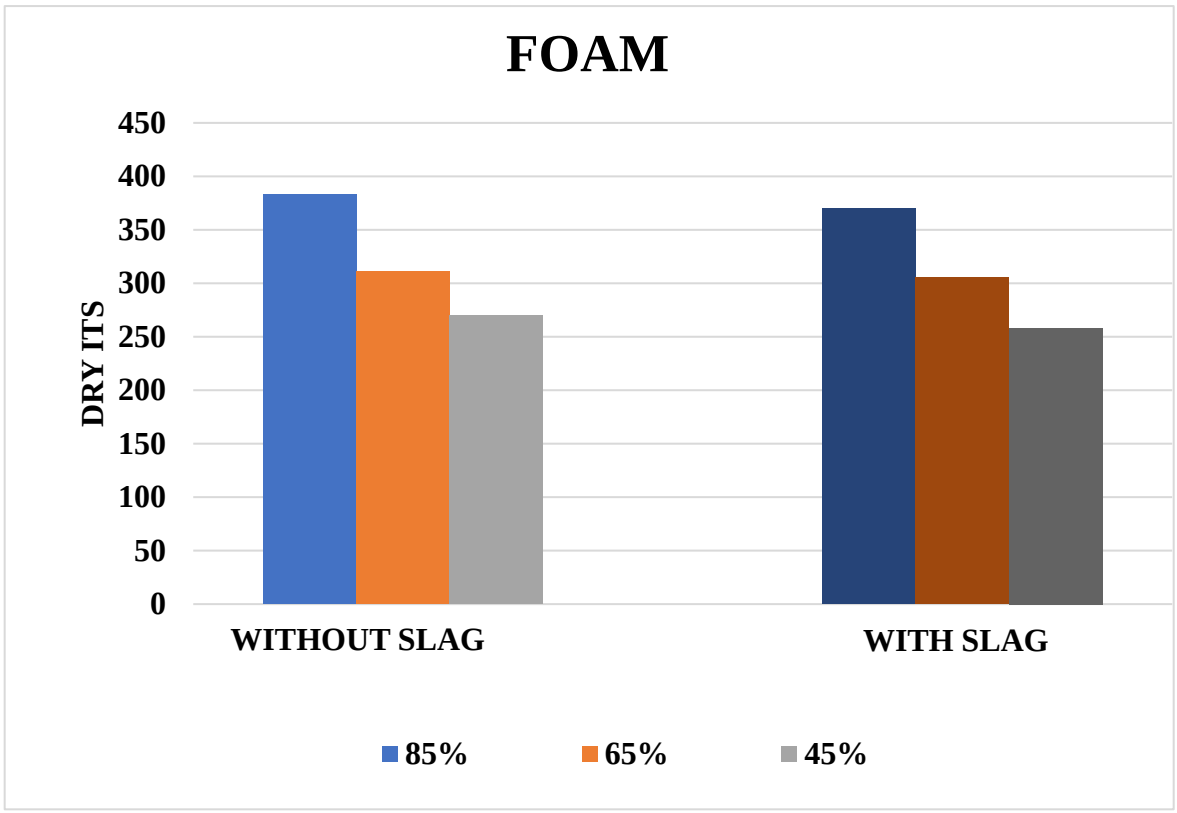

Fig 6.7: Variation of Dry ITS (kPa) with RAP content and slag content

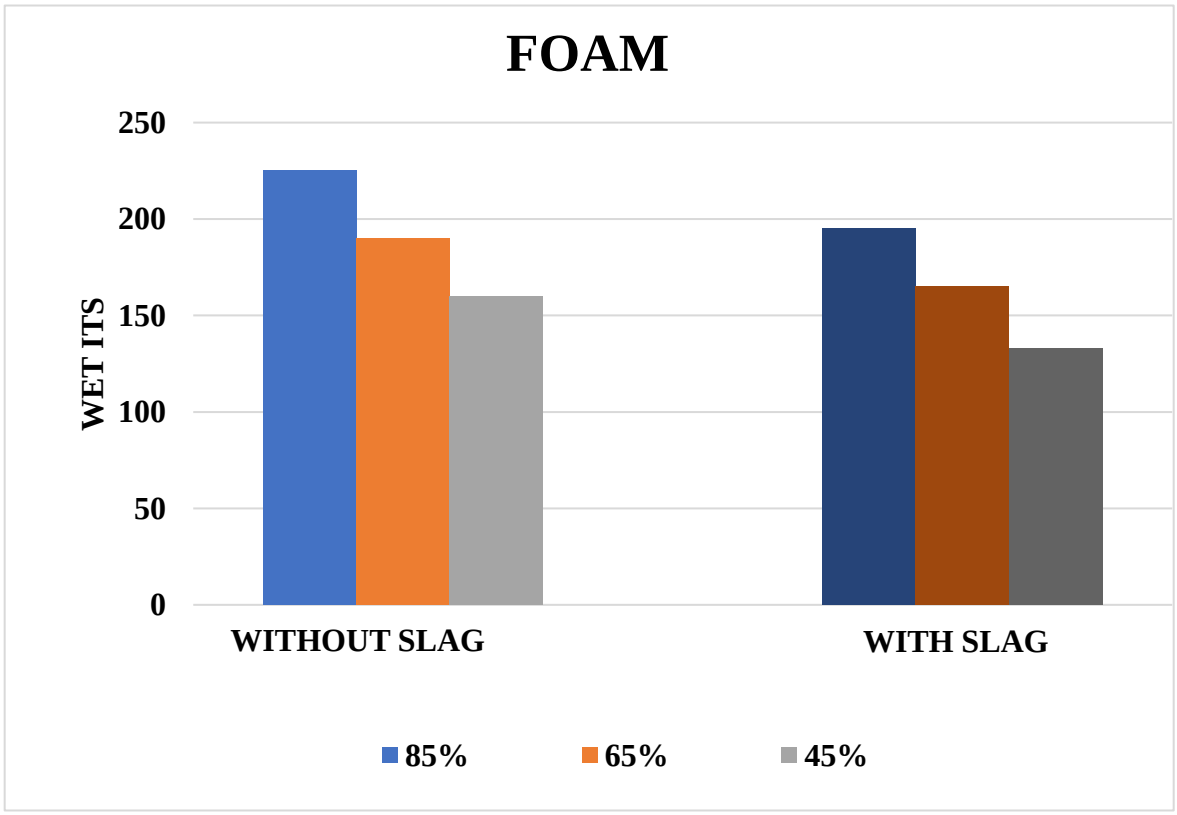

Fig 6.8: Variation of Wet ITS (kPa) with RAP content and slag content

6.2.2 Resilient Modulus Test

Figures 6.9, 6.10, and 6.11 show the fluctuation of resilient modulus with RAP % and Slag content for the VG-10 binder at 25°C, 35°C, and 45°C, respectively. Keeping all other factors fixed, 25°C had higher resilient modulus than 35°C and 45°C for all mixes. This finding suggests that the slag content of FBM has a considerable impact on the sample mix's resilient modulus. All FBM samples displayed increased resilience modulus with increasing RAP concentration and eventually decreased for a given binder grade. For all mixes, the maximum robust modulus was recorded at 65 percent RAP concentration. This can be due to the softening of aged binder in 65 percent RAP combinations compared to 45 percent RAP mixtures. The inclusion of an extra-stiff binder (recovered binder) lowers the cohesion of the mix at 85 percent RAP content, resulting in a lower resilient modulus value. All combinations displayed improved resilience modulus with slag concentration for the specific grade of binder and RAP component.

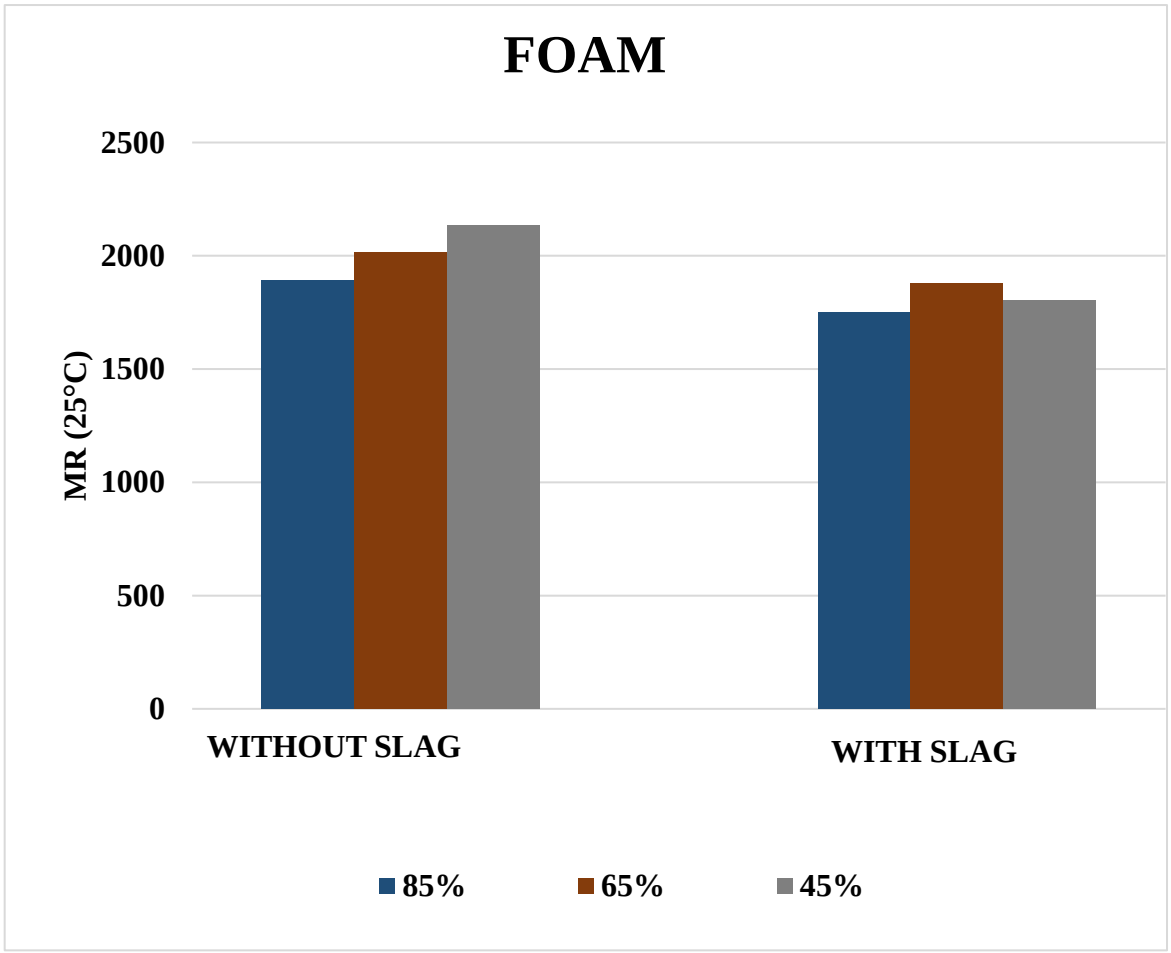

Fig 6.9: Variation of MR at 25°C (MPa) with RAP percentage and slag content

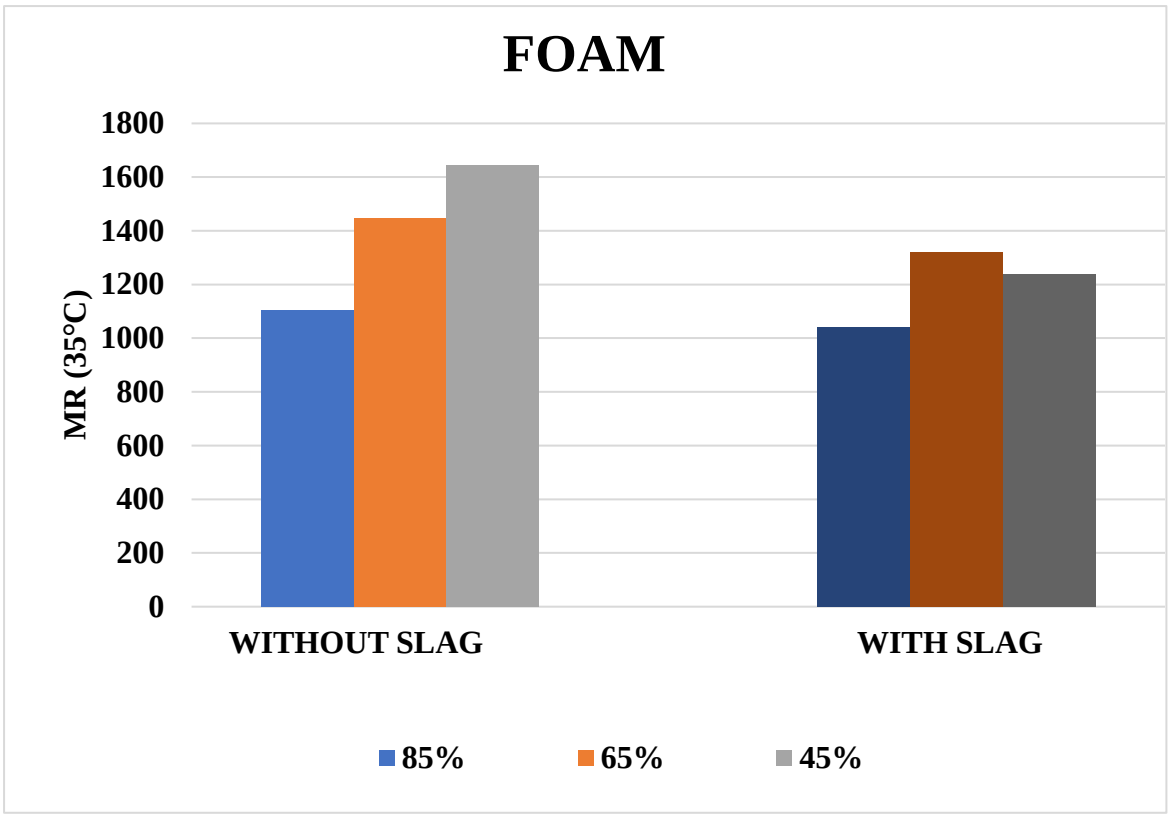

Fig 6.10: Variation of MR at 35°C (MPa) with RAP percentage and slag content

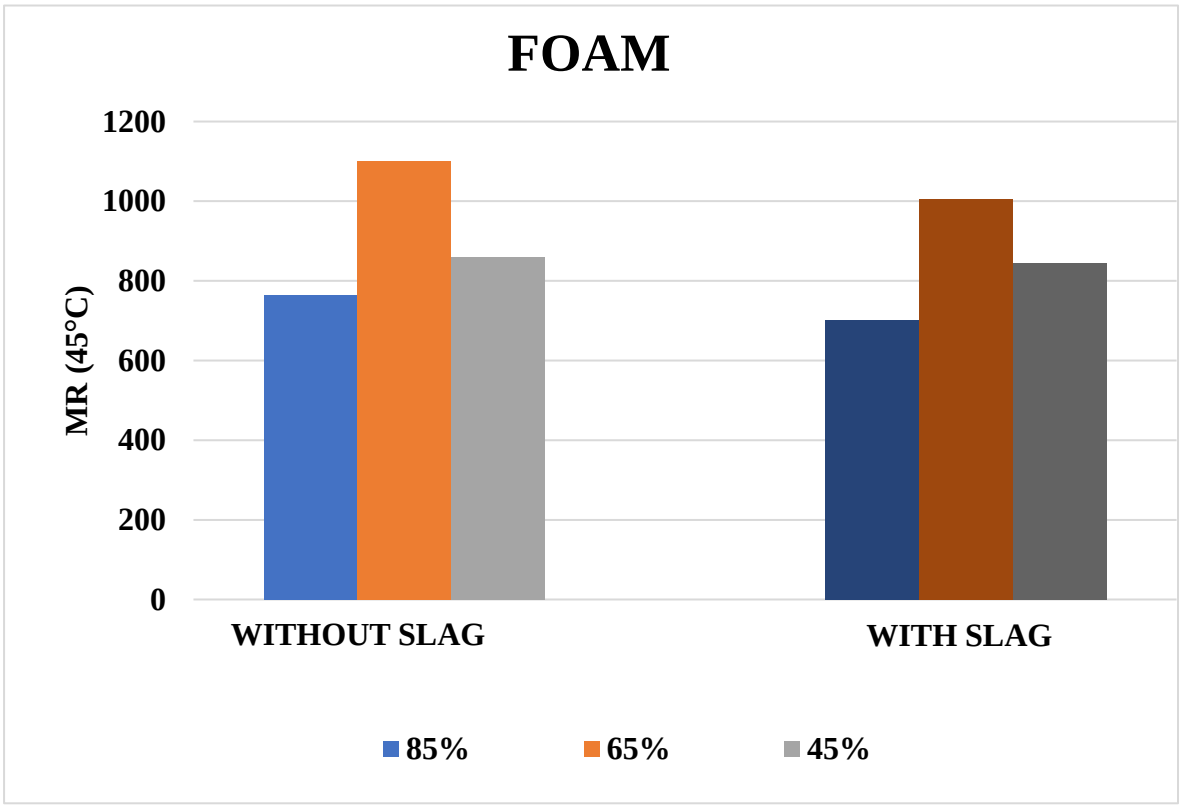

Fig 6.11: Variation of MR at 45°C (MPa) with RAP percentage and slag content

6.2.3 Tensile Strength Ratio

Considering FBM has a large low early strength, void content, a slow rate of strength growth, and a low binder concentration, its strength properties are greatly reliant on the moisture present. As a result, moisture susceptibility is an important element in determining FBM performance. The ITS tests were carried out on a marshal compactor, the findings for dry ITS, wet ITS, and TSR values for VG 10 binder are already shown in Tables 6.2. The specification specifies 225 kPa and 100 kPa as the minimum acceptable values for dry and wet ITS, respectively (Asphalt Academy, 2020; IRC 37, 2012). Furthermore, the literature states that if the value falls below 100 kPa, the mix can be redeemed by applying an active filler like as cement or lime (Asphalt Academy, 2020). According to the literature, in the case of EBM, a TSR value less than 40% suggests questionable material (Kushwaha and Swampy, 2019). Figure 6.12 depicts the fluctuation of TSR with RAP content and slag content. In the current study, the TSR value for all mixes is greater than 50%, which is greater than the minimal criterion of 40%.

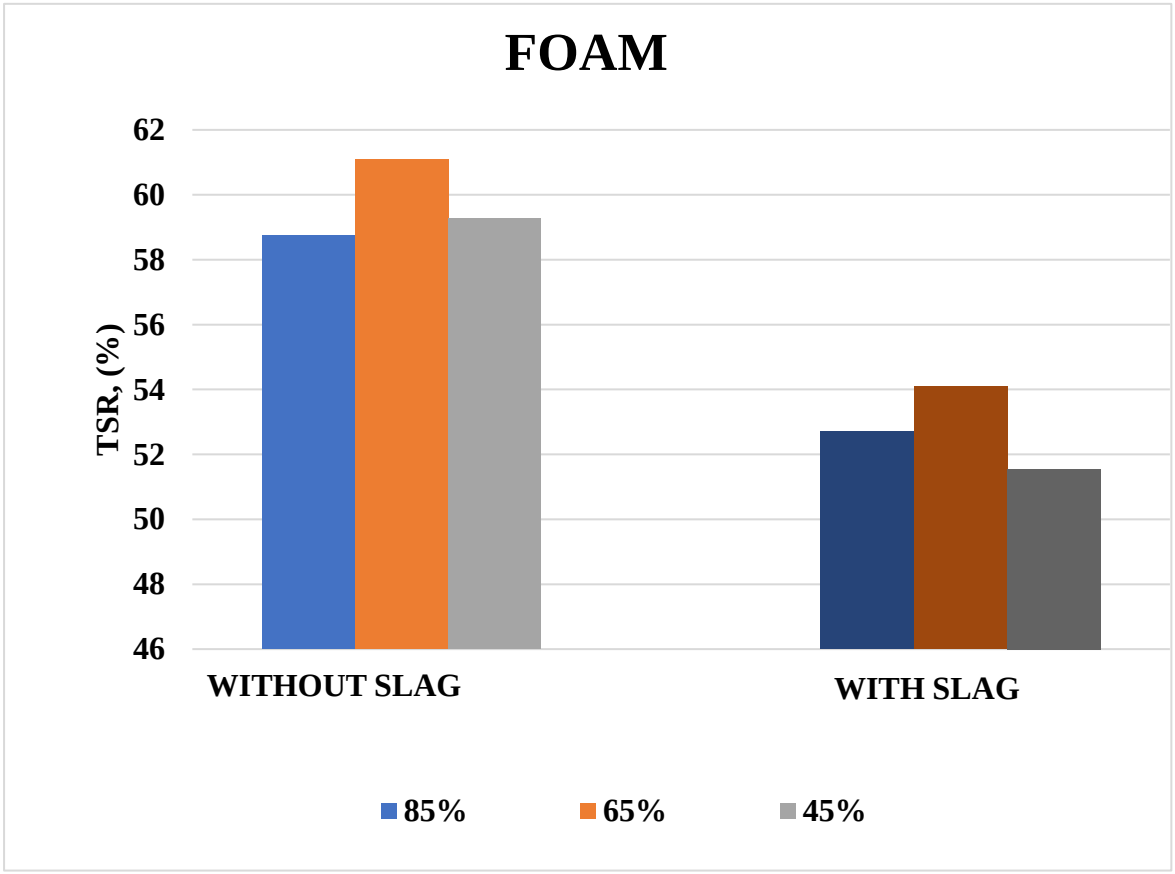

Fig 6.12: Variation of TSR with RAP percentage and slag content

6.3 X-ray Diffraction Analysis

Phase compositions of fine-grain FCS particles were ascertained using the XRD test. The fundamental idea guiding identification of minerals using the X-ray diffractogram (XRD) methodology is that each crystalline substance possesses unique properties and an atomic structure that diffracts X-rays in a certain pattern. The output chart typically records the diffraction peaks in terms of 2, where is the X-ray beam's glancing angle. After that, Bragg's rule is used to translate the data into lattice spacing "d" in Angstroms.

$$d = \lambda / 2n \, Sin\theta \quad \textbf{(6.1)}$$

where, λ = wavelength of X-ray specific to target used

n = an integer

Results of the XRD tests on the fine-grain FCS, stone dust, RAP + FCS mix, and RAP + NA mix samples are displayed in the figures below in turn at 6.13, 6.14, 6.15, and 6.16 respectively. These figures show that the major minerals are spinel quartz, forsterite, Whewellite, and entatite. The presence of the phases in the samples was investigated using XRD analysis. Using the Bruker D8 Advance and Cu K (= 1.54056 A°) between 2 values of 5 and 80° at a scan rate of 2°/min, powder X-ray diffraction patterns of raw ferrochrome slag were produced. The individual XRD patterns was compared with the JCPDS-recommended library/database, phase identification analysis was performed (PDF-2 database 2003).

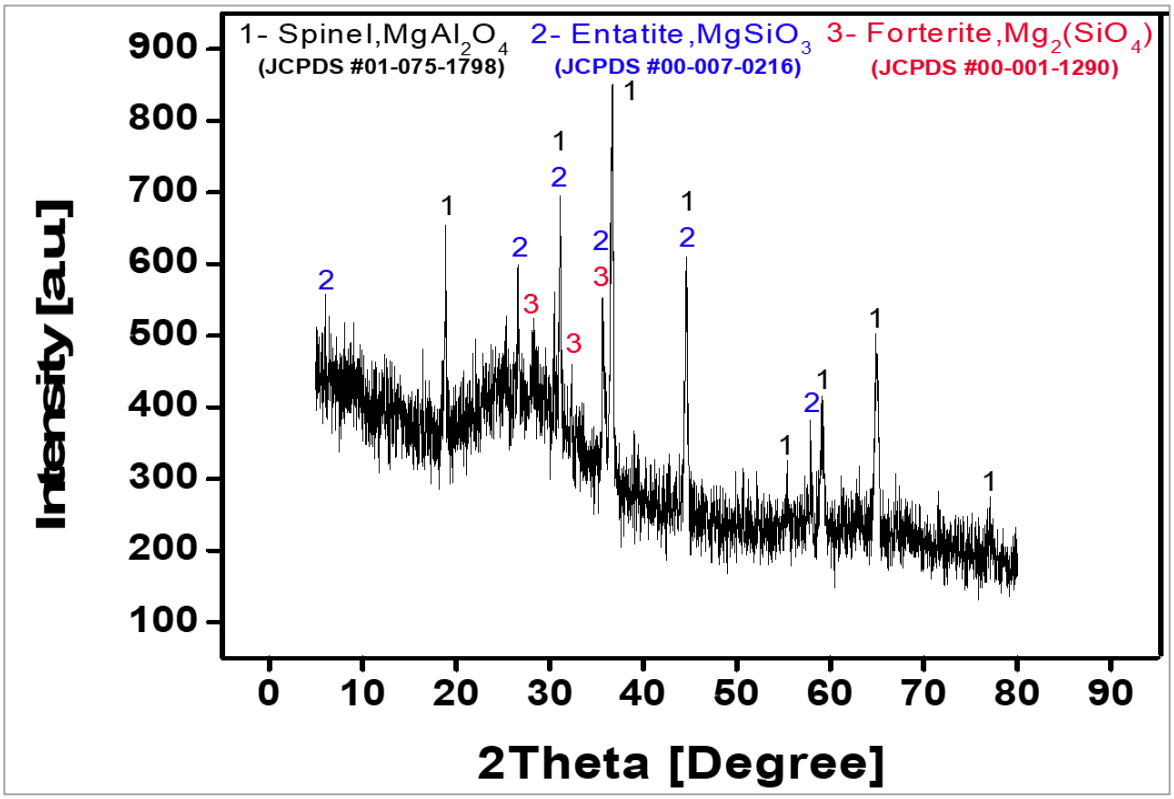

Fig 6.13: X-ray diffraction pattern of ferrochrome slag used

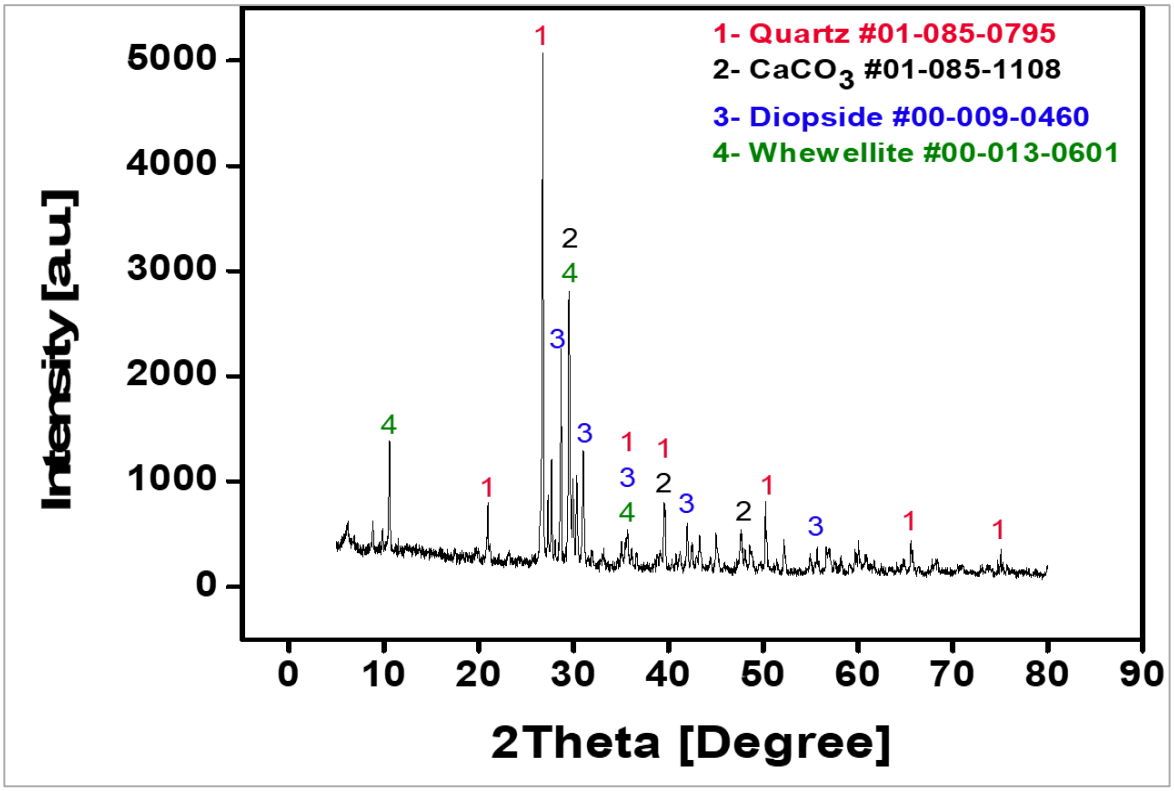

Fig 6.14: X-ray diffraction pattern of Stone Dust used.

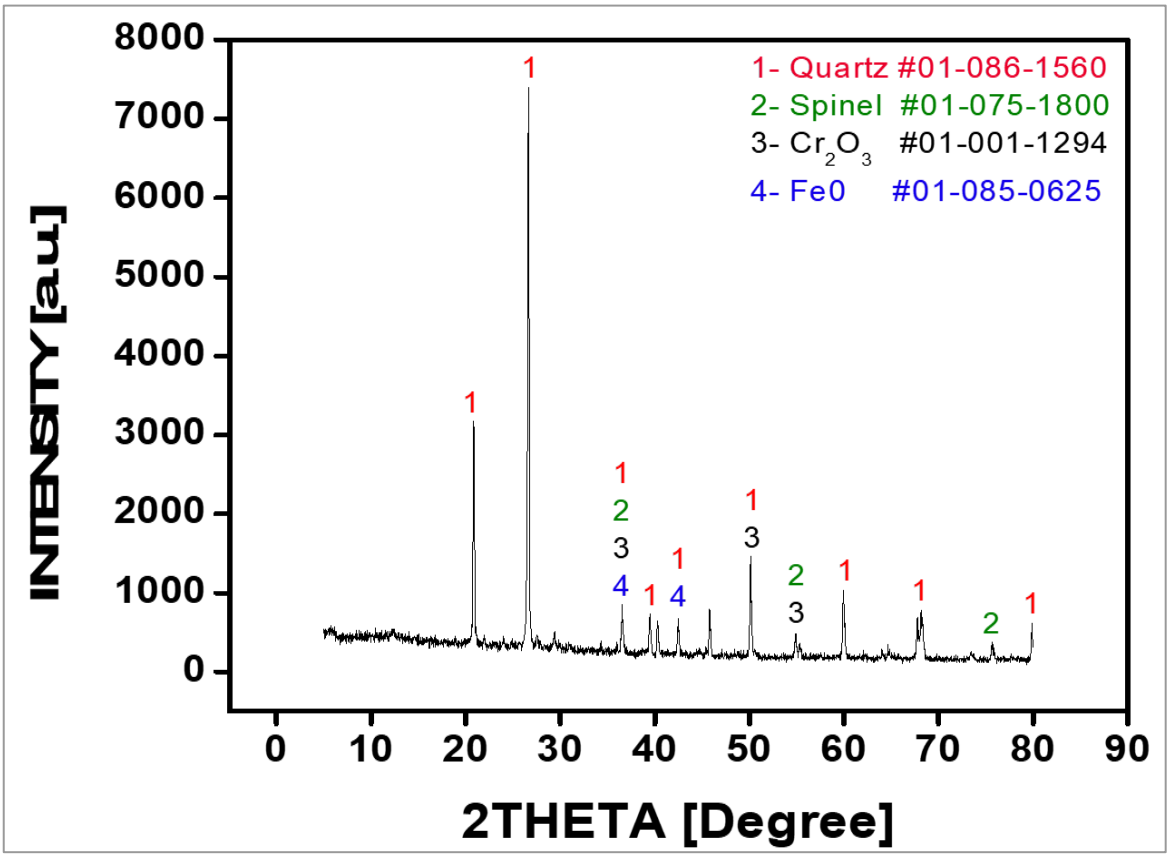

Fig 6.15: X-ray diffraction pattern of RAP+FCS mix.

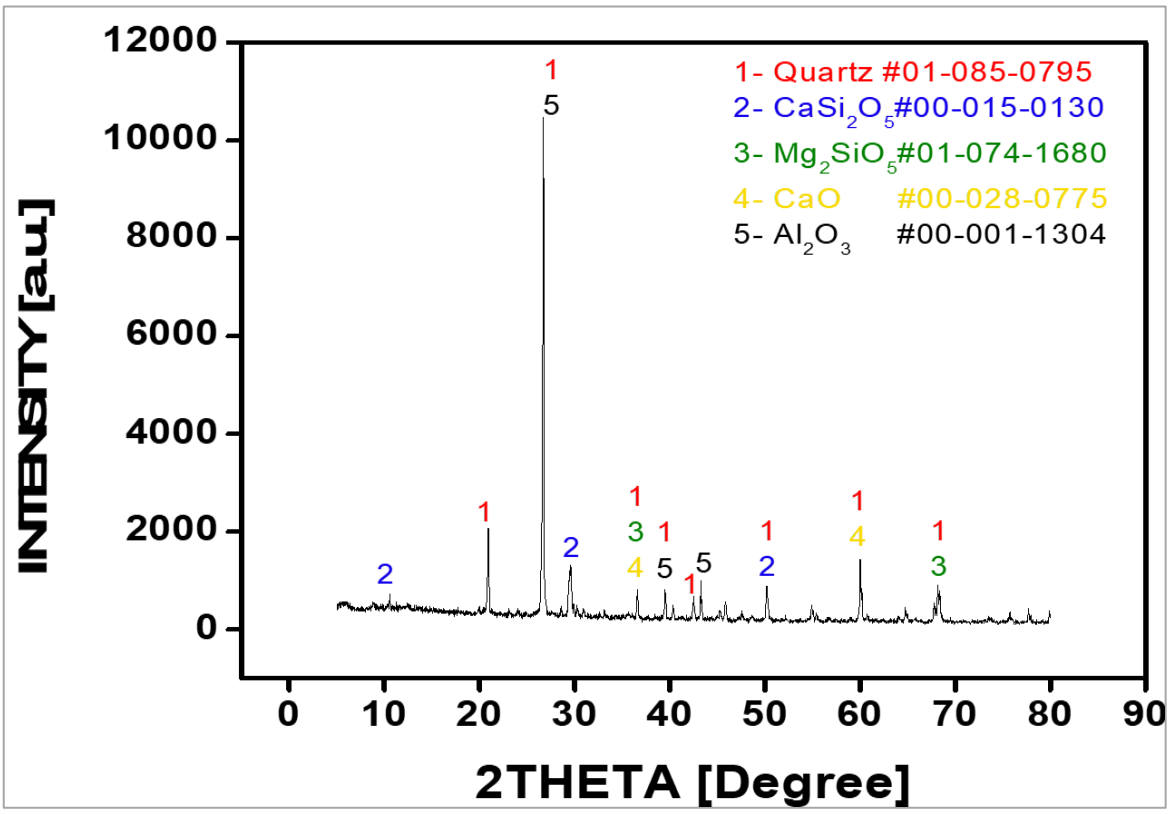

Fig 6.16: X-ray diffraction pattern of RAP+NA mix

CHAPTER 7

CONCLUSION

The current study aimed that the influence of RAP content and ferrochrome slag content utilization on characterization of foam bitumen mix and emulsion bitumen mix. Thus, this includes the performance of both the mix, which determine the optimum parameters for the best mix performance using DoE analysis. Based on data obtained from the laboratory studies as well as analyses carried out, the following findings are made.

Foaming features of the binders in term of half-life and expansions ratio were also evaluated by varying the water content. Optimum foaming water content and optimum foaming bitumen content were obtained to have an acceptable and best value of expansion ratio and half-life.

Emulsion characteristics of binder in terms of total fluid content and optimum emulsion content were evaluated by varying both the parameters. Optimum emulsion content was obtained through ITS value to have a best value of EBM.

The effect of RAP material content, ferrochrome slag content and two types of binder (foam bitumen and bitumen emulsion) on the performance of FBM and EBM have been evaluated through the DoE approach. The experiments were designed conferring to the 2^3 factorial designs using RSM method. The performance of FBM and EBM samples was evaluated by preparing the samples with each grade of bitumen at three different percentages of RAP material (45%, 65%, and 85%), at two different slag content (with slag and without slag). Performance tests such as dry ITS and wet ITS, and MR at different temperatures were carried out on the samples having different RAP material content and binder. Also X-ray Diffraction Analysis was carried out to evaluate the different phase of mix and raw material to check whether there is a possibility of leaching.

7.1 Comparison between mix containing rap and slag

The TSR values determined by ASTM D4867 for cold bituminous mixtures containing RAP were comparable to the slag content mix. This indicates that RAP offer resistance to damage by moisture. Whereas, TSR values determined by ASTM D7870 for the cold recycled foam mixtures were equivalent to the conventional mix, which indicates lower susceptibility to moisture damage. But in emulsion-based mixtures, higher RAP percentage mixtures are more resistant than conventional mixtures. This implies that increase in content of RAP improves moisture resistance.

The resilient modulus values of RAP and natural aggregate mixes were found to be more compared to the RAP and ferrochrome slag mixes at selected test temperatures. Thus it indicates that addition of RAP in mix makes it more stiffer. Higher modulus values were gained for 65% RAP incorporated in bituminous mix. These conclusions therefore show that RAP inclusion enhances the bituminous mixes' characteristics. The sole negative is that, depending on whether the RAP gets blended with natural aggregate or ferrochrome slag, the ultimate performance of the mix containing RAP mostly depends on materials characteristics in the mix and its optimization.

7.2 Comparison between foam bitumen and bitumen emulsion

Foamed bitumen mix performed better in moisture susceptibility when compared to the emulsion-based bitumen. Additionally, compared to specimens containing emulsion, those containing foam bitumen demonstrated a slower proportion in increase on permanent deformation. It may be observed that mixes derived out of foam bitumen performed relatively better than conventional and mixes of emulsion. However, when fatigue life is the criterion, cold emulsion mixes performed better.

7.3 Suggestion for future work

The following work may be pursued in future studies in light of the constraints observed in the laboratory during inquiry and development of the DoE-based predictive models:

- Life Cycle cost analysis is to be done to indicate the economic benefits in utilizing higher RAP bituminous mix and higher ferrochrome slag content
- Investigating the utilization of RAP in different layers of road pavement.
- The parameters of the foam bitumen mix utilised in this study were established using varied slag and RAP contents for a single bitumen source, the predictive model's accuracy can be increased further by include various grades of binder.
- Test sections may be constructed with different RAP percentage and slag percentage and actual field performance may be evaluated.

Therefore, in order to better understand the performance, a large-scale field trial must be carried out.

REFERENCES

i. Annual Report (2012-2013)"; Ministry of Road and Transport and Highways, Government of India. p. 96 (Appendix 17). Retrieved 3 April 2013.

ii. AASHTO T 324 (2004), "Standard Method of Test for Hamburg Wheel-Track Testing of Compacted Hot-Mix Asphalt (HMA)" AASHTO, Washington DC.

iii. Abel F (1978), "Foamed asphalt base stabilization", 6th Annual Asphalt Paving Seminar, Colorado State University.

iv. Analysis of Rates for Delhi (2013), Central Public Works Department (CPWD), Government of India, published by Director General (works), CPWD, Nirman Bhavan, New Delhi.

v. Asphalt Academy (2009), "Technical guideline: Bitumen stabilized materials", A guide for the design and construction of bitumen emulsion and foamed bitumen stabilized materials, TG2, First Edition, Asphalt Academy, Pretoria, South Africa.

vi. Asphalt institute (1989) "Asphalt Cold Mix Manual". Manual Series No. 14 MS-14), Third Edition, Lexington.

vii. AST D1856, (2004). "Standard Test Method for Recovery of Asphalt from Solution by Abson Method", American Society for Testing and Materials, Annual Book of ASTM Standards, Volume 04.03

viii. asphalt Institute and Asphalt Emulsion Manufacturers Association (1007). •A Basie "Asphalt Emulsion Manual". Manual Series No. 19. Third Edition, Asphalt Institute and Asphalt Emulsion Manufacturers Association, USA.

ix. AST D2041, (2011) "Standard Test Method for Theoretical Maximum Specific Gravity and Density of Bituminous Paving Mixtures", American Society for Testing and Materials, Annual Book of ASTM Standards, Volume 04.03.

x. AST D4402-02 (2002), "Standard test Method for viscosity determinations of asphalts at elevated temperatures using a rotational viscometer", American Society for Testing and Materials, Annual Book of ASTM Standards, Volume 04.03.

xi. ASTM D4867, (2009) "Standard Test Method for Effect of Moisture on Asphalt Concrete paving Mixtures, American Society for Testing and Materials, Annual Book of ASTM Standards, Volume 04.03.

xii. AST D6307(2010), "Standard Test Method for Asphalt Content of Hot-Mix Asphalt by Ignition Method", American Society for Testing and Materials, Annual Book of ASTM Standards, Volume 04.03.

xiii. ASTM D7369 (2011) "Standard Test Method for Determining the Resilient Modulus of Bituminous Mixtures by Indirect Tension Test", American Society for Testing and Materials, Annual Book of ASTM Standards, Volume 04.03.

xiv. Barinov, E. N. (1990). "Formation and properties of bituminous foams. Chemistry and Technology of Fuels and Oils", 26(10), 544-548.

xv. Brennen M., Tia M., Alschachi A and Wood L.E, 1883. Laboratory Investigation of the use of foamed bitumen for recycled bituminous pavements. Transportation Research Record 911. Pp 80-87.

xvi. CSIR-Council for Scientific and Industrial Research, (1998). "Foamed Asphalt Mixes Mix Design Procedure", Contract Report CR-98/077, SABITA and SIR Transportek, Pretoria, South Africa.

xvii. Das, S. K., and Yudbir,(2005), "Geotechnical Characterization of some Indian Fly ashes", Journal of Materials in Civil Engineering, ASCE,17(5), pp.544- 552.

xviii. D'Angelo, J. A., Harm, E. E., Bartoszek, J. C., Baumgardner, G. L., Corrigan, M. R. Cowsert, J. E., ... & Yeaton, B. A. (2008). Warm-mix asphalt: European practice (No. FHWA-PL-08-007).

xix. Fu P. Jones. Di Man eY a sprai in Mallea, E: A. (2000). "Investigation of the cuing mechanism of foamed asphalt mixes based on micromechanics principles" Journal of Materials in Civil Engineering, 22(1), 29-38.

xx. Gaudefroy, V. OLARD: F. Le Quernec, F., & De La Roche, C. (2008, August) "laboratory investigations on the Total Organic Compounds emissions of half-warm mix asphalt technology versus traditional hot mix asphalt. Symposium on Asphalt Pavements and Environment (ISAP).

xxi. He G. and Wong W. (2007) "Laboratory study on permanent deformation of foamed asphalt mix incorporating reclaimed asphalt pavement materials", Construction and Building Materials Vol. 21, No. 8, P 1809-1819.

xxii. IRC 37: (2012), Technical Guideline for Design of Flexible Pavements.

xxiii. IS:1203, "Methods for Testing Tar & Bituminous Materials: Determination of penetration", Bureau of Indian Standards, New Delhi.

xxiv. IS:1205, "Methods for Testing Tar & Bituminous Materials: Determination of softening point", Bureau of Indian Standards, New Delhi.

xxv. 1S:2386 (Part 3) - 1963 (2002), "Methods of Test for Aggregates for Concrete – Specific Gravity, Density, Voids, Absorption and Bulking", Bureau of Indian Standards, New Delhi.

xxvi. Jenkins, K. J., & Van de Ven, M. F. C. (2001), "Guidelines for the mix design and performance prediction of foamed bitumen mixes". SATC 2001.

xxvii. Kauppi, M. and Pekka, N., (2007). "Production, characteristics and use of Ferrochrome slags", Infacom 7.

xxviii. Kim Y., Im S., and Lee H. (2011), "Impacts of Curing Time and Moisture Content on Engineering Properties of Cold In-Place Recycling Mixtures Using Foamed or Emulsified Asphalt", ASCE J. Materials in Civil Engineering, Vol. 23, No. 5, pp.542-553.

xxix. Lind BB, Fallman AM, Larsson LB (2001) Environmental impact of ferrochrome slag in road construction. Waste Manag 21:255–264.

xxx. Lane, B., Kazmierowski, T. And Alkins, A. (2008). "Sustainable Pavements: Environmental, Economic, and Social Benefits of In Situ Pavement Recycling". Transportation Research Records: Joumal of the Transportation Research Board 2008. Transportation Research Record: Journal of the Transportation Research Board, No. 2084, pp. 100-103.

xxxi. Leach, R., & Beer, T. (2000). ENVIRONMENTAL ASSESSMENT OF EMULSIONS. Publication AP-R153/00. Austroads Inc.

xxxii. R.M. Mulungye, P.M.O. Owende, K. Mellon, Finite element modeling of flexible pavements on soft soil subgrades, Mater. Des. 28 (2007) 739–756.

xxxiii. Singh, M., Upadhayay, S.N., Prasad, P.M., (1996)," Preparation of special cements from red mud", Waste Management 6 (8), 665–670.

xxxiv. Singh S.R. and Panda, A.P (1996), "Utilization of fly ash in geotechnical construction", Proc. Indian Geotechnical Conf., Madras, Vol. 1, pp:547-550.

xxxv. Tossavainen, M., (2005). "Leaching results in the assessment of slag and rock materials as construction material", Doctoral thesis, Lulea University of Technology, 1402-1544.

xxxvi. Wu S, Xue Y, Ye Q, Chen Y (2007) Utilization of steel slag as aggregates for stone mastic asphalt (SMA) mixtures. Build Environ 42:2580–2585.

xxxvii. Y. Huang, R.N. Bird, O. Heidrich, A review of the use of recycled solid waste materials in asphalt pavements, Resour. Conserv. Recycle. 52 (2007) 58–73.

xxxviii. Yilmaz, M., VuralKo, B., (2009). "Effect of ferrochromium slag with neat and polymer modified binders in hot bituminous mix", Indian Journal of Engineering & materials science, vol. 16: 310-318.

xxxix. Yilmaz, A., Karasahin, M., (2010). "Mechanical properties of ferrochromium slag in granular layers of flexible pavements, materials and structures", vol. 43: 309-317.

xl. www.ferro-alloys.net (2013) "Ferro alloy industries around the world". Browsed on 10.4.2013.

UTILIZATION OF FERROCHROME SLAG IN BITUMEN BASE STABILISATION

Ouriginal

Document Information

Analyzed document	Dissertation_Utkarsh Singh.pdf (D142999233)
Submitted	2022-08-17 09:39:00
Submitted by	Manpreet Singh
Submitter email	manpreetsingh2@thapar.edu
Similarity	4%
Analysis address	manpreetsingh2.thapar@analysis.urkund.com

Sources included in the report

SA	**Thapar Institute Of Engineering And Technology / NIPUN MADAAN FINAL THESIS Revised!.pdf** Document NIPUN MADAAN FINAL THESIS Revised!.pdf (D76002549) Submitted by: manpreetsingh2@thapar.edu Receiver: manpreetsingh2.thapar@analysis.urkund.com	4
SA	**Sardar Vallabhbhai National Institute Of Tech / P19TP009_SAURABH GARG_DISSERTATION_13072021.pdf** Document P19TP009_SAURABH GARG_DISSERTATION_13072021.pdf (D110444319) Submitted by: ajs@ced.svnit.ac.in Receiver: ajs.svnit@analysis.urkund.com	3
W	URL: https://researchbank.swinburne.edu.au/file/63088b2f-5c6f-437f-bd1e-6654913c37e9/1/anuththara_kirindigoda_hewage_thesis.pdf Fetched: 2021-11-01 13:19:13	1
SA	**Thapar Institute Of Engineering And Technology / USE OF STONE MATRIX ASPHALT (2) (1) (1).docx** Document USE OF STONE MATRIX ASPHALT (2) (1) (1).docx (D110188149) Submitted by: manpreetsingh2@thapar.edu Receiver: manpreetsingh2.thapar@analysis.urkund.com	1
SA	**SAGE University / 18ENG7CIV0003_Naveen_Shankar_PhD_Thesis.docx** Document 18ENG7CIV0003_Naveen_Shankar_PhD_Thesis.docx (D121400994) Submitted by: phdcell@sageuniversity.in Receiver: phdcell.sage@analysis.urkund.com	1
W	URL: https://pdfs.semanticscholar.org/23f9/acbe2544ef67d54d8f5577bcdf3341c010a6.pdf Fetched: 2022-06-23 07:52:42	5
W	URL: https://www.researchgate.net/publication/324052664_Impact_of_Recycled_Asphalt_Pavement_on_Properties_of_Foamed_Bituminous_Mixtures Fetched: 2020-05-30 12:51:46	2
W	URL: https://www.omicsonline.org/open-access/significance-of-rap-content-and-foamed-binder-content-on-mechanisticcharacteristics-of-recycled-foamed-bituminous-mixes-2165-784X-1000220.php?aid=72575 Fetched: 2019-09-30 15:14:50	1
SA	**Rajiv Gandhi Proudyogiki Vishwavidyalaya / thesis...vijay.docx** Document thesis...vijay.docx (D139916867) Submitted by: ashokgagorni@gmail.com Receiver: ashokgagorni.rgpv@analysis.urkund.com	1